Lab on a Chip

RSC Publishing

CRITICAL REVIEW

View Article Online
View Journal | View Issue

Published on 08 May 2013. Downloaded by University of Cambridge on 31/05/2013 13:14:32.

Cite this: *Lab Chip*, 2013, **13**, 2210

Paper-based microfluidic point-of-care diagnostic devices

Ali Kemal Yetisen,* Muhammad Safwan Akram and Christopher R. Lowe

Dipstick and lateral-flow formats have dominated rapid diagnostics over the last three decades. These formats gained popularity in the consumer markets due to their compactness, portability and facile interpretation without external instrumentation. However, lack of quantitation in measurements has challenged the demand of existing assay formats in consumer markets. Recently, paper-based microfluidics has emerged as a multiplexable point-of-care platform which might transcend the capabilities of existing assays in resource-limited settings. However, paper-based microfluidics can enable fluid handling and quantitative analysis for potential applications in healthcare, veterinary medicine, environmental monitoring and food safety. Currently, in its early development stages, paper-based microfluidics is considered a low-cost, lightweight, and disposable technology. The aim of this review is to discuss: (1) fabrication of paper-based microfluidic devices, (2) functionalisation of microfluidic components to increase the capabilities and the performance, (3) introduction of existing detection techniques to the paper platform and (4) exploration of extracting quantitative readouts *via* handheld devices and camera phones. Additionally, this review includes challenges to scaling up, commercialisation and regulatory issues. The factors which limit paper-based microfluidic devices to become real world products and future directions are also identified.

Received 6th February 2013,
Accepted 18th March 2013

DOI: 10.1039/c3lc50169h

www.rsc.org/loc

1. Introduction

Since its origins[1] in the 1990s, polydimethylsiloxane-based[2] microfluidics have made little progress towards becoming real world products. They have limited diffusion and impact in other disciplines and have not solved problems that are otherwise unsolvable.[3] The disconnect stems from the fact that developers of microfluidic devices are often fundamentally not interested in building practical products whereas the end-users are only interested in cheap and simple technologies that solves their own problems.[4] There has been a lot of promise in the field, but not a lot of delivery.[5] However, this is changing, and for this, capillary-based microfluidics might be the answer. Recently, paper has been functionalised as a substrate to construct microfluidic devices for use in rapid diagnostic tests.[6] Patterning paper into regions of hydrophilic channels demarcated by hydrophobic barriers (or air) provides microfluidic devices that offer four basic capabilities on a single analytical device: (i) distribution of a sample into multiple spatially-segregated regions to enable multiple assays simultaneously (or replicates of an assay) on a single device; (ii) moving the sample by capillary action (no pumps are needed); (iii) compatibility with small volumes of sample,

Fig. 1 The array of rapid tests: urinalysis,[8–15] immunoassays,[16–20] veterinary diagnostics,[21–24] food safety,[25–28] environmental,[29–34] biothreats,[35–37] drug abuse.[38–41] Rapid diagnostic tests often have lower specificity and sensitivity than their laboratory bench counterparts. The majority of these tests are simple and provide a yes/no answer where response time is critical to the user.

Department of Chemical Engineering and Biotechnology, University of Cambridge, Tennis Court Road, Cambridge, CB21QT, United Kingdom.
E-mail: ay283@cam.ac.uk; Fax: +44 (0) 1223 334160; Tel: +44 (0) 1223 334162

This journal is © The Royal Society of Chemistry 2013

Published on 08 May 2013. Downloaded by University of Cambridge on 31/05/2013 13:14:32.

which is essential when sample size is limited (*i.e.* tears, saliva, urine from neonates and drops of blood from finger sticks); and (iv) facile elimination of hazardous waste since the devices can be disposed of by incineration.[7]

This article aims to review industrial applications and commercial opportunities of paper-based microfluidic devices. This review discusses existing technologies in the market, the origins of paper-based microfluidics, materials, capabilities, the principles of capillary flow, sensing mechanisms, readout technologies, performance, reproducibility, mass manufacturing techniques, routes to commercialisation and regulatory issues, as well as updating the topics previously covered in other reviews.[42–46] The review will be concluded by a discussion of gaps within the field and how to overcome the perceived limitations of paper-based microfluidics. This review will not discuss high-end applications of microfluidics such as laboratory-based technologies that do not apply to resource-limited settings. In this review, ''paper'' refers to cellulosic materials (*i.e.* filter paper and chromatography paper) unless otherwise specified. In *in vitro* diagnostics industry, the term ''membrane'' is exclusively used to describe nitrocellulose in the lateral flow format.[47] To be compatible with the terminology in the industry, this review does not refer to nitrocellulose as paper. However, the review will also discuss nitrocellulose-based technologies due to their close relationship to paper-based devices.

1.1 Healthcare burden in the developing economies

Despite the increasing trend of urbanisation around the globe, 55% of inhabitants of the developing world still live in rural regions.[48] As poverty stays as a subjective parameter, the majority of the developing world's population relies on agriculture and livestock commodities.[49,50] In resource-limited settings, inhabitants lack access to technical services and human resources that are often present in urban areas. Affordable technologies that can enable local communities in developing regions to improve healthcare,[51] environmental safety,[52] animal health,[53,54] and food quality[55] will play key roles in achieving post Millennium Development Goals[56] agenda beyond 2015. Diagnosis is the first step to treat a condition: yet, the major stumbling block in monitoring and controlling diseases/contaminations remains delivering simple, low-cost and robust diagnostic tests.[57] Several factors that have accelerated the emphasis on point-of-care diagnostics for the developing world include lack of infrastructure,[58] shortages in trained personnel,[59] increase in healthcare associated infections,[60,61] preservation of the life span of cost-effective drugs[62] and increases in spurious/counterfeit medicines[63] as well as mitigating the possibility of epidemic-to-pandemic transitions of infectious diseases.[64] In terms of impact, low-cost diagnostics can reach under-served communities, *i.e.* the bottom of the pyramid.

Responding to global initiatives, economic and minimally instrumented diagnostics for resource-limited settings are emerging rapidly despite the limited interest from commercial partners.[64–66] Diagnostics for resource-limited settings does not always receive attention from large companies while limited research activity in smaller biotechnology companies and academia struggle to make an impact in creating real world products, scaling up and achieving market penetration. This aspect parallels the disinterest of industrial partners in these applications due to the limited market and low-profit margins.

Medical diagnostics in the developing world for poverty-related conditions are often ineffective and out-dated. In healthcare, when diagnostic equipment is absent, healthcare workers make their decisions based on observed symptoms. WHO's Integrated Management of Childhood Illness (IMCI) is an example of a systematic diagnosis and treatment guideline with minimum requirements for instrumentation and based on signs and symptoms.[67] However, such systematic guidelines are time consuming and fall short when (i) distinguishing asymptomatic diseases, (ii) detecting multiple infections at a time, (iii) identifying the window period (*i.e.* the timeframe between infection and diagnosis) and (iv) quantifying results (*i.e.* concentrations of analytes and viral load). Despite the odds, systematic guidelines remain the most cost-effective and practiced method with little or no requirement for equipment.

Veterinary diagnostics is another critical field which can be linked to human health. In developing world regions, humans constantly interact with animals for transportation, power, clothing and basic food. The close human-animal relationship often carries risk factors in public health with economic consequences. A wide array of communicable diseases, also known as zoonoses, can be transmitted from livestock or wildlife to humans in various ways. Pathogenic infections which arise as a consequence of zoonotic cross-species transmission are a significant cause of infection among humans.[68,69] Acquired infections have serious health consequences including HIV,[70] SARS coronavirus[71] and influenza.[72] Potentially, many of these diseases can spread over long distances to become pandemics (*e.g.* vector-borne West Nile virus). Zoonotic diseases often disable the potential and efficient production of food of animal origin and act as a hindrance to international trade.

Food safety is another silent public health concern. Foodborne illnesses are the direct consequence of ingesting food that contains infectious and toxic agents. Major examples in this category include salmonellosis and campylobacteriosis infections (*via* eggs, poultry, and unpasteurised milk), enterohaemorrhagic *Escherichia coli* (O157:H7 serotype) and cholera (*via* water, rice, vegetables, seafood).[73]

The same argument applies to environmental monitoring. Despite international efforts, waterborne diseases due to contaminated water and inadequate sanitation remain a major global health issue which continue to fuel diarrhoeal diseases. Today, very few developing countries have programmes for testing water supplies in rural regions.[74] Access to safe drinking water, contamination from industrial sources (*e.g.* lead and mercury), human dwellings, chemicals from agriculture, water treatment or materials, and microbial safety, are among historical challenges to be tackled. Today simple platform technologies that can answer an important question: ''Is this water contaminated?'' are needed more than ever.[75]

The WHO has set seven guidelines for the development of diagnostics in resource-poor settings. These tests must be: (i) affordable, (ii) sensitive, (iii) specific, (iv) user-friendly, (v)

Published on 08 May 2013. Downloaded by University of Cambridge on 31/05/2013 13:14:32.

rapid and robust, (vi) equipment-free, and (vii) delivered to those who need it, corresponding to the acronym "ASSURED".[62] Although the design trend towards low-cost remains a priority, major markets are demanding more sensitivity and specificity from rapid diagnostics assays in global markets. Operating with low-volume clinical samples with minimum user manipulation, being lightweight and eliminating sharps (*i.e.* needles) are considered additional desirable characteristics of rapid tests.

1.2 Existing technologies

Dipsticks and lateral flow are the established assay formats for point-of-care testing. The first paper-based diabetes dipstick test was proposed in the 1950s to quantify glucose in urine, followed by its commercial introduction to the consumer markets in the 1960s.[76] After the urine is introduced, the results are compared to a colour-coded chart to determine the glucose concentration as a semi-quantitative result. Today, commercial urinalysis dipsticks have been widely adapted for a number of analytes.[9–15] Traditionally, these tests come with a colourimetric chart or with detection equipment such as Urisys 1100® Urine Analyser (Roche).

Parallel to the development of dipstick tests, latex agglutination assays and radioimmunoassays can be considered the forerunners of lateral flow tests, and date back to 1950s.[77,78] Although nitrocellulose membranes have been used historically for filtration purposes,[79] they have been adapted as a substrate for molecular detection in 1970s.[80–82] In the 1980s, serological lateral flow tests started emerging,[83] particularly the human pregnancy test,[84] derived from the development of hCG beta-subunit radioimmunoassay.[85] Since then, commercial rapid lateral flow tests expanded beyond clinical diagnostics to veterinary, food, environmental applications, biodefence and drug abuse (Fig. 1).[86–93]

The majority of these tests come in different sizes, shapes and configurations. These assays are available without (Fig. 2A–C) or with housing units (Fig. 2D–G). Nowadays, multiplexing of rapid tests is becoming fairly common. Fig. 2H illustrates a lateral-flow format that separates each single lateral flow test strip into multiple channels. The assay is multiplexed in the sense that a single sample is analysed simultaneously but in reality the test strips are still separate reactions occurring independent of the other reactions.[94,95] Similarly, SNAP® 3Dx® Test is another multiplex assay that can test four pathogens simultaneously.[96]

Lateral flow immunoassays can be subdivided into two major types: direct (*i.e.* double antibody sandwich assays) and competitive (*i.e.* inhibitive) formats. The assay format typically consists of a number of segments that join together and are supported by a backing card. These segments include the sample pad, conjugate pad, reaction membrane and an absorbent pad (Fig. 3A). All these components are typically enclosed in a plastic cassette (housing). Other formats such as flow-through (vertical format) (Fig. 3B) are more complex than lateral flow tests. Execution of such assays often requires multiple steps: Sample placement on the device, washing and addition of analyte-colloidal gold conjugates. Due to the multistep nature of the flow-through format, it gained relatively less

Fig. 2 Commercial rapid tests. (A) Determine™ HIV 1/2 Ag/Ab Combo. © 2013 Alere. All rights reserved. (B) Determine™ TB LAM Ag test. © 2013 Alere. All rights reserved. (C) QuickVue Influenza A + B test. Courtesy of Quidel Corporation. (D) Clearview® Malaria P.f. Test. © 2013 Alere. All rights reserved. (E) Directigen™ EZ Flu A + B. Courtesy of Beckton Dickinson. (F) ICON HP. Courtesy of Beckman Coulter. (G) Immuno*Card* STAT!® *E. coli* O157 Plus. Courtesy of Meridian Bioscience. (H) A multiplex lateral-flow assay. RAID™ 5 for the determination of biological threat agents. Courtesy of Alexeter Technologies.

 This journal is © The Royal Society of Chemistry 2013

Published on 08 May 2013. Downloaded by University of Cambridge on 31/05/2013 13:14:32.

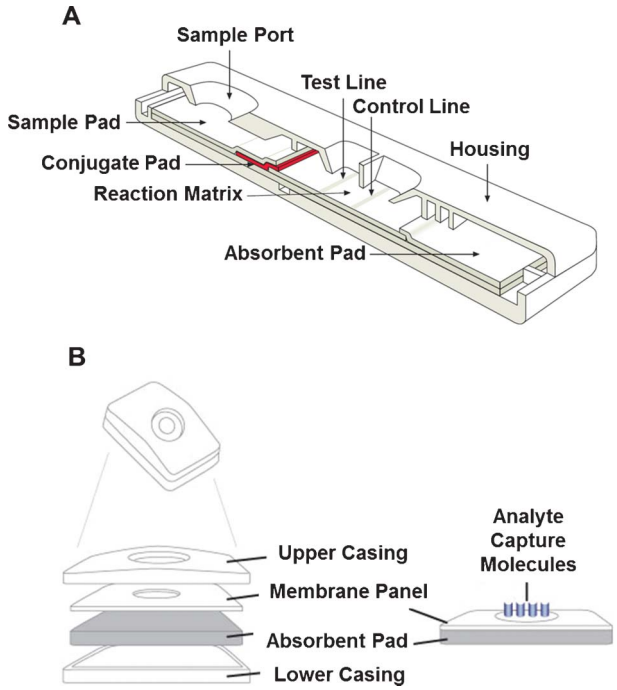

Fig. 3 Schematic view of a typical (A) lateral flow assay. Courtesy of Merck Millipore Corporation. (B) flow-through assay. Courtesy of PATH.

acceptance because of its requirement of skilled personnel to operate the devices.[97]

Sample preparation is the first step in rapid testing. Lateral flow tests are prone to matrix effects (*e.g.* from blood and urine).[98] Today, many of the existing assays require the removal of contaminants from the samples to improve detection selectivity and sensitivity, and decrease assay run time. Depending on the sample, specific components might be removed from the sample to improve the signal to noise ratio.[99] Sample preparation suffers from problems such as inhomogeneity, interfering agents, inhibitors, and reducing the viscosity of samples such as whole blood and food samples. Increasing the levels of sensitivity often requires tedious sample preparation steps, and often applies to samples with low traces of target molecules or cells. The ideal sample preparation step must be cost-effective and is potentially executed in one step. The desired outcome of the sample preparation step is concentrating the target analytes and reducing the background noise for matrix interferences.

The test process begins with introducing a sample to the proximal end of the strip where the sample pad is located. This step is often followed by addition of buffer solution to facilitate capillary flow. The sample pad then renders the sample compatible with the assay and releases the sample. The treated sample is wicked by capillary action to the conjugate pad which is previously impregnated with particulate conjugates. The sample re-mobilises the dried conjugate, and a target analyte (if present) in the sample interacts with the conjugate. Next, the sample and conjugate couples migrate to the reaction matrix, which consists of two bands where antibodies have previously been immobilised. These two bands act as a capture mechanism for the conjugate along with the analyte. Nitrocellulose has been the material of choice as the reaction matrix in lateral flow assays for the last two decades. The attractiveness of nitrocellulose relates to its ability to bind irreversibly and hydrophobically to proteins by absorption. However, unlike filter paper, commercially adopted nitrocellulose is a hydrophobic material due to its cellulose acetate blends. Therefore, the use of a nitrocellulose membrane requires the deposition of surfactants. There have been attempts to replace nitrocellulose in the diagnostics industry with other materials such as nylon, polyvinylidene fluoride and Fusion 5 from Whatman, but they have not made an impact due to high-costs, manufacturing challenges and the requirement for novel chemistry. In addition, the diagnostics industry often resists replacement of current manufacturing practices.[47] This resistance is validated by the fact that other membranes could not match the signal-to-noise ratio of nitrocellulose and therefore failed to challenge its dominant position. Table 1 shows all the components of a typical lateral flow assay and their limitations. Depending on the captured conjugate, the presence or absence of a target analyte can be interpreted by naked eye or specialised equipment. In the case of positive results in direct assays, a test line appears along with a control line where the antibody is immobilised. In the case of a negative result, the conjugated particles bypass the test line and are captured at the control line. For competitive assays, positive results are indicated when the test line is absent along with a control line.[100]

Lateral flow tests are often low-cost, lightweight, portable and require minimum sample preparation, but the growing demand for better sensitivity is challenging its current format.[97] Some examples of the requirement for high-sensitivity include cardiac markers, biothreat applications and single cell detection. For all these applications, lateral flow tests must develop novel materials and detection techniques (*i.e.* new labelling approaches). Progress in detection technologies, materials, readout devices and manufacturing techniques will increase the repeatability and sensitivity of lateral flow assays. However, all these new advances must maintain the ultimate attractiveness of lateral flow tests: Sample-to-answer in a single step.

A common misperception of the lateral-flow format is that it is neither quantitative nor can be multiplexed. While difficult, particularly on a manufacturing scale, multiplexed, quantitative, reader-based systems (or any combination thereof) are already in the market. Some examples of such readers include Sofia Fluorescent Immunoassay Analyser (multiplex assays),[18] BD Veritor™ System (multiplex tests),[17] SNAP® Reader (quantitative tests)[96] and Astute140™ Meter (multiplex and quantitative tests).[101] However, in the absence of such readers, subjective interpretation constitutes a challenge in low-infrastructure settings. Overcoming such challenges by improving the existing technologies or developing novel diagnostics could reduce the large burden of disease in the developing world.[102]

Published on 08 May 2013. Downloaded by University of Cambridge on 31/05/2013 13:14:32.

Table 1 Components of a typical lateral flow assay

Component	Function	Material	Pretreatment	Limitations
Sample pad	Modulate any chemical variability in the sample, treat the crude sample and release the assay adjusted sample	100% cotton linter, glass fibre, rayon and filtration materials	Impregnation with pH buffer, surfactants, blocking reagents, additives and drying	The potential of flooding or surface flow and the inability to adjust the pH or filter out contaminants are the major concerns
Conjugate pad	Couple the analyte in the sample with the conjugate and release the sample	Glass fibres, polyesters, and rayon	Immersion of the pad in aqueous solutions (*e.g.* proteins, surfactants, polymers), drying at high temperatures	The critical issues include variations in the uptake of pretreatment solutions, conjugates, and inconsistent binding and release of conjugates, fast/slow release of conjugate and inconsistencies in binding of conjugates to hydrophobic fibres
Reaction membrane	Facilitate as a capturing mechanism and form visible bands when analyte is present/absent	Nitrocellulose, nylon and polyvinylidene fluoride	Rewetting agents (*i.e.* surfactants), electrostatic attraction to bind proteins, deposition of test and control lines, drying at elevated temperature, blocking	Inconsistencies with reaction membranes are caused by irreproducibility, shelf life issues, flammability, vulnerable to environmental conditions (*e.g.* humidity), low tensile strength, possible scoring during manufacturing, protein incompatibility with surfactants, inconsistencies in flow characteristics due to desiccation, protein inability to bind covalently or directionally to nitrocellulose
Waste reservoir	Serve as the sink for excessive sample and prevent wicking towards the reaction membrane	100% cotton linter, high-density cellulose	None	This membrane might release the excessive fluid back into the assay and cause false positives
Backing	Keep all the components in one place, provide rigidity and facilitate easy handling	Polystyrene, vinyl (poly vinyl chloride or PVC), and polyester	Lamination and cutting	Issues include variations in component overlaps, inconsistencies in run time and fluid front conformation, tendency to curl, causing liners and adhesives to pinch or wrinkle
Adhesive	Hold the assay components in place and be compatible with proteins during storage	Diagnostic grade medium tack adhesives (*e.g.* GL187 pressure-sensitive adhesive)	None	This material might flow into components of the strip and cause hydrophobic batches, possible destabilisation of proteins, and build up excessively on blades during cutting
Cassette	Preserve the assay from environmental conditions and prevent contamination, expose the sample pad, maintain the alignment of components, indicate the position of test and control lines	Low-cost plastics	None	The sample might run out across the surface of the pad and pool inside the cassette, also the housing unit might crush the sample pad, overcompress the sample pad, causing limiting the rate of absorption

This journal is © The Royal Society of Chemistry 2013

Published on 08 May 2013. Downloaded by University of Cambridge on 31/05/2013 13:14:32.

1.3 The origins of paper-based microfluidics and their advantages

Impregnating paper strips with hydrophobic materials such as paraffin and wax to prevent cross contamination of reaction zones dates back to 1902.[103] The first fabrication technique for the impregnation of paper with paraffin to create confined spaces for qualitative spot testing appeared in 1937.[104,105] Fig. 4A illustrates the earliest paper-based device. Formation of paper plates in filter paper prevented spreading of the spot over a large surface. Forming confined spaces also allowed uniformity in both area and tint of the spot, thus enabling the estimation of the concentrations from the intensity of colouration. Paraffin wax was suggested for the formation of water-repellent zones on filter paper due to its general inertness to chemical reagents and its practicality for the formation of diverse patterns. In this case, an embossing tool or dye comprising a metal tube is warmed and dipped into paraffin, which is transferred to a sheet of filter paper to form uniform rings. By this method, paraffin can be embedded in filter papers as a series of confined absorbent areas in a one-step process. The area over which the paraffin wax spreads could be controlled by varying the temperature of the printing tool, the pressure, the time of contact and the pore size of the filter paper. A diagnostic application comprising the detection of the concentrations of nickel and copper salts was demonstrated. Further, a wax impregnated assay was proposed for the determination of pH, water testing and biological analyses for the composition of urine and blood. Later, General Motors (Warren, Michigan) adapted these assays for the analysis of micro samples of the major elements and for the analysis of trace amounts of elements.[106]

Following these studies, in 1949, filter paper was impregnated with paraffin to demonstrate preferential elution of pigment mixtures (Fig. 4B).[107] In this study, a custom die was fabricated, whence a piece of paraffin paper was placed on top of a filter paper and the heated die was pressed on the paraffin paper. The progress of elution was monitored as each fraction passes a beam of monochromatic light. The advantages of using confined patterned channels were also realised: speeding up the diffusion process and working with smaller quantities by reducing the reagent consumption. However, realisation of the wax impregnation technique required complex fabrication techniques, again failing to receive attention from the diagnostics industry. Instead, the diagnostics industry has continued to generate solutions for the cross contamination issues of dipstick tests.

Considerable time has been devoted to attempts to curtail the run over between adjacent reagents in dipstick tests. Much of the emphasis has been directed to three basic concepts in preventing cross contamination: These are (1) forming hydrophobic barriers between reagent zones,[92,108–115] (2) absorbing runover liquid by bibulous layers placed beneath reagent bearing layers,[116] and (3) physically separating adjacent reagent zones.[117] Proposed barriers comprised of materials that are impervious to water such as ethyl cellulose, silicones, polystyrene, rosin, waxes, paraffin, printer varnish and cellulose esters. Impregnation with wax prevented cross contamination of reaction zones in dipstick assays. As an alternative to forming hydrophobic barriers, test device carrier matrices which comprise of absorbent underlayers, were fabricated to prevent runover from one matrix to another.[116] In addition, coating the base support with a hydrophobic

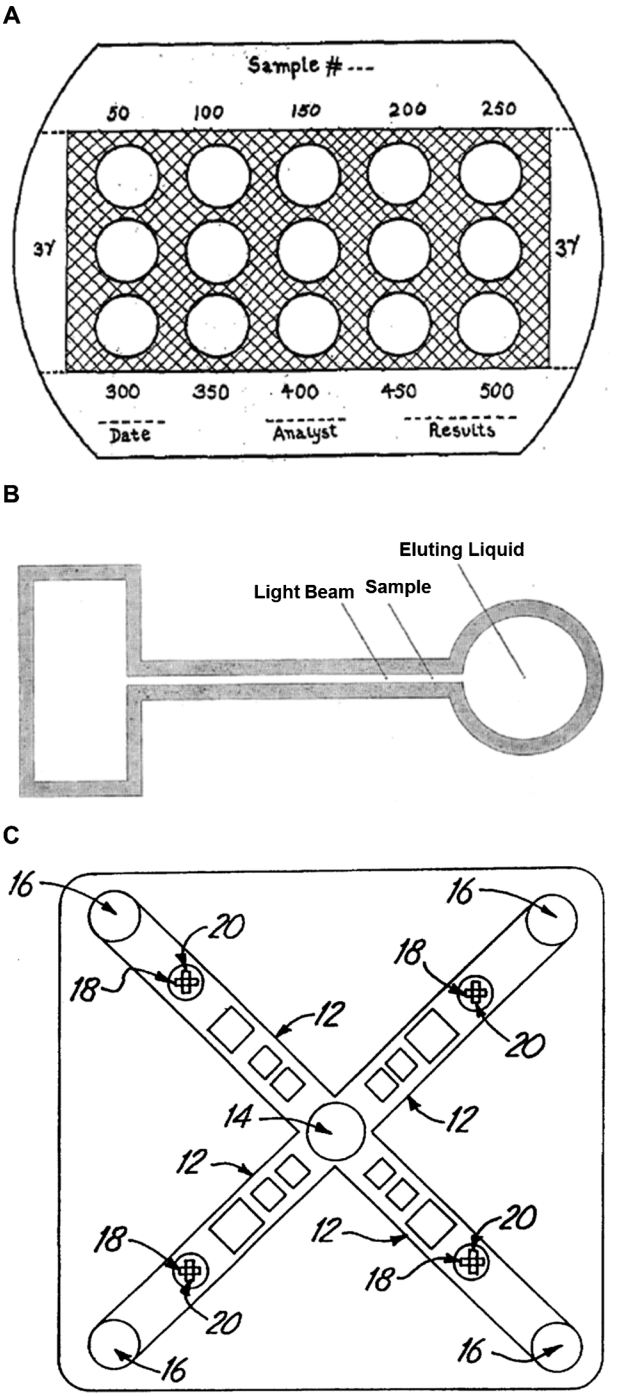

Fig. 4 Schematics of the earliest paper-based formats and wax impregnation of paper. A) Formation of water-repellent zones in filter paper and by paraffin printing. Adapted with permission from ref. 104. Copyright (1937) American Chemical Society. B) Automatic paper chromatography. Adapted with permission from ref. 107. Copyright (1949) American Chemical Society. C) A device for simultaneously performing multiple competitive immunoassays. Adapted with permission from ref. 118.

Published on 08 May 2013. Downloaded by University of Cambridge on 31/05/2013 13:14:32.

material to increase the contact angle, was also used.[117] There were also two-dimensional assays which were capable of performing simultaneously a plurality of immunoassays to detect the presence of analytes in a sample (Fig. 4C).[118]

In addition to the developments outlined above, over the last two decades, microfluidics has made some progress from clean rooms towards being real world products.[119] Microfluidics has been proposed as a suitable technology for point-of-care diagnostics.[120–123] The need and requirement for cost-effective microfluidic-based diagnostics has also been expressed, but deployment of such diagnostics to the developing world faces design, cost-effectiveness and manufacturing challenges.[124,125]

2. The prospects for paper-based microfluidics

2.1 Materials

Is paper a material overlooked by diagnostics manufacturers for decades? Can paper overcome the limitations of nitrocellulose such as hydrophobicity? Can an entire analytical assay be built upon a single material such as paper? If so, can paper meet the performance requirements and reduce costs to manufacturers? All these questions need to be addressed in order to exploit paper for diagnostics devices. Here, we evaluate the notion of adapting paper as a replacement for all the solid phase materials currently used in lateral flow assays. To be a competitive material, paper-based assays must meet the following requirements: (i) process biological samples in small volumes, (ii) complete the test within a short duration and (iii) comparable to existing nitrocellulose-based assays in specificity and sensitivity. In addition, paper must provide sufficient protein binding to allow the formation of sharp and intense capture lines or zones while keeping the level of nonspecific background low.

Chemistry of paper. Paper is a thin sheet of material that is produced by pressing together cellulosic fibres. Paper can be made from many raw sources such as wood (printing paper), cotton (filter and chromatography papers), jute, flax (linen), hemp, bamboo, ramie, sisal, bagasse, grass and straw. Today, wood constitutes 90% of the raw material in the industry due to the fact that processing of non-wood plants is more costly.[126] A high-concentration of lignin in wood causes paper to discolour and eventually self-destruct.[127] Lignin consists of chromophores and thus, paper made from 100% cotton is desirable in diagnostics applications. Historically, nitrocellulose is produced through esterification of cellulose with a nitrating acid (*i.e.* sulphuric acid and nitric acid) (Fig. 5).[128] Sulphuric acid serves as a catalyst to produce the nitronium ion and the degree of esterification is controlled by the concentration of water in the reacting mixture. The solubility and flammability is determined by the degree of nitration. In theory, during esterification, all three OH groups can be replaced by nitro (NO_2) groups that results in cellulose trinitrate (14% nitrogen). However, most nitrocellulose compounds are dinitrates (1.8–2.8 nitro groups) leading to 10.5–13.5% nitrogen.[129] For example, Protran nitrocellulose membranes (Whatman) have a degree of substitution of hydroxyl groups in the range of 1.9–2.4 after nitration.[130] When the degree of esterification is high (nitrogen content $> 12.6\%$), nitrocellulose is referred to as guncotton.[129]

Physical characteristics of paper. In this section, we explain the properties of paper for microfluidic applications: surface characteristics, surface area, capillary flow rate, pore size, porosity and thickness. The selection of the grade of paper depends on the application of the assay. There is no single type of paper that can possess the desired characteristics for all applications. Commercial paper grades often differ in porosity, particle retention and flow rate. Filter and chromatography papers are manufactured using high-quality cotton linters with a minimum α-cellulose content of 98%. The majority of filter papers are designed for general filtration and exhibit retention levels down to 2.5 μm.[131] These filter papers come in different degrees of purity, hardness and chemical resistance.

In paper-based microfluidics, most of the studies have exploited chromatography and filter papers, although some investigators also explored unconventional paper types and their chemically modified grades. Due to their low porosity and surface tension effects, printing paper has been shown not to be a suitable material for constructing hydrophilic channels for liquid transport.[132] On the other hand, high porosity might be a drawback due to uncontrolled diffusion of hydrophobisation materials. For example, filter papers with larger pore sizes than the standard grade can swell their cellulose fibres and constrain the capillary flow. In addition, studies investigating kitchen towels showed that the diffusion of hydrophobisation materials is uneven and incomplete.[132]

The surface area of the paper is critical due to its impact on reagent deposition, sensitivity, specificity and reproducibility. When other parameters are kept constant, the surface area declines nonlinearly with pore size, increases nonlinearly with porosity and increases linearly with thickness.[133] The internal surface area of porous membranes is given as $m^2\ g^{-1}$ of polymer. The surface area ratio can be calculated by multiplying the internal surface area by the basis weight. Surface area is expressed as m^2 internal surface area/m^2 frontal area. Commercially available immunochromatographic assays have surface area ratios of 50–200.[134]

Capillary flow rate is another important parameter for paper-based microfluidics. It is defined as the migration speed of a sample front moving along the length of the membrane strip. The capillary flow rate is a key parameter in the performance of the assay due to the fact that the effective concentration of the analyte present in the sample is inversely proportional to the square of the change in the flow rate.[134] The capillary flow rate is critical in achieving consistent sensitivity depending on the location of the detection line/zone. When the test line/zone is placed furthest from the inlet, the analyte will be slower as it passes through the capture line. Measuring capillary flow rate is not a preferred parameter in the industry as speed decays exponentially when the fluid front travels along the membrane.[134] Instead, capillary flow time is measured. This parameter is the time required for the sample to move along and saturate the membrane with a defined length. Capillary flow time is inversely related to the flow rate

 This journal is © The Royal Society of Chemistry 2013

Published on 08 May 2013. Downloaded by University of Cambridge on 31/05/2013 13:14:32.

and it is implicitly related to the performance of the assay.[134] It can be expressed in s cm^{-1}.

Pore size and pore size distribution are important parameters in selecting porous materials for the construction of microfluidic devices. The pore size (nominal or absolute) relates to the size of particles retained by the filter.[135] Traditionally, membranes are characterised based on their nominal pore size. Nominal size is the diameter of the largest pore in the filtration direction. Determination of pore size experimentally is accomplished by forcing hard particles through the membrane. Due to the complexities and impracticalities associated with this technique, the bubble point[136] is adopted as an alternative experimental parameter to determine the pore size. Experimental determination of the bubble point consists of forcing air (or isopropanol) through a wetted substrate and measuring the pressure requirement. The bubble point is predominantly governed by the diameter of the largest pore in the membrane, and therefore this correlation can be used in the development of the membranes to infer the pore size. The correlation between bubble point and largest pore size is linear for pore sizes between 0.1 μm and 3 μm, but the relationship is more complex for pore sizes greater than 3 μm.[134] For membranes with large pore sizes, this correlation is not a reliable parameter to control the consistency of the membranes. The pore size is not an accurate indicator for estimating the flow rate due to the fact that the pore size corresponding to the bubble point is located at the high end of the distribution. The pore size distribution (PSD) defines the range of pore sizes in the membrane and it determines the capillary flow rate as a function of the aggregate pore size. PSD is useful in distinguishing membranes with identical pore size ratings.

Porosity is another parameter that is defined as the volume of air in the 3D membrane structure.[133] Not to be confused with pore size, porosity is an independent parameter that is not correlated with the pore size. It is traditionally defined as the void volume of the membrane. This can aid in estimating the total volume of sample required for wet-out. When pore size distribution and thickness are kept constant, the capillary flow rate increases linearly as the porosity of the membrane increases. Porosity is considered a key parameter due to its influence on the capillary flow rate.

Paper thickness also influences the following parameters: (i) bed volume, (ii) tensile strength and (iii) signal visibility. Bed volume is the total accessible volume of the membrane for the sample and it is a function of membrane dimensions and porosity. As the thickness increases, the bed volume also increases. In paper-based microfluidics, bed volume is especially important in the absence of an absorbent pad since it determines the total amount of sample wicked up. Alterations in the bed volume can also make an impact on the width of the test and the control lines. For example, the spread of the reagents on a thin sheet of paper is greater than on thicker paper due to restricted downward penetration of the reagents. When the capture reagents spread over a wide area, the diffusion of the detector reagents will be the same. Thus, lower colour intensities and sensitivities will be attained. As the paper thickness increases, the absorption of the sample also increases, thus eventually altering the mass of the analyte that passes to the capture line. In addition, although the detector reagent bound in nitrocellulose membranes is not visible deeper than 10 μm from the surface due to the opacity of nitrocellulose, paper might provide an improved signal visibility.[134] The visibility of the signal is a function of the thickness and the opacity of paper. The percentage of visible signal[134] can be expressed as the following (eqn (1)).

$$\%\ \text{visible signal} = \frac{\text{visible depth}(\sim 10\ \mu\text{m})}{\text{membrane thickness}} \quad (1)$$

If the paper thickness is too thin, it might break during high-speed manufacturing. In paper-based microfluidic devices, paper is utilised as a reaction matrix and is often non-laminated. Therefore, paper thicknesses <50 μm might be impractical during routine processing unless they are covered with laminating sheets. During in-line roll-to-roll manufacturing, the equipment used to manufacture the strips should not exceed the wet/dry tension limit of the chosen paper.

The colour of the paper is important because it plays a role in image analysis. Paper should be white, preferably with no tinge or hue. Paper tends to turn yellowish to brownish upon prolonged storage due to exposure to humidity, high temperatures and sunlight. Acceptable limits of colour decay must be identified and compensated for during the readout.

Paper as a component of a lateral flow test. In this section paper is evaluated as a sample pad, conjugate pad, reaction matrix and absorbent pad. Paper might be adapted to adjust the pH, filter out the unwanted interfering analytes and, for blood samples, to separate red blood cells (RBC) from the plasma. The ideal blood separator should be capable of separating the red blood cells from the plasma with an efficiency comparable to conventional centrifuges.[137,138] In lateral flow tests, the historic material choice for blood separators has been glass fibre. It works effectively as a blood separator and is capable of attracting RBCs to the surface and trapping them within the depth of the matrix. For paper-based microfluidics, there have been two different approaches to separate RBC from the plasma: (i) agglutination of RBCs and (ii) adapting a commercial separation membrane.

The first attempt used chromatography paper as a substrate to induce RBC agglutination. Antibodies (anti-A,B) were spotted onto a paper substrate and resulted in large aggregates which could not pass through the pores of the paper, whence the RBC could be filtered out and the plasma separated.

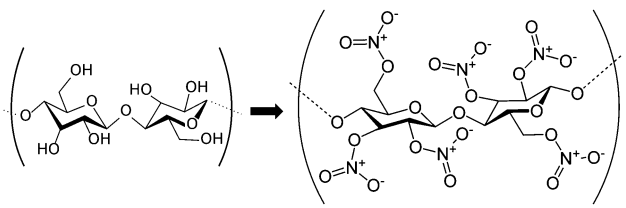

Fig. 5 Esterification of cellulose with nitrating acid to produce nitrocellulose.

Published on 08 May 2013. Downloaded by University of Cambridge on 31/05/2013 13:14:32.

However, this technique can only be used for A, B or AB blood types, but not for blood type O, which is 44% of the human population.[139] Given the fact that people with O blood types cannot use the assay, this method has limited applicability for designing rapid tests. Another paper-based microfluidic device assembly included Whatman plasma separation membranes (*e.g.* LF1, MF1, VF1 and VF2). In this study, chromatography paper and blood separation membranes were sealed using a wax dipping method (see section 2.2).[140] Although this assembly method is not compatible with other fabrication techniques (*e.g.* wax printing), it stands out as a robust and amenable method for mass manufacturing. Other studies describing lateral flow assays adapted GX PSM and Pall Vivid GX plasma separation filters[141] from the Pall Corporation.[142,143]

The function of the conjugate pad is to capture the coloured colloidal particles and dry them on the pad without damage. When the sample flows through this pad, it releases the coloured colloidal particles in a controlled manner. However, these particles can aggregate permanently when they touch each other. The common characteristic of colloidal particles is that they are negatively charged hydrophobic particles coated with antibodies to enable capturing the target analyte. An ideal conjugate base should be negatively charged and be hydrophilic, thus allowing the facile release of the conjugates from the matrix.[97]

The characteristics of an ideal reaction matrix are consistency throughout the surface pore size, thickness, protein binding capacity, flow characteristics, defined test lines and stability on storage. In order to fabricate rapid tests with consistency, the membrane must irreversibly capture reagents at the detection zones such as test and control lines. The material from which the substrate is made plays a critical role in the binding characteristics. When the assay is run, protein binding properties should not be altered. Protein binding capability of the membrane is dependent on the paper surface area available for immobilisation. The most important asset of paper is that it is hydrophilic in nature. However, paper requires chemical activation to immobilise antibodies. Many key concerns have been expressed about the performance characteristics of paper by members of the *in vitro* diagnostics industry.[47] Colloidal gold and latex labels used in the industry require more open pore materials such as glass fibre and polyester in which to be stabilised and from which to be released. Surface quality is another key parameter in optimising the performance of paper-based microfluidics. Paper has relatively rough surface characteristics, and not surprisingly, this poses a challenge for quantitative measurements.

Historically, paper is adapted as an absorbent pad: however, in the absence of an absorbent pad, the volume of sample analysed is determined solely by the bed volume. In this circumstance, if the capture line is located further from the origin, the volume of sample analysed decreases. This also affects the quantity of analyte and detector reagent complex captured. Locating the line closer to the origin can improve kinetics. Other options include using thicker paper matrices or stacking paper layers on top of each other.

2.2 Fabrication techniques

Paper-based microfluidics can be fabricated in 2D or 3D to transport the fluidics in both the horizontal and vertical dimensions depending on the complexity of the diagnostic application. Fabricating paper-based microfluidic devices can be subdivided into two general categories: (i) physical blocking of pores[140,144] and (ii) two-dimensional shaping/cutting.[145–148] Table 2 provides with an overview of the fabrication techniques.

Wax patterning. Constructing hydrophobic barriers in a paper matrix is a simple way to prevent mixing of detector reagents and achieve multiplexed assays. These devices are known as microfluidic paper-based analytical devices (μPADs). Of the current approaches, wax-based fabrication techniques have proved amenable to laboratory-scale manufacturing of paper based microfluidic devices since they are low-cost methods that use non-toxic reagents. Examples of wax patterning methods include: wax (i) screen printing, (ii) dipping and (iii) printing. In wax screen printing, solid wax is rubbed through a screen onto a paper sheet,[144] the paper is placed on a hot plate (or oven) to allow the wax to melt and diffuse into the paper, thus forming hydrophobic barriers (Fig. 6A). Another method that eliminates the necessity for complicated instrumentation is wax dipping (Fig. 6B).[160] This fabrication technique requires an iron mould that can be formed by laser cutting. The pattern can be transferred onto a piece of paper by dipping an assembled mould (sealed by magnets) into molten wax. The optimum temperature and dipping time are 120–130 °C and 1 s, respectively. Although, both wax dipping and screen printing do not require high-cost fabrication equipment, they suffer from inflexibility in patterning and low reproducibility between batches. A recently explored technique involved wax printing (Fig. 6C).[155,156] A sheet of paper is fed into a wax printer and then processed by a heat cycle (heated on hot plate or oven). This process can be completed within a few minutes, and is capable of producing 10 s to 100 s of copies of devices. As in the case of modelling the fluid movement, Washburn's equation can be used to predict the spreading of molten wax and the final width of hydrophobic barriers in paper substrates (eqn (2)).[156,162]

$$L = \sqrt{\frac{\gamma D t}{4\eta}} \tag{2}$$

where L is the distance covered by the wax front, η is the viscosity, γ is the effective surface tension, D is the average pore diameter and t is the time. It should be noted that the viscosity of molten wax is a function of time and exposed heat. Therefore, the characteristics of final hydrophobic barriers to be formed in a paper substrate are defined by the initial deposited wax on paper.[156] The inner width of the hydrophobic channel can be defined as the following:

$$W_C = W_P - 2L \tag{3}$$

where W_C is the inner width of the hydrophobic channel, W_P is the inner width of the printed channel, and L is the additional distance that the wax spreads perpendicular to the length of

 This journal is © The Royal Society of Chemistry 2013

Published on 08 May 2013. Downloaded by University of Cambridge on 31/05/2013 13:14:32.

Table 2 Methods for fabricating 2D paper-based microfluidic devices

Fabrication technique	Substrate	Equipment	Consumables	Limitations
Photolithography[6,149]	Chromatography paper	Lithography equipment, UV lamp printer, hot plate	SU-8 photoresist, organic solvents	Vulnerable to bending Clogs paper pores due to SU-8
Silane and UV/O_3 patterning[150]	Filter paper	Quartz mask, clamps, mercury lamp, UV cleaner	Octadecyltrichlorosilane, organic solvents, nitrogen stream	Requires organic solvents Needs a customised mask Requires assembly of components for each batch Consumes time during UV exposure
PDMS printing[151]	Filter paper	Desktop plotter	PDMS	Inconsistent control over hydrophobic barrier formation Requires a curing step
Inkjet etching[152,153]	Filter paper	Modified inkjet printer	Polystyrene, organic solvents	Uses organic solvents Requires multiple printing steps
Plasma treatment[154]	Filter paper	Customised masks, hot plate or oven, vacuum plasma reactor	Alkenyl ketene dimer, solvents	Demands a customised mask is to create different patterns
Wax printing[155,156]	Filter and chromatography papers	Xerox ColorQube 8570 (printer: ~$650), hot plate	Wax cartridges (single unit: $62)	Unstable at high-temperatures
Alkenyl ketene dimer (AKD) printing[157]	Filter paper	Modified inkjet printer	AKD, solvents	Requires a heating cycle
Screen printing[144]	Filter paper	Customised masks	Solid wax	Inconsistent deposition of wax/ink deposited through the mask renders low resolution
Flexographic printing[158]	Chromatography and clean room papers	Commercial printing equipment	Polystyrene, solvents	Requires frequent cleaning to avoid contamination Printing quality depends on smoothness of paper surface Requires sequentially printing layers
Subtractive laser treatment[159]	Parchment paper	CO_2 laser cutting and engraving system	None	Requires specialised laser equipment Fluid flow is limited and requires coating to allow fluid flow.
Wax dipping[140,160]	Filter paper	Customised masks, heating unit	Solid wax	Inconsistent between batches due to the variation in dipping time
Computer controlled knife shaping[145,146] and CO_2 laser cutting[148]	Chromatography paper and nitrocellulose	X–Y plotter or CO_2 laser.	None	Wastes raw material Yields low-mechanical stability
Printed circuit technology[161]	Filter paper	Desktop printer, thermal transfer printer, printed circuit board, electric iron	Sheet copper, ferric trichloride water solution, paraffin	Requires multistep processes

the channel. Here, L is a function of time, heat and the porosity of paper. The assumptions of this model include (1) the heat source has a constant temperature and it is uniform across the surface of the plate, (2) the distance that the wax spreads in the paper from the edge of the printed line is constant, (3) the viscosity of the wax does not change, (4) the amount of wax is not limiting and (5) natural convection is negligible.

In wax impregnation techniques, features sizes vary depending on the method of fabrication, but the typical size for a hydrophilic channel or assay region ranges from 0.5 mm to 4 mm (the average width of a channel is ~1–2 mm) and the typical width of a hydrophobic barrier is ~1 mm (Fig. 8A–C). A

Published on 08 May 2013. Downloaded by University of Cambridge on 31/05/2013 13:14:32.

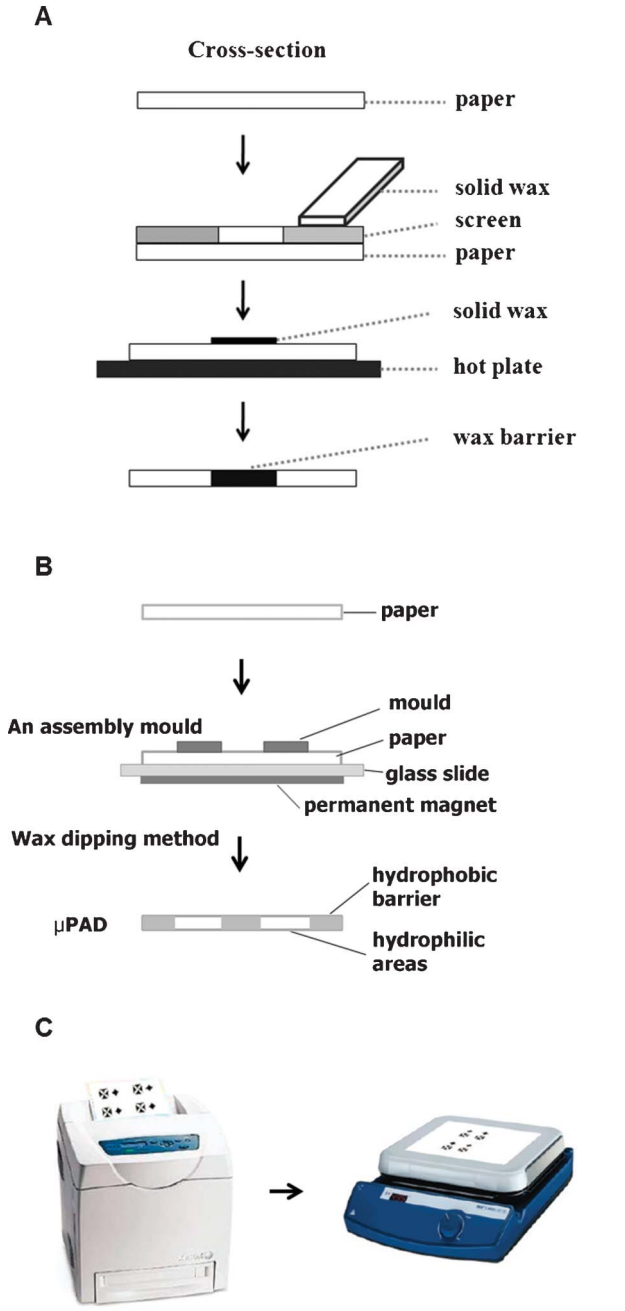

Fig. 6 Fabrication techniques for paper-based microfluidics. (A) Screen printing. Adapted with permission from ref. 144. Copyright (2011) RSC publishing (B) Wax dipping. Adapted with permission from ref. 160. Copyright (2011) Elsevier. (C) Wax printing. A hydrophobic barrier penetrates through the thickness of the paper to create a hydrophilic channel. Adapted with permission from ref. 156. Copyright (2009) American Chemical Society.

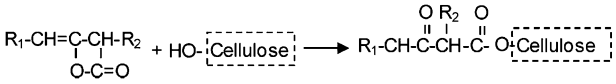

Fig. 7 The reaction of alkyl and alkenyl ketene dimers with cellulose. Adapted with permission from ref. 157. Copyright (2010) Elsevier.

detailed comparison of features sizes in relation to wax-impregnation methods is available.[163] A significant weakness of 2D wax impregnated microfluidic devices is that the assays require being suspended in the air during wicking to prevent mixing of reagents. In addition, ambient (hot) air conditions and long-term storage in the developing world may cause wax to melt, thus deforming the channels.

Alkyl ketene dimer (AKD) printing. The selective hydrophobisation of paper using cellulose reactive hydrophobisation agents is another way of fabricating paper-based microfluidic channels.[154,157] The fibre surface can be chemically modified by applying cellulose reactive agents to paper. Such reagents tend to react with the OH groups of cellulose, leading to imparting hydrophobicity to the cellulose fibres (Fig. 7). Modified inkjet printing was exploited to deposit an alkyl ketene dimer, followed by a curing step to create hydrophilic-hydrophobic contrast patterns. Digital patterns are printed using alkenyl ketene dimer and heptane solution (5% (v/v)). However, the printed samples must be heated in an oven at 100 °C for 8 min to cure the alkenyl ketene dimer. Channels with a width of up to 300 μm can be achieved (Fig. 8D). Hydrophobic channels sustain a contact angle of 110–125° with water. In this technique, printed hydrophobic patterns are invisible to the naked eye, and the paper substrate also retains flexibility. Forming paper-based microfluidic devices by alkyl ketene dimer printing has potential for scaling up for commercial use.

Flexographic printing. Flexographic printing of polystyrene enables direct roll-to-roll production of paper-based microfluidics.[158] First, a substrate paper is fixed to an impression roll. The required amount of ink is applied to the ink reservoir, followed by transferring the polystyrene solution onto an anilox roll (a hard cylinder) with microfluidic patterns. The excess polystyrene solution from the anilox can be removed by a blade. The anilox then distributes the polystyrene solution onto the printing plate comprising relief patterns. Eventually the system prints the patterns on the paper substrate. The speed of printing can be controlled by accelerating or decelerating the anilox. The pressure between the plate roll and the impression roll is optimised to achieve ink penetration into the paper. However, one-step printing is not enough to penetrate the ink into the paper substrate to form hydrophobic barriers. For this reason, a 5% (w/v) solution of polystyrene in xylene was printed as a uniform layer on the backside and the patterned layer was printed on the front side. Notably this method requires at least two sequential printing cycles to obtain waterproof barriers. The nominal width of the channel obtained by this method is 1 mm (Fig. 8E). Because flexographic printing is based on existing manufacturing techniques, it is compatible with large-scale production, with printing speeds up to 60 m min^{-1}.

Two-dimensional shaping/cutting. While there are compelling attributes of wax-patterned paper, cut paper channels affixed to suitable plastic cassettes offer benefits. There are two ways of forming 2D paper and nitrocellulose networks: (i) computer controlled X–Y knife plotters[145,146] and (ii) CO_2 laser cutting (for nitrocellulose).[147] The earliest demonstration was shaping paper or nitrocellulose in two dimensions using a

 This journal is © The Royal Society of Chemistry 2013

Published on 08 May 2013. Downloaded by University of Cambridge on 31/05/2013 13:14:32.

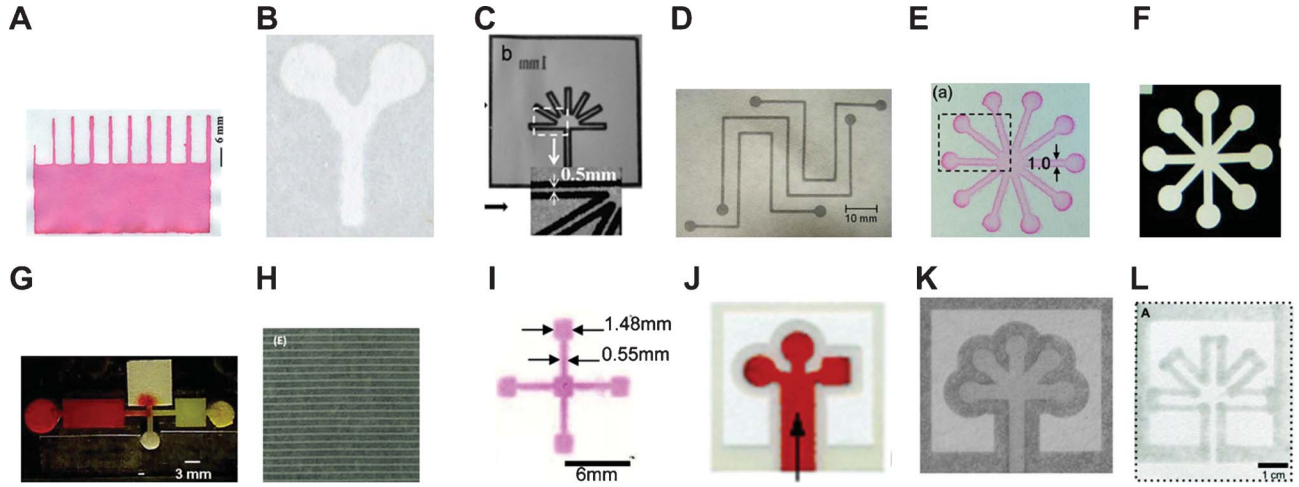

Fig. 8 Fabrication of paper-based microfluidic devices. (A) Wax screen-printing. Adapted with permission from ref. 144. Copyright (2011) RSC publishing (B) Wax dipping. Adapted with permission from ref. 160. Copyright (2011) Elsevier B.V. (C) Wax printing. Adapted with permission from ref. 155. Copyright (2009) WILEY-VCH Verlag GmbH & Co. (D) AKD printed paper-based microfluidic patterns. Adapted with permission from ref. 157. Copyright (2010) Elsevier B.V. (E) Flexographic printing. Fluidic structures formed into chromatography paper and clean room paper. Adapted with permission from ref. 158. Copyright (2010) American Chemical Society (F) Computer controlled knife shaping. Adapted with permission from ref. 146. Copyright (2009) American Chemical Society (G) CO_2 laser cutting. Adapted with permission from ref. 195. Copyright (2011) Springer-Verlag (H) Laser treatment. Adapted with permission from ref. 159. Copyright (2011) RSC publishing (I) Inkjet etching of poly(styrene) with toluene on paper. Adapted with permission from ref. 152. Copyright (2008) American Chemical Society (J) Chromatography paper patterned with photoresist. Adapted with permission from ref. 6. Copyright (2007) Wiley-VCH Verlag GmbH & Co. (K) FLASH. chromatography paper by printing the pattern with an ink-jet printer. Adapted with permission from ref. 149. Copyright (2008) RSC publishing (L) A microfluidic system based on PDMS printed in filter paper. Adapted with permission from ref. 151. Copyright (2008) American Chemical Society.

computer controlled X–Y knife plotter. The device comprises of a knife that rotates on a turret, thus allowing the cutting different shapes and fine features (Fig. 8F). When the blade angle and downward force are adjusted, a variety of porous substrates could be cut with a single pass of the knife. However, when paper is being cut, it is necessary to have at least three sequential overlapping cuts to prevent tearing of the paper. In CO_2 laser cutting of nitrocellulose, lateral dimensions down to 1.5 mm can be achieved (Fig. 8G).[147] After the cutting process, unwanted sections must be removed. These devices might find applications in specialised point-of-care applications where resources may be more accessible than in resource-poor environments, and where the cost of the diagnostic device is less of a concern. These types of microfluidic devices are analogous to current lateral-flow assays, but the microfluidic component offers the potential for more sophisticated capabilities than have been available previously. Since nitrocellulose can also be used in these devices, the components of standard lateral-flow formats can be incorporated easily, thus offering a lower barrier to market than devices made entirely out of paper. It should be noted that these devices are not mechanically rigid relative to wax-printed paper channels and therefore require vinyl or polyester plastic films as backing or sealing substrates. The packaging reduces evaporation and protects the assay from contamination. A drawback of such a technique is the resulting high-cost device.

Other fabrication methods. Investigators also experimented with a number of methods that were soon replaced with those listed above. These methods include two methods based on photolithography,[6,149] silane and UV/O_3 patterning,[150] PDMS printing,[151] inkjet etching,[152,153] plasma treatment (using a screen),[154] printed circuit technology[161] and subtractive (dehydrophobization) laser treatment (Fig. 8H–L).[159] These laboratory-scale fabrication techniques failed to prove amenable for mass manufacture due to their multistep nature and relatively high cost.

Three-dimensional (3D) paper-based microfluidics. These devices are analogous to the flow-through rapid tests already in the market. 3D devices are advantageous for certain applications because they (i) accommodate more assays on the same footprint of a device than a 2D device; (ii) enable fluid movement in three dimensions through multiple layers of paper, which opens the potential for multi-step assays in a compact device; and (iii) move fluid through the thickness of paper (the *z*-direction) and laterally (the *x*-,*y*-plane). This latter characteristic minimises the quantity of sample that is lost in swelling the paper, increases distribution times and decreases the necessary sample volume for an assay.

Maintaining contact between hydrophilic features in each layer of a 3D paper-based microfluidic device is the key fabrication challenge for these devices. There are two general methods for achieving this goal. They include: (i) affixing one layer of paper to another in an ordered, layer-by-layer manner; and (ii) assembling all layers and then applying an outer clamp, adhesive, or protective coating to hold the layers in contact with one another. The first approach was used in the original method for fabricating 3D paper-based microfluidic devices.[164] In both approaches, reagents are deposited onto individual layers before assembling the final 3D device.

This original method uses alternating layers of patterned paper and patterned double-sided adhesive tape.[164] Holes are

Published on 08 May 2013. Downloaded by University of Cambridge on 31/05/2013 13:14:32.

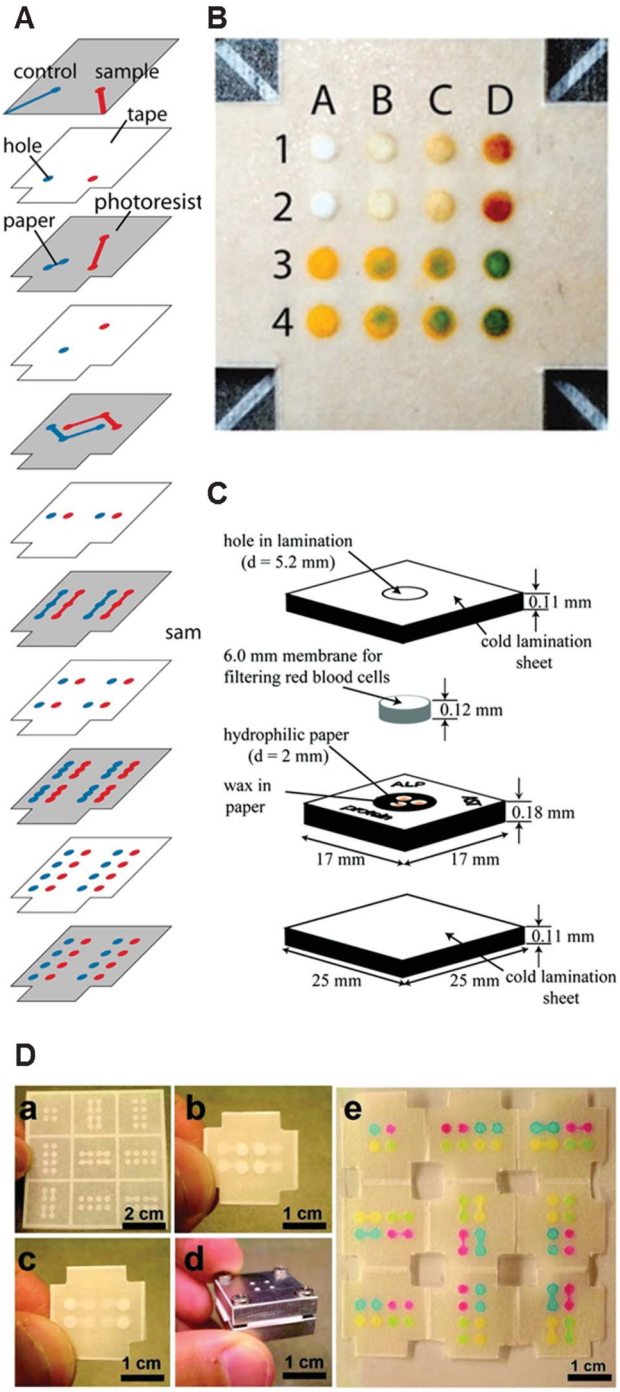

Fig. 9 Three-dimensional microfluidic devices. (A) Schematic of the layers for the construction of a three-dimensional microfluidic device. Adapted with permission from ref. 164. Copyright (2008) National Academy of Sciences, USA (B) The final colourimetric assay for glucose and proteins were prespotted in the detection zones. Adapted with permission from ref. 164. Copyright (2008) National Academy of Sciences, USA (C) Design of a flow-through device. Adapted with permission from ref. 142. Copyright (2012) American Chemical Society (D) Three-dimensional paper-based device assembled using the principles of origami, also called. Adapted with permission from ref. 166. Copyright (2011) American Chemical Society.

cut in the tape in locations that match the desired hydrophilic features in the layers of patterned paper. The holes are then filled with cut paper to create hydrophilic connections between layers of paper (Fig. 9A and B). This type of 3D device is useful for prototyping new technologies in paper-based microfluidic devices, but the tedious assembly method might not be amenable to mass production. An alternative assembly strategy uses hydrophilic spray adhesive (rather than double-sided adhesive tape) to glue layers of patterned paper together.[165] This approach works well in a laboratory setting, it is rapid (minutes are required to assemble a device) and enables the fabrication of 10 s to 100 s of 3D devices simultaneously. The second method involves layering pieces of paper on top of one another and then using cold lamination techniques to hold the layers together and seal the devices (Fig. 9C). This approach has only been demonstrated on 3D devices containing only a few layers of paper, so questions remain on its feasibility for more layers.[142,143] Inspired from the traditional Japanese art of paper folding, Origami, a related approach involves layering or folding patterned paper into a 3D stack (*o*PAD), and then using a pre-fabricated clamp (or lamination) to hold the stack together (Fig. 9D).[166,167] Incorporating folding into the design also enables devices that can be opened and altered during the course of an assay or sample preparation step.[168] However, such a procedure raises questions of reproducibility and safety when individuals with different skill sets are manipulating devices containing potentially biohazardous waste. Despite obvious capabilities of paper-based microfluidics in fluid manipulation, quantitation and multiplexed detection, these assays have received criticism from the rapid diagnostics industry based on the innate inconsistency of the paper matrix, their complex fabrication procedures and limited reproducibility. In addition, cloth-based substrates,[169] threads[170–172] and silk fabric[173] (*i.e.* weaving) were reported to be low-cost materials in fabricating 3D microfluidic devices. However, the reproducibility of the assays using these materials is under debate.

Packaging. Enclosing a capillary-based microfluidic device can overcome the following limitations: (i) potential contamination in the transportation or operation steps, (ii) impact of evaporation on the reagents and the sample caused by limited wicking or increasing the time required for the assay to saturate, (iii) contamination or leakage of samples when the assay contacts with any surface and (iv) susceptibility to light. Enclosed paper-based microfluidics can also protect reagents and ease handling to achieve robust assays. There are a number of ways to seal or enclose paper-based microfluidic devices and prevent the issues created by open channels. Traditionally, lateral flow assays are backed by a plastic membrane and enclosed with a plastic housing (Fig. 3A). Further considerations in developing sealing applications for paper-based microfluidics should consider the potential impact on the wicking properties and the flux of fluid flow. Furthermore, these assays should employ sealing materials that are disposable and compatible with paper or nitrocellulose and sensors.

Pressure-sensitive tapes. The first impermeable layers adopted to seal paper-based microfluidics were pressure-sensitive tapes.[164] These tapes display poor adhesion when

 This journal is © The Royal Society of Chemistry 2013

Published on 08 May 2013. Downloaded by University of Cambridge on 31/05/2013 13:14:32.

the channels are wet and at slightly higher ambient temperatures, the pressure-sensitive adhesive diffuses into the paper and reagent zones, thereby severely affecting their consistency in flow. Also, conventional pressure-sensitive tapes cannot provide the required initial tack and residual bond when the assay is wet. For this reason, diagnostic grade medium tack adhesives (*e.g.* GL187 pressure-sensitive adhesive, Lohmann) should be used in these devices. Such biocompatible acrylic adhesives have been adopted by the *in vitro* diagnostics industry.[174]

Toner sealing. In order to prevent natural convection and control the moisture content within the assay, paper can be sealed using commercially available laser toners. Toner sealing is an assembly technique that does not require the use of thick plastics or pressure-sensitive adhesives in the enclosure of 2D paper-based microfluidic devices.[175] Using a laser printer, multiple layers of toner are deposited on the paper, which creates a thin layer of plastic that is thermally bonded to the paper. The bond prevents the toner further diffusing into the paper or being detached when the paper is wet. Laser toners also provide advantages in the printing of calibration charts, labels or instructions on the paper. However, there are also challenges involved with toner sealing: first, a single layer of toner on paper comprises of defects such as cracks and holes, potentially causing leakage. Therefore, four or five layers of toner for each side of the device are required for fully enclosed sealing. Other limitations include (i) interference with wicking due to printing excess layers, (ii) compatibility with thermally insensitive reagents (must survive the process of passing through a fuser heated to about 180 °C), (iii) requirement of adding the detection reagents before the toner deposition and (iv) potential incompatibility with the toner chemistry.

Cold lamination. Self-adhesive laminating has been adapted to enclose the top and the bottom of a flow-through paper-based microfluidic device.[142,143] It has been shown that cold lamination sheets similar to pressure-sensitive tapes could protect the assay. In addition, the laminating sheets hold the assay components, such as filter and plasma separator, in place. Unlike pressure-sensitive tapes, cold laminating sheets can provide improved mechanical strength during operation. However, the laminating process requires benchtop equipment.

2.3 Capabilities

Analytical assays employing paper-based microfluidic devices require several capabilities beyond a platform for running the assay. For example, a typical quantitative assay requires a platform, a fixed sample volume, a fixed assay time, a reader, sometimes a power supply for the reader (*i.e.* to power absorbance, fluorescence or electrochemical assays), and reagents that provide selectivity and sensitivity. Traditional lateral flow assays are less demanding, but still require a fixed sample volume and assay time. The ideal paper-based microfluidic device would incorporate solutions to many (if not all) of these requirements directly in the device, thus enabling point-of-care assays that require minimal effort and manipulation by the user. The ideal device would require only that the user adds a sample and then interprets the readout. Incorporating solutions to these requirements into the paper-based device also offers an opportunity to simplify an assay and reduce its cost. It is in this context that paper-based microfluidic devices might offer a distinct advantage over more traditional dipstick and lateral-flow devices. Fluidic channels in a paper-based microfluidic device can be designed to separate a sample into multiple regions where multiple functions can occur on the device simultaneously. Three-dimensional paper-based microfluidic devices are particularly attractive in this context since each thin ($\sim$180 μm-thick) layer of paper within a device could (in principle) perform a different function to facilitate the overall assay.

Functional elements can be incorporated into paper-based microfluidics to have precise control over the flow of fluids in the channels. The capabilities of the current assays can be subdivided into categories based on the simplicity of conducting an assay: (1) self-contained assays (the user only adds the sample and interprets the readout); (2) assays that involve some user intervention (*e.g.* immunoassays, push-button designs, adding multiple fluids to a device); and (3) designs that require multiple external equipment operations or instrumentation. Several recent studies have made progress towards the goal of fully-integrated analytical devices. These include creating fluidic channels in paper that provide fixed volumes of sample to the assay reagents within the device, timers,[176,177] power sources[178,179] (*i.e.* paper batteries) and pre-processing steps directly in a paper-based microfluidic device. Related efforts have focused on creating new types of assay reagents as well, with a particular focus on achieving selectivity and sensitivity (particularly signal amplification) using thermally-stable reagents which are important for creating robust point-of-care diagnostics that do not require storage at reduced temperatures to prolong the shelf-life of the device.[180]

An important challenge in the context of point-of-care analytical devices involves minimizing the number of external steps and equipment involved in conducting the assay. A number of studies using paper-microfluidic devices, however, have taken a different approach that is more analogous to the types of studies that have emerged in polymer-based microfluidic devices. External equipment is used along with paper-based microfluidic devices to demonstrate capabilities in paper that were possible in polymer-based microfluidic devices as well. Examples of this approach include separation,[181] acoustic mixing[182] and thermochromic displays.[183] Table 3 shows recently developed capabilities of capillary-based microfluidic devices. These capabilities ideally should be consistent with the characteristics of low-cost ($\sim$\$0.01), lightweight, operation under limited infrastructure settings and the requirement for low sample volumes ($\sim$5 μl).

Switches and valves. These mechanisms play an important role in multi-step protocols such as signal amplification. The first example of a paper-based microfluidic switch was built to control capillary wicking in fluid channels. This was accomplished by cutting a channel into two pieces and manually separating the channels to allow or inhibit the capillary flow (Fig. 10A).[154] Three-dimensional paper-based microfluidic devices can be constructed in such a way that allows fluid movement. The principle of the valve mechanism is based on closing the gap between two vertically aligned fluidic channels by applying pressure (Fig. 10B).[184] Closing the gap allows

Published on 08 May 2013. Downloaded by University of Cambridge on 31/05/2013 13:14:32.

Table 3 Capabilities of capillary-based microfluidics

Function	Substrate	Platform	Capabilities
Valves[184]	Chromatography paper	3D	Consists of single-use on buttons. Fluids are delivered by closing the gap of physically separated paper membranes allowing wicking continuously. It also requires single use adhesive tapes.
Multi-step processes[147]	Backed nitrocellulose	2D	A device comprising multiple inlets per outlet can be built. Geometry of the networks and dissolvable barriers were functionalised to restrict or allow wicking.
Fluidic timers[176]	Backed nitrocellulose	3D	Embedded timing mechanism. The capability is formed by specific wax and dye deposition that construct the signalling feature.
Disconnects[185]	Nitrocellulose and cellulose pads	2D	Consists of multiple converging inlets controlling the arrival of each fluid to a specific detection area. It also achieves a programmed disconnection of fluid sources for multi-fluid step applications.
Separation[186]	Chromatography paper	3D	The mechanism consists of a gold electrochemical microcell on polyester allowing chromatographic separation. It may perform separation and quantification of complex solutions.
Thread mixing[170–172]	Mercerised cotton and plasma-treated cotton	3D	Threads can be sewn in different combinations such as branching woven arrays to facilitate capillary action. Potential materials include rayon, hemp, nylon, polyester, wool, silk or combination of these materials. They are proposed as an alternative to reduce the fabrication complexity involved in 3D paper-based microfluidics.
Acoustic mixing[182]	Polyester-cellulose clean room paper	2D	A convective actuation mechanism that functionalises surface acoustic waves. The mixing function employs a Y-channel structure pattern on paper.
Dilution[187]	Nitrocellulose	2D	Adapts adjacent fluid flows for dilution.
Flow visualization[188]	Backed nitrocellulose	2D	Visualization and measurements of fluid flow can be demonstrated by using fluorescence and electrochemical marking methods.
Metering[189]	Chromatography paper	3D	Provides control over when and how fluids are delivered into detection areas.
Fluidic batteries[179]	Chromatography paper	3D	Galvanic cells incorporated into the device are capable of powering a surface-mount UV LED and on-chip fluorescent assay.
Fluidic diode[190]	Cellulose paper	2D	A two-terminal component that allows and stops wicking. It can be also used as a delay mechanism.
Thermochromic displays[183]	Photo paper	3D	Consists of electrically conductive wires and thermochromic inks on the opposite sides of paper. The colour change is achieved by passing current through the wires and heating the thermochromic inks.
Text display[191]	Paper towel (softwood fibres)	2D	Capable of reporting haemagglutination reactions in written text.

fluids to wick along the connected channels. The single-use 'on' buttons can be activated using a ballpoint pen (pin pressure). Such devices can be fabricated as a single platform and used for more specialised purposes. A single device can be adjusted to perform replicates of a particular assay (or analyte) based on the given sample. These assays can find applications in which the volume of the sample is limited or multiple repetitions are required to meet an analytical standard. Paper-based microfluidic valves are conceptually analogous to field-programmable gate arrays in electronics. Vertical channels are connected by double-sided tape (or pressure-sensitive glue). Such designs also require cellulose powder, custom made tapes with holes (laser or punch cut), complex fabrication techniques and alignment issues with multiple layers.

Another approach to paper-based valves is to build 2D microfluidic networks with programmable fluidic disconnects.[185] The assay employs multiple converging fluid inlets to control the arrival time of each fluid to a detection zone (Fig. 10C). The system comprises of a fluidic network and a fluid reservoir to allow programmed disconnection of fluid

 This journal is © The Royal Society of Chemistry 2013

Published on 08 May 2013. Downloaded by University of Cambridge on 31/05/2013 13:14:32.

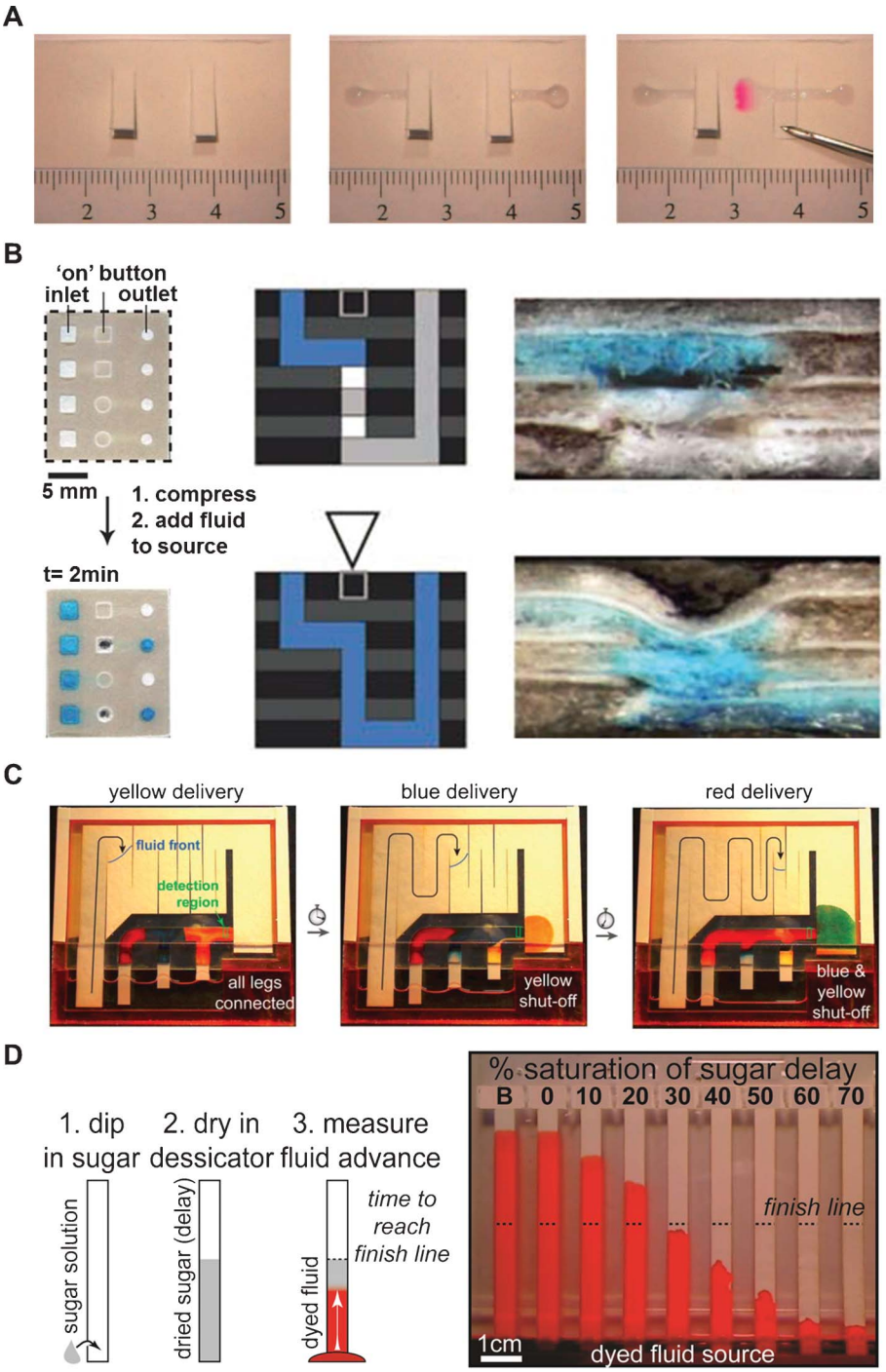

Fig. 10 Switches and valves. (A) A switch triggers solution to wick into the reaction site and allow the indicator to change colour. 3D microfluidic devices fabricated in layered paper and tape. Adapted with permission from ref. 154. Copyright (2008) American Chemical Society (B) Top view of the assembled device with four 'on' buttons. Here an aqueous blue dye was added to the four inlets. Buttons 2 and 4 (top to bottom) of the device were compressed and the device allows the dye to be wicked and reach the outlet. Schematic representations and images of the cross sections. Adapted with permission from ref. 184. Copyright (2010) RSC publishing. (C) Automated sequential fluid delivery in a 2D paper network. Each leg wicks buffer from a single reservoir and wet the dried dyes. Each coloured fluid arrives sequentially to the detection zone and the system is switched off as the fluid contact resolves. Adapted with permission from ref. 185. Copyright (2011) RSC publishing. (D) Dissolvable fluidic time delays. Adapted with permission from ref. 192. Copyright (2012) Chemical and Biological Microsystems Society.

sources that are required for multi-step delivery. The 2D microfluidic network has legs with different lengths and the legs are dipped in the fluid reservoir. As the fluid level drops, the legs disconnect in their order of length and programmable sequence.

Published on 08 May 2013. Downloaded by University of Cambridge on 31/05/2013 13:14:32.

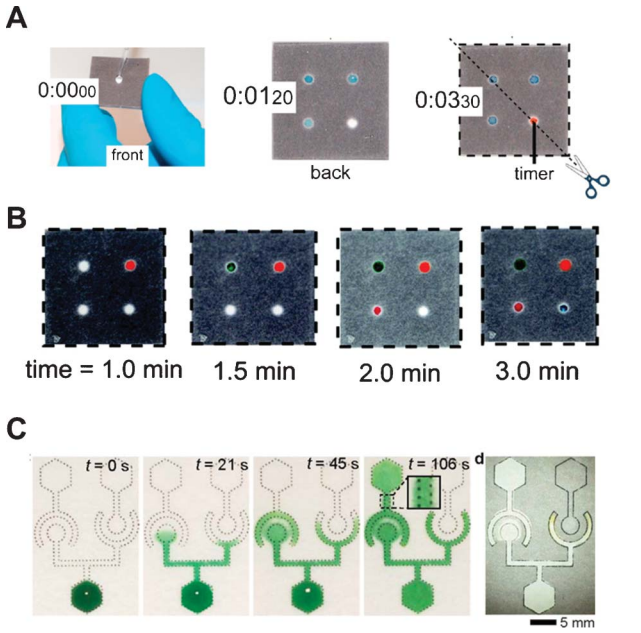

Fig. 11 Fluidic timers and metering. (A) Example of a fluidic timer that was built in a 3D paper-based microfluidic device. The orange circle indicates the feature of the fluidic timer and it signals the end-point of the assay. The blue circles show the results of a multiplex assay. Below is the image of the cross-section of the fluidic timer. Adapted with permission from ref. 176. Copyright (2010) American Chemical Society. (B) Time lapse images of 3D microfluidic device with metering capability. The wax concentrations are 0, 15.7, 31.4, and 47.1 μg × μm^{-3}. Adapted with permission ref. 189. Copyright (2010) American Chemical Society. (C) Fluidic diodes. Time-sequential photographs show the fluid wicking towards two oppositely-configured diodes and the photograph of the movement of human blood serum by the diodes. Adapted with permission from ref. 190. Copyright (2012) RSC publishing.

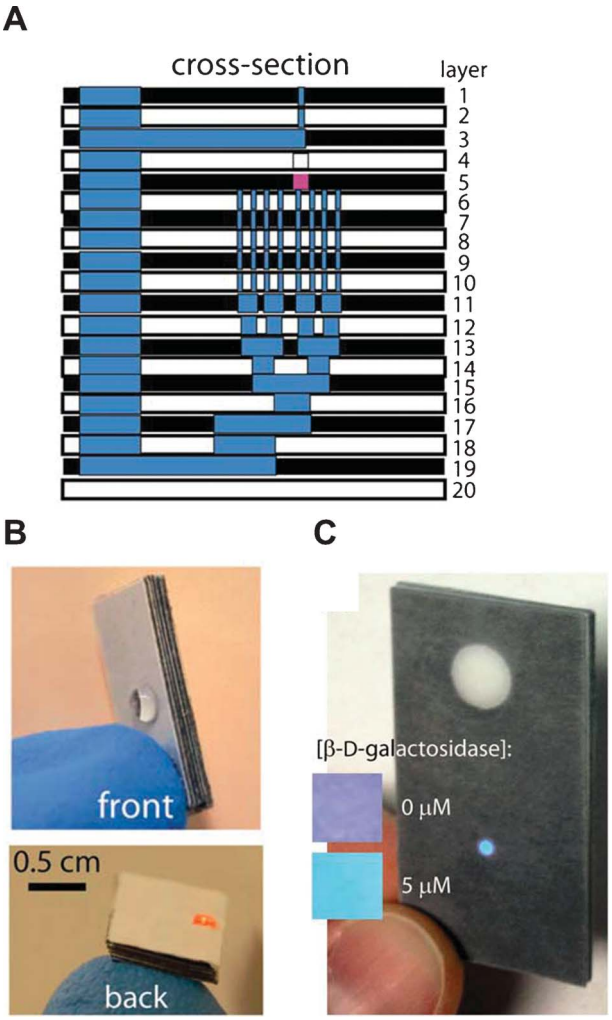

Fig. 12 The fluidic batteries can be made from galvanic cells that are incorporated into a paper-based device. (A) Schematic of a fluorescent assay on a paper-based microfluidic device for detecting β-D-galactosidase. (B) A red LED illuminates when the fluidic battery is on. (C) Colourimetric output of the on-chip fluorescence assay. Adapted with permission from ref. 179. Copyright (2012) RSC publishing.

Recently, dissolvable fluidic time delays were suggested for 2D microfluidic networks (Fig. 10D).[192] Feasibility studies demonstrated the impregnation of nitrocellulose using sucrose to create time delays in seconds to hours. The mechanism can be tuned by adjusting the concentration of sucrose. Due to the possibility of evaporation, the housing unit plays a key role in its reduction. Furthermore, the impregnated sucrose in nitrocellulose (or paper) should not interfere with the analytes that are measured. Also, it should be noted that mixing of the sample with sucrose increases the viscosity. In terms of practicality, this simple delay mechanism stands out as a component that is compatible with high-volume manufacturing, unlike 3D systems.

Other potential delay mechanisms that have not been demonstrated are the following: (1) partially impregnating paper or nitrocellulose with wax, AKD and polystyrene and (2) crushing the paper or nitrocellulose volume.

Mixing. Capillary-driven passive mixing has a number of limitations, including non-uniformities and poor control of fluidics in mixing as different fluids move along the channel. The quality of the paper's texture and alignment of fibres governs reproducibility. Paper-based microfluidics can be integrated with threads to build mixing capabilities.[170–172] Threads can be sewn to create 3D passageways to transport liquid by capillary action. The capabilities can be integrated with sensing mechanisms to allow qualitative or semiquantitative analysis. Another way of mixing fluids is to use surface acoustic waves to drive mixing.[182] However, the acoustic mixing method requires miniature battery-powered circuits.

Fluidic timers and metering. To know the exact end point of the assay is very important. Recently, 3D paper-based microfluidic devices enabled the end point of a time-dependent assay to be monitored (Fig. 11A).[176,177] The mechanism automatically starts when the sample is added and does not require any external equipment. The timing function is based on the wicking time of a sample. The time period can be controlled by the quantity of wax present in the paper. The signalling is achieved through observing a dye in the assay. The fluidic timers can automatically calibrate the assay to compensate for differences in wicking rates (can be caused by viscosity or humidity variations). This approach is critical for

 This journal is © The Royal Society of Chemistry 2013

Published on 08 May 2013. Downloaded by University of Cambridge on 31/05/2013 13:14:32.

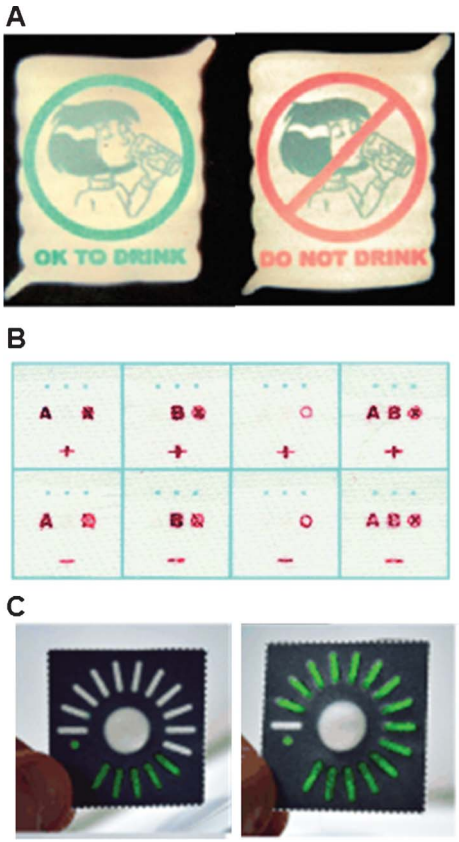

Fig. 13 Displays for paper-based microfluidics. (A) A thermochromic display that indicates safe *vs.* unsafe drinking water using images. Such displays may allow communicating complex messages or can find applications in locations where multiple languages are spoken. Adapted with permission from ref. 193. Copyright (2009) RSC publishing. (B) Text and patterns reported by the blood test device displaying eight ABO RhD blood types. Adapted with permission from ref. 191. Copyright (2012) Wiley-VCH Verlag GmbH & Co. (C) Quantitation of the concentration of hydrogen peroxide in a paper-based analytical device without external equipment. Adapted with permission from ref. 194. Copyright (2012) Wiley-VCH Verlag GmbH & Co.

reading the assay on time. The development of functions that can indicate the time when the assay should be read and no longer valid will be key advancements in building integrated paper-based devices.

3D paper-based microfluidics can be functionalised to control the movement of the capillary-driven flow (Fig. 11B).[189] Such a capability enables the control of the fluid flow to detection zones with appropriate time delays. This device introduces new capabilities to paper-based assays that require multiple steps in which reagents might interact with a substance for a particular period of time. In addition, metering can also be used in the simultaneous display of results for multiple analytes.

Constructing fluidic diodes is another approach that enables the control of fluids during wicking in a 2D paper-based device (Fig. 11C).[190] The fluidic diode consists of a two-terminal component that allows or prevents capillary flow along the channel. Potential applications include trigger and delay valve mechanisms. Such systems can comprise of functional circuits that can manipulate multiple fluids in a sequential manner.

Power. Fluidic batteries can be constructed in paper-based microfluidic devices to generate power when a sample is introduced to the device. Such a device might comprise of galvanic cells that are integrated into the microfluidic channels.[179] Fig. 12A illustrates such galvanic cells and the complexity associated with constructing such assays. The assay was demonstrated for powering a surface-mount UV LED (Fig. 12B) and on-chip fluorescence assay (Fig. 12C). The current size (20 layers) and fabrication process are suitable for laboratory prototyping, but additional improvements in the design will be required before the approach can be applied more broadly.

Displays. Thermochromic displays are among the earliest readout technologies demonstrated for use in paper-based platforms.[193] The principle is based on passing an electrical current through wires situated on the paper to heat thermochromic inks and obtain a colour change (Fig. 13A). However, this display capability requires a power supply. The first example of an equipment-free display was demonstrated on reporting ABO RhD blood types using paper text and symbols (Fig. 13B).[191] Determining the presence or absence of certain antigens on the surface of red blood cells based on the principle of haemagglutination reactions is well known. The device comprises of contrasting hydrophobic–hydrophilic channels as text patterns and functionalised sites for RBC and antibody interactions. When the antibody in a text pattern does not conjugate with the antibody of the RBCs, the non-agglutinated RBCs are washed out with saline solution. Similarly, if the haemagglutination reaction occurs, agglutinated RBC lumps will stay inside the fibre matrix and cannot be removed. In addition, individual inoculation of each drop of blood samples to the channels, saline-washing and drying steps makes the assay labour intensive and prone to operator error. Although the assay is helpful to obtain yes/no answers in haemagglutination assays, it cannot be used in quantification and multiplexing for other analytes. Recently, another assay for the quantitation of the concentration of hydrogen peroxide (a model analyte) was reported (Fig. 13C).[194] The 3D paper-based microfluidic device consisted of hydrophilic paper, HEPES buffer impregnated on a paper disc, a layer containing hydrogen peroxide, food dye in a paper disc, double-sided tape and a piece of hydrophobic paper. The principle of the assay is based on the selective changes in the wetting properties of paper. In this assay, hydrogen peroxide oxidatively cleaves the detection reagent and the elimination reaction yields hydrophilic by-products. The hydrophilic by-products allow the sample to wick through the device, followed by interaction with the food dye, thus resulting in a colour change in the detection region. The time required to wet the detection region can be correlated with the concentration of the analyte. The assay enables quantitation by either (i) tracking the time required for a sample to react and pass through a hydrophobic detection reagent in a single conduit or (ii) counting the number of coloured bars after a fixed assay period. However, such reactions presented in this study are rare in chemistry. Further development in the assay chemistry is needed to expand the scope of this method for quantitative analysis. In

Published on 08 May 2013. Downloaded by University of Cambridge on 31/05/2013 13:14:32.

this study, standard printer paper was also adopted in some layers to achieve more reproducible coverage of a detection reagent on the printer paper than on filter/chromatography paper.

Other processes. Multi-step chemical processing sequences can be useful in sample pretreatment.[195] 2D microfluidic networks can be configured to have multiple inlets per outlet to enable controlled transportation of reagents within a single device.[147] This process can be accomplished by modifying the geometry of the network or by using dissolvable barriers. Sequential reagent delivery was demonstrated by constructing a nitrocellulose-based network comprising of three staggered inlets which lead to a common segment of the body. When increasing volumes of reagents were wicked up by the segregated channels, the fluid with the shortest path reaches the detection region first, followed by the fluids from medium and longest inlets.

Paper-based separation devices represent an approach to differentiate analytes in complex samples to prevent interference.[181] Sample preparation often involves concentration or dilution. This study employs adjacent flow streams to enable hydrodynamic focusing, diffusion-based analyte extraction from a complex mixture, and single and serial dilutions.[187]

3. Theoretical studies

Achieving consistent control over the time of flow velocities and time of detection is important to fabricate reproducible paper or nitrocellulose-based assays. Control parameters are especially critical to carry out multi-step processes. The flow in traditional PDMS-based microfluidics is characterised by the Hagen-Poiseuille law with pressure-driven flow at low Reynolds numbers.[196] However, the flow through paper pores could be characterised by plug flow, thus allowing a reduction in Taylor-Aris dispersion.[197–199] Capillary fluid transport is the ability of a liquid to flow in constricted spaces without the assistance of external forces such as pumps. Based on the intermolecular forces between the porous fibres and the fluid, capillary action is driven by hydrophilicity, surface tension and porosity. In lateral flow assays, the fluid front migrating into a dry membrane is affected by the viscous resistance of the wetted area. In this section, the governing equations of the wet-out and fully wetted flow for constant width and varying-width channels are discussed.

3.1 Paper wet-out

Constant-width channels. The one-dimensional transport of fluids in porous substrates can be described by Washburn's equation, which represents the distance moved by the fluid front that is proportional to the square-root of time (eqn (2)).[162] Here L is the distance covered by the fluid front, t is the time, D is the average pore diameter, γ is the effective surface tension, η is the viscosity. It should be noted that this equation is valid in the presence of a non-limiting reservoir and a constant cross sectional area that is maintained throughout the length. This equation agrees well with the experimental data; however, inconsistencies can arise depending on the characteristics of paper. In paper-based microfluidics, this equation assumes that (i) the pore sizes of the paper matrix are the same; (ii) no impurities exist in the paper; (iii) the hydrophobic channels formed by the diffusion of wax or cut edges are consistent and do not affect the capillary force. When this equation is rearranged and combined with experimental data, it can also be used to estimate the average pore diameter of the paper substrate. It is key to note that the transport time of fluids can be controlled by altering the surface chemistry, impregnation of hydrophilic/hydrophobic barriers and channel width.

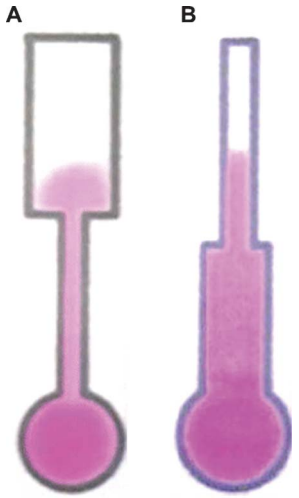

Fig. 14 A) The constricted fluid flow and B) the abundant fluid flow. Adapted with permission from ref. 132. Copyright (2012) Springer.

Constricted flow. When two strips with different constant widths are introduced to a non-limiting reservoir, they both achieve the same transport time and decrease in velocity as the fluid front moves through the strip. In the case where a narrow channel connects to a wider channel, the non-limiting fluid reservoir is violated and the velocity of the fluid front decreases as it migrates through the wider channel (Fig. 14A).[147] This is because the mass flow along the channel (or volumetric flow rate) is conserved and the flow rate of the fluid front decreases. A practical application can be realised when the transport time of a sample or a reagent is employed as an adjustable parameter.[147]

Abundant flow. This flow type is the migration of a fluid from a channel towards another channel of smaller width. Compared to the constricted flow, the abundant flow could be considered a non-limiting reservoir. This configuration shows that varying the initial channel reservoir width does not make an impact on the flow rate as long as it is wider than the next channel (Fig. 14B). This phenomenon is driven by sufficient fluid to feed and sustain the transition point. The experimental data confirms that flow from a channel with a larger width can act as a non-limiting reservoir for the fluid flowing into a channel with a smaller width when equal depths are assumed.[132]

 This journal is © The Royal Society of Chemistry 2013

Published on 08 May 2013. Downloaded by University of Cambridge on 31/05/2013 13:14:32.

Table 4 Comparison of proposed detection mechanisms for paper-based microfluidics. Published sensors include medical diagnostics, environmental sensing and food contamination testing

Sensor	Analyte
Molecular dyes or enzymatic reactions	Bovine serum albumin,[6,161,203] glucose,[6,7,119,152,204] (pH and human serum albumin),[152] (bendiocarb, carbaryl, paraoxon, malathion),[205] (paraoxon and aflatoxin B1),[206] ketones,[184] antibodies to the HIV-1 envelope antigen gp41,[207] lactate,[204] uric acid,[119,204] red cell antigens A, B, and D,[208,209] (urinary acetoacetate and salivary nitrite),[210] total iron,[144] heavy metals[211] (Hg(II), Ag(I), Cu(II), Cd(II), Pb(II), Cr(VI), Ni(II)), organic solvents,[212] hydrogen peroxide,[213] volatile organic compounds,[214] E. coli strain K12 ER2738,[215] (*E. coli O157:H7*, *Salmonella typhimurium*, and *L. monocytogenes*),[216] iodide,[217] particulate metals[218](Fe, Ni, Cu), (alkaline phosphatase and aspartate aminotransferase),[142] (aspartate aminotransferase and alanine aminotransferase),[143] aerosol oxidative activity,[219] reactive phosphate[220]
Electrochemical sensing	Glucose,[178,221–223] lactate,[221,222] uric acid[186,221](Kfouri 2010), ascorbic acid,[186] (cholesterol and ethanol),[222] Pb(II),[223–225] Cd(II),[225] cancer and tumor markers,[226–229] hydrogen peroxide,[178] (pH, K+ and NH4+),[230] dopamine,[231] paracetamol and 4-aminophenol,[232] 1-butanethiol[233]
Nanoparticles	DNase I,[234] adenosine,[167,234] human immunoglobulin G,[153] human chorionic gonadotropin,[235] (*Pseudomonas aeruginosa*, *Staphylococcus aureus*),[236] glucose,[237] Hg(II),[238] PfHRP2,[235] goat IgG,[239] prostate-specific antigen,[240] Cu^{2+},[241] HIV DNA,[242] *Mycobacterium tuberculosis*,[243] immunoglobulin E[244] and Cd^{2+}[245]
Electrochemiluminescence	(2-(Dibutylamino)-ethanol, and nicotinamide adenine dinucleotide),[246] tumor markers,[228,247,248] carcinoembryonic antigens,[249] dopamine,[250] (Pb^{2+} and Hg^{2+})[251] and genotoxic activity[252]
Chemiluminescence	Glucose,[253] uric acid,[253,254] tumor markers[227,255]
Fluorescence	Fluorescein isothiocyanate-labeled bovine serum albumin,[256] DNA,[257] nucleic acids,[258] lung cancer associated miRNA,[259] nucleic acid hybridisation[260] and Asian soybean rust[261]
Hybrid techniques	Dual Electrochemical/Colourimetric (Au(III), Fe(III))[262]
Genetically engineered bacterial whole-cell	Bacterial quorum signaling molecules-*N*-acylhomoserine lactones[263]

3.2 Fully-wetted flow

Constant-width channels. The flow characteristics of a fluid in a pre-wetted channel can be described by Darcy's law (1856) which is based on the Navier–Stokes equations by assuming homogeneity.[200–202] It describes the fluid flow in porous media and can be used to express the flow of a fluid in a straight paper substrate with a channel of constant width.

$$Q = -\frac{\kappa WH}{\eta L}\Delta P \tag{4}$$

where Q is the volumetric flow rate, κ is the fluid permeability of the paper, η is the viscosity, WH is the area of the channel perpendicular to flow and ΔP is the pressure difference along the flow direction over the length L. When the channel width is constant, the time taken for the fluid front to migrate a certain distance can be described as the following:

$$t = \frac{V}{Q} = \frac{V\eta L}{\kappa WH\Delta P} = \frac{\eta L^2}{\kappa \Delta P} \tag{5}$$

where V = the volume of the fluid at the time instant t. The variation in pressure is governed by the capillary force therefore, ΔP is assumed to be constant. If permeability of paper is constant, then the geometric shape is the defining factor that affects the flow rate of the fluid.[132,195] Therefore, when the width of a channel is constant, the length L is the only parameter that influences the time taken for the flow.

Varying-width channels. Darcy's law can also be applied to channels with varying widths. The volumetric flow rate can be determined in serially connected straight channels of varying widths by imposing equality of the volumetric fluxes in the segments of different widths.

$$Q = -\frac{\Delta P}{\left(\frac{\forall}{\kappa}\sum_{i=1}^{N}\frac{L_i}{W_iH_i}\right)} \tag{6}$$

where W_iH_i is the area of segment of the channel perpendicular to flow, L_i is the length of segment i of the channel in the direction of flow, and ΔP is the pressure difference across the length of the channel. The estimation of total volumetric flux through a paper strip with N segments in series and parallel is analogous with Ohm's law.[195] An analogous approach reveals that ΔP is the fluidic counterpart to voltage change, Q is the fluidic counterpart to current, and

$$\frac{\eta L_i}{\kappa W_iH_i} \tag{7}$$

is the fluidic counterpart to the resistance. While in series the total end-to-end resistance of a string of fluidic components connected in series is the sum of all the fluidic resistances.

Published on 08 May 2013. Downloaded by University of Cambridge on 31/05/2013 13:14:32.

Table 5 The principles of colourimetric reactions in commercial urinalysis tests[a9–15]

Assay	Measurement principle	Reactive ingredient	Reaction
Glucose	Based on glucose oxidase, peroxidase and chromogen reactions. If the pad indicates yellow or greenish, the glucose levels are normal.	2.2% w/w glucose oxidase (microbial, 1.3 IU); 1.0% w/w peroxidase (horseradish, 3300 IU); 8.1% w/w potassium iodide; 69.8% w/w buffer; 18.9% w/w non-reactive ingredients	$\text{Glucose} + O_2 \xrightarrow{\text{glucose oxidase}} \text{Gluconolactone} + H_2O_2$ $\text{Chromogen} + H_2O_2 \xrightarrow{\text{peroxidase}} H_2O + \text{dye}$
Protein	Based on protein error principle for albumin. The tests pad can change colour from yellow to greenish blue in the presence of albumin.	0.3% w/w tetrabromophenol blue; 97.3% w/w buffer; 2.4% w/w non-reactive ingredients	$\text{tetrabromophenol blue (pH 3, yellow)}$ $\xrightarrow{\text{protein}} \text{tetrabromophenol blue (>pH 4.6, blue)}$
Blood	Pseudoperoxidative activity of haemoglobin and myoglobin can catalyse oxidation of an indicator in the presence of organic hydroperoxide and yields green colour.	6.8% w/w diisopropylbenzene dihydroperoxide*; 4.0% w/w 3,3′,5,5′-tetramethylbenzidine; 48.0% w/w buffer; 41.2% w/w non-reactive ingredients	$H_2O_2 + \text{chromogen}$ $\xrightarrow[\text{peroxide}]{\text{haemoglobin}} \text{oxidised chromogen} + H_2O_2$
Leukocytes	Presence of esterase from granulocytes yields a violet colour.	0.4% w/w derivatised pyrrole amino acid ester*; 0.2% w/w diazonium salt; 40.9% w/w buffer; 58.5% w/w non-reactive ingredients.	$\text{Indoxyl or pyrole carbonic acid ester}$ $\xrightarrow[\text{exterase}]{\text{granulocytic}} \text{Indoxyl or pyrole}$ $\text{Indoxyl or pyrole} + \text{diazonium salt}$ dye (purple)
Nitrite	Nitrite reacts with *p*-arsanilic acid to form a diazonium compound, which couples with the quinolone compound to produce a pink colour	1.4% w/w *p*-arsanilic acid*; 1.3% w/w 1,2,3,4-tetrahydrobenzo(h)-quinolin-3-ol; 10.8% w/w buffer; 86.5% w/w non-reactive ingredients	$\text{Nitrite} + p\text{-arsanilic acid}$ $\rightarrow \text{diazonium compound}$ $\text{3-Hydroxyl-1,2,3,4 tetrahydrobenz}-(h)$ $-\text{quinoline}$ $+\text{diazonium compound}$ $=\text{pink colour}$
pH	Based on pH indicators which change colour in the range of 5–9 (orange to turquoise).	0.2% w/w methyl red; 2.8% w/w bromthymol blue; 97.0% w/w non-reactive ingredients	$\text{H}Ind\,(\text{acid form}) + H_2O \rightleftharpoons H_3O^+$ $+Ind^-\,(\text{conjugate base of the indicator})$
Ketone	Based on Leagal reaction. In the presence of sodium nitroprusside in alkaline medium, acetoacetic acid and acetone form a complex (violet).	7.1% w/w sodium nitroprusside; 92.9% w/w buffer	$\text{Acetoacetic acid} + \text{Na nitroprusside} + \text{glycine}$ $\xrightarrow{\text{alkaline}} \text{violet to purple colour}$
Urobilinogen	Based on Ehrlich Aldehyde reaction. Aldehyde or diazonium compounds in the presence of urobilinogen yields an azo compound (red).	0.2% w/w *p*-diethylaminobenzaldehyde*; 99.8% w/w non-reactive ingredients	$p\text{-diethylaminobenzaldehyde} + \text{urobilinogen}$ $=\text{azo compound (red)}$
Bilirubin	When bilirubin with a diazonium salt couples and produces acid, an azo compound (red) is inline.	0.4% w/w 2,4-dichloroaniline diazonium salt*, balanced with buffer and nonreactive ingredients	$\text{bilirubin} + \text{diazide} \xrightarrow{\text{acid}} \text{azobilirubin}$

[a] *Product specific.

Analogously, in parallel channels, the fluidic resistances add in reciprocals. In multisegmented strips in series, the transport time can be estimated as the following:

$$t = \frac{\eta}{\kappa \Delta P}(L_1 W_1 + L_2 W_2)\left(\frac{L_1}{W_1} + \frac{L_2}{W_2}\right) \tag{8}$$

 This journal is © The Royal Society of Chemistry 2013

Published on 08 May 2013. Downloaded by University of Cambridge on 31/05/2013 13:14:32.

In this equation, the heights of the paper segments are assumed to be the same. The cases in which $W_2 > W_1$, the time of transport will be greater for W_2/W_1. Volumetric flux in parallel strips or channels with hydrophobic barriers can be estimated using the same analogy.

4. Detection techniques

A wide array of detection mechanisms have been proposed for paper-based microfluidic devices. Applications for such detection methods include medical diagnostics, food pathogens and environmental testing. Table 4 provides an overview of established sensing mechanisms in paper-based microfluidics. Although the majority of these studies are focused on healthcare, limited studies were reported on environmental applications and food safety. No application of veterinary diagnostics has so far appeared in the literature. Sensing mechanisms demonstrated in the literature with the exception of molecular dyes are dependent on handheld readers. Excluding other types of sensor technology could be attributed to high costs, electrical component requirements and integration incompatibility with paper-based assays. Unsurprisingly, to date, most studies have exploited mature sensing mechanisms such as colourimetric and electrochemical sensing in paper-based microfluidic devices.

4.1 Sensing mechanisms

Colourimetric detection. Molecular and enzymatic dyes represent the simplest and most used method for detection. Colourimetric sensing can produce semi-quantitative readouts with the help of a calibration chart. Commercial urinalysis dipsticks such as Chemstrip (Roche) and Multistix 10 SG (Siemens Healthcare) are based on a colourimetric detection mechanism. Table 5 shows the principles of colourimetric tests in the market. In paper-based microfluidic devices, multiple detection zones are employed to capture different analytes within the same device. After the fabrication of hydrophobic patterns in paper, detection zones can be formed by spotting reagents in the detection zones. In such multiplex assays, an enzymatic or a chemical reaction between the target analyte in the sample and previously immobilised reagents take place. These reagents can be enzymes, acid–base indicators or dyes. Early examples of colourimetric sensing in paper-based microfluidics were demonstrated using pH, glucose and protein assays in artificial urine.[6,152] When samples were introduced to the paper-based microfluidic assay, they were distributed into the reaction zones. This process eventually yields a colour change and enables visual determination of analyte levels using a calibration chart. In the glucose assay, the positive result was recorded when the colour shifted from clear to brown, based on the enzymatic oxidation of iodide to iodine. Similarly, positive results in protein assays can be interpreted from a colour change of tetrabromophenol blue from yellow to blue. While these assays saturate within a minute, they require at least 10 min for colour development. Other published studies include biomedical testing,[119,142,143,210,215] environmental monitoring,[205,211,212,214,218] and food safety applications[206,216] (Fig. 15A and B). A disadvantage of the colourimetric sensing in lateral-flow and flow through assays is the inhomogeneity of the colour distribution, and thus, the judgment of the final colour can be challenging with the naked eye.[152] In addition, colourimetric sensors are influenced by the background noise of the paper or the sample. For example, blood assays require either usage of serum/plasma samples or a blood separator. Despite all these drawbacks, colourimetric sensing has been the most adopted sensing mechanism, and can be quantified by a calibration chart, a handheld reader[264,265] or a camera phone.[7,266]

Electrochemical sensing. Electrochemical detection has been exploited widely due to its maturity and well-understood working principles. Traditionally, electrochemical sensors comprise of three electrodes: a counter electrode, a working electrode and one or multiple reference electrodes. Carbon inks are well-known materials used in the fabrication of counter and working electrodes, whereas silver/silver chloride ink is used for the fabrication of reference electrodes (Fig. 15C). In paper-based assays, reaction zones comprise of this multiple-electrode mechanism (Fig. 15D). Early examples of electrochemical sensing included analytes such as glucose,[221,222] lactate,[221,222] uric acid,[221] cholesterol,[222] tumour markers,[226] dopamine[231] and drugs.[232] There were also environmental monitoring applications such as heavy metals.[221,223–225] Further usefulness of electrochemical sensing was demonstrated for the detection of glucose using a commercial handheld glucometer as a readout device.[222]

Fabrication of an electrochemical sensing platform requires an additional step involving the deposition of conductive inks on the paper matrix. All these electrodes and electronic wires were screen printed using graphite and silver inks, respectively. When the sample was introduced to the device the liquid was wicked up into the sensing zones and the amperometric measurement was initiated *via* the glucometer. Gold is another material that can be adopted for use in the fabrication of electrochemical electrodes. Sputtering through a shadow mask can be used to deposit the electrodes on the paper matrix.[232] In the fabrication of electrodes, screen-printing was adapted and these electrodes were characterised by cyclic and square wave voltammetry. The analysis in these experiments was based on chronoamperometry with optimised potential for the hydrogen peroxide production.

Historically, in contrast to colourimetric sensing, electrochemical sensing has demonstrated fast sensor responses and higher sensitivities, down to nM ranges. Electrochemical detection is also independent of the ambient light and is less prone to interference from the colour/deteriorations of paper, but requires reading equipment. Although the attractive attributes of electrochemical detection such as maturity, miniaturisation and low levels of interference from paper, the requirement for a detection instrument increases the complexity (see equipment-free ASSURED criterion) and the cost per test. Finally, investigators should question the necessity of using patterned paper when employing electrochemical sensing. A comparable assay could have been achieved on the dipstick and the lateral-flow format.

Published on 08 May 2013. Downloaded by University of Cambridge on 31/05/2013 13:14:32.

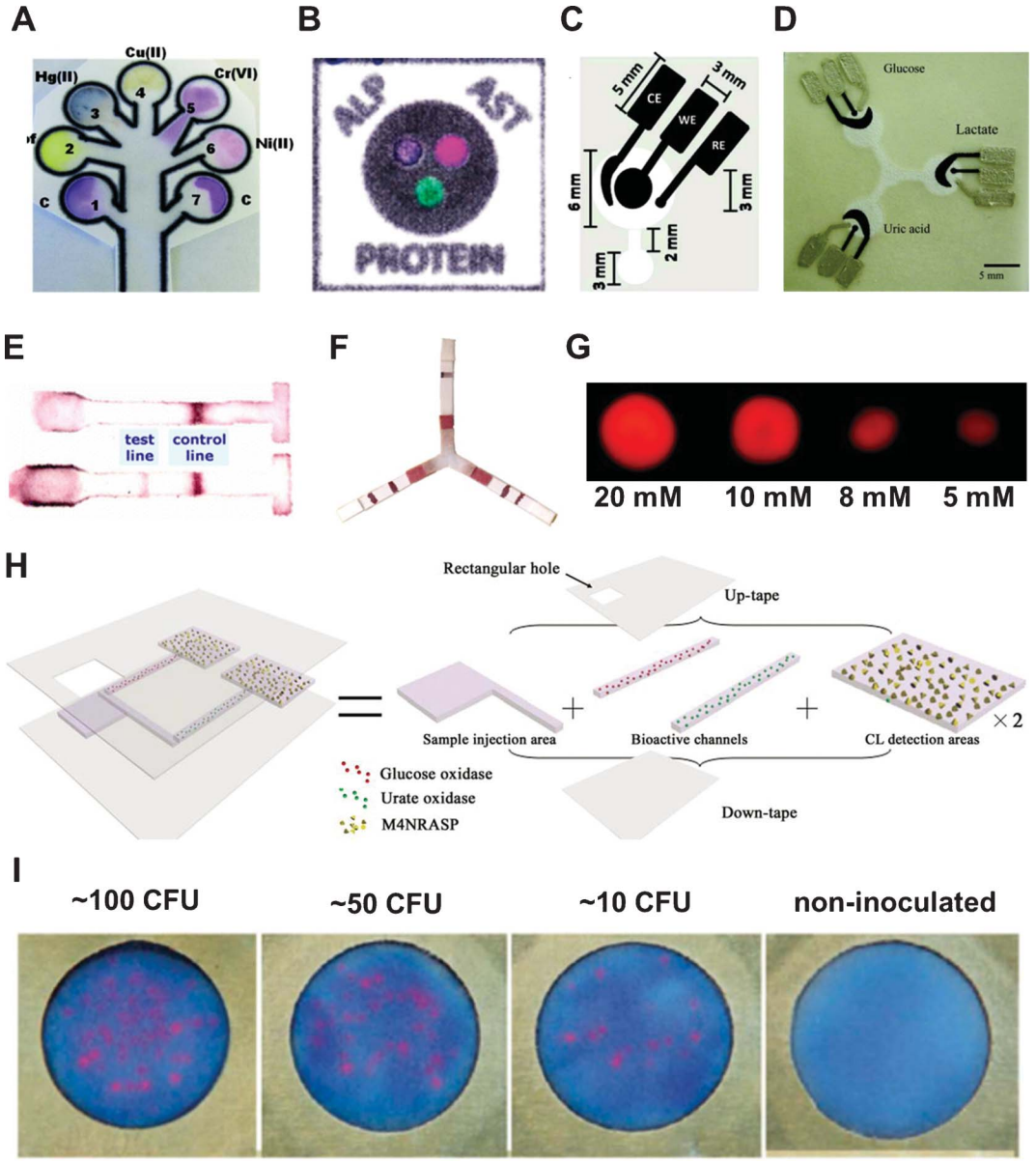

Fig. 15 Examples of sensing mechanisms for paper-based microfluidics. (A) Colourimetric detection of heavy metals. Adapted with permission from ref. 211. Copyright (2011) American Chemical Society. (B) Colourimetric detection of liver function. Adapted with permission from ref. 142. Copyright (2012) American Chemical Society. (C) The schematic of dual electrochemical/colourimetric determination of gold and iron. Adapted with permission from ref. 262. Copyright (2010) American Chemical Society. (D) Electrochemical sensing of glucose, lactate and uric acid. Adapted with permission from ref. 221. Copyright (2009) American Chemical Society. (E) Antibody conjugated/gold nanoparticle sensing of Immunoglobulin G. Adapted with permission from ref. 153. Copyright (2010) American Chemical Society (F) Antibody conjugated gold nanoparticle detection of *Pseudomonas aeruginosa* and *Staphylococcus aureus*. Adapted with permission from ref. 236. Copyright (2011) Elsevier B.V. S. (G) ECL emission from a paper-based device at different concentrations. Adapted with permission from ref. 246. Copyright (2011) American Chemical Society. (H) Schematic of the construction of a CL sensor in paper-based microfluidics. Adapted with permission from ref. 253. Copyright (2011) RSC publishing. (I) Fluorescent sensing for the growth of bacteria. Adapted with permission from ref. 215. Copyright (2012) RSC publishing.

Nanoparticle-based detection. Colloidal gold and monodisperse latex are the historical detector reagents for lateral flow assays.[267] Antibody conjugated gold nanoparticles are widely adopted in commercial lateral flow tests because gold nanoparticles have extinction coefficients that are higher than common organic dyes. In addition, their qualitative interpretation does not require a reader. Alternatively, monodisperse latex is often coupled with fluorescent dyes, coloured dyes, and magnetic or paramagnetic components. Coupled with dark colours, monodisperse latex particles can exhibit high contrast on nitrocellulose or paper. Even greater sensitivities of latex particles can be obtained when they are coupled with different colours or fluorescent dyes, thus enabling multiplexing, but their interpretation can require a handheld reader.

 This journal is © The Royal Society of Chemistry 2013

Published on 08 May 2013. Downloaded by University of Cambridge on 31/05/2013 13:14:32.

Because of their relatively small size (20–40 nm), colloidal gold particles can be dispensed in high density on the test lines. This constitutes the reasoning behind why colloidal gold is preferred over monodisperse latex particles (100–300 nm) in visually interpreted rapid assays. Another advantage of using colloidal gold is that it has higher colour intensity compared with coloured latex particles and higher intensities constitute easier discrimination of weak positive signals.

In paper and nitrocellulose-based microfluidics, the feasibility of using nanoparticle-based detection has been demonstrated with metabolites,[153,234,237,240,244,268] bacterial agents,[236] in key disease diagnosis such as HIV,[242] malaria,[235] tuberculosis[243] (requires PCR amplification) and in environmental monitoring applications.[238,241]

The first systematic study employing nanoparticle-based detection was in multianalyte immunochemical detection on filter paper using inkjet printers (Fig. 15E).[153] In the preparation of immunosensing inks, human IgG and, anti-human IgG and colloidal gold-labeled anti-human IgG solutions were adopted. First, filter paper is soaked in 1.8% (w/v) solution of polystyrene in toluene for 2 h and then dried at room temperature. Following this, a hydrophilic pattern was etched on the polystyrene-impregnated paper by ejecting toluene droplets to create test and control lines. This process dissolves the polymer and re-exposes the hydrophilic layer. This printing cycle was repeated nine times in order to have sufficient hydrophilicity on paper. Next, immunosensing inks were dispensed on test and control lines. This required 60 printing cycles and followed a second inkjet-etching step in which the remaining hydrophilic areas and connecting flow channel were formed by dispensing toluene in nine printing cycles. Then, the entire patterned paper strip was soaked in BSA in PBS buffer for 1 h for blocking followed by air drying. Next, polyvinylpyrrolidone surfactant in water was applied on the sample inlet area and conjugate area. Eventually, colloidal gold-labeled anti-IgG solution was incrementally spotted onto the conjugate area to prevent overflow of the colloidal gold into the hydrophilic channel. In this study, although the fabrication technique described eliminates the necessity of using multiple pads (*i.e.* sample pad, conjugate pad, reaction membrane and absorbent pad), it adds complexity in its fabrication, higher cost and lower reproducibility. It should also be noted that the assay is not compatible with fabrication techniques involving wax. Although this study employed inkjet printing, industrial efforts aimed at introducing modified inkjet printers were costly and not feasible due to the requirement for large dispensing heads and their connection to large-diameter umbilical systems.[97]

Other nanoparticle-based assay studies focused on improving the sensitivity of current lateral flow tests by using paper network platforms. The 2D nitrocellulose-based microfluidic networks enabled multistep processes to amplify the signal in immunoassays, and thus improve the limit of detection.[235,268] These cards can contain reagents stored in a dry form and the assay can be activated by adding the sample and water. Such devices can also be activated by a single-user step. They are also capable of multistep processes such as delivering rinse buffers and signal amplification reagents to the capture regions.

Although these devices were demonstrated using porous materials that include nitrocellulose and cellulose, the nitrocellulose piece could be replaced by cellulose or another porous materials depending on assay requirements.[269] Other 2D paper networks involved integrating the inlets of a number of lateral flow assays[236] (Fig. 15F), adopting folding techniques[242] and microplate paper platforms.[243] Furthermore, a method for patterning narrow lines of biomolecules onto a matrix was reported (Fig. 16).[270] The system consists of a syringe pump (SP1) that drives the biomolecule solution through a needle while another syringe pump (SP2) drags the needle tip across the membrane. This method enables laboratory-scale deposition of nanoparticle conjugates onto nitrocellulose membranes for prototyping.

Electrochemiluminescence (ECL). This sensing mechanism is based on luminescence generated by electrochemical reactions. When electrochemically generated intermediates undergo exergonic reactions, they result in an electronically excited state. This state emits light upon relaxation to a lower level state and therefore enables readouts without the requirement of a photodetector. ECL is considered attractive because it has the advantage of both luminescence and electrochemical methods. Applications to date include analytes,[225,246] tumour markers,[228,247,249] and ions.[251]

The first reported sensing mechanism was based on orange luminescence.[246] This study demonstrated the detection of 2-(dibutylamino)-ethanol (DBAE) and nicotinamide adenine dinucleotide by readouts of luminescence from the sensors. The principle of ECL sensing mechanism is based on $Ru(bpy)_3^{2+}$ and DBAE. At the electrode, the amine is oxidised (eqn (10)) and forms a radical cation $[DBAE^{\bullet}]^+$ (eqn (11)), followed by deprotonation and forming a reducing $DBAE^{\bullet}$ radical (eqn (12)). Then, this radical reduces $Ru(bpy)_3^{3+}$ to an excited state (eqn (13)). Later, $Ru(bpy)_3^{3+\bullet}$ emits at 620 nm while relaxing to the ground state.[271] This mechanism serves as a coreactant that is oxidised solely by the electrode.

$$Ru(bpy)_3^{2+} - e^- \rightarrow Ru(bpy)_3^{3+} \quad (9)$$

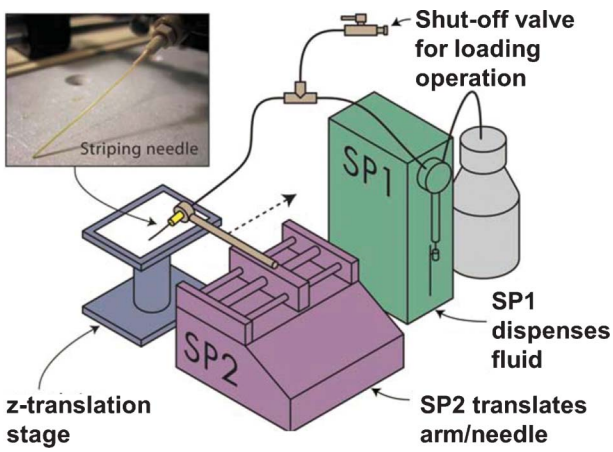

Fig. 16 Schematic showing the system components of a laboratory-scale protein striping device. Adapted with permission from ref. 270. Copyright (2010) RSC publishing.

Published on 08 May 2013. Downloaded by University of Cambridge on 31/05/2013 13:14:32.

$$\mathrm{DBAE} - e^- \rightarrow [\mathrm{DBAE}^\bullet]^+ \quad (10)$$

$$[\mathrm{DBAE}^\bullet]^+ \rightarrow \mathrm{DBAE}^\bullet + \mathrm{H}^+ \quad (11)$$

$$\mathrm{Ru(bpy)}_3^{3+} + \mathrm{DBAE}^\bullet \rightarrow \mathrm{Ru(bpy)}_3^{2+\bullet} + \text{products} \quad (12)$$

$$\mathrm{Ru(bpy)}_3^{2+\bullet} \rightarrow \mathrm{Ru(bpy)}_3^{2+} + h\nu \quad (13)$$

In ECL, electrochemical potential initiates and rules the chemiluminescence reaction. Electrodes were printed using screen printing and adding an ECL active luminophore followed by drying. The substrates were laminated onto a Zensor screen-printed electrode using an office laminator. In this study, the cyclic voltammetry of $\mathrm{Ru(bpy)}_3^{2+}$ was used to characterise the electrodes. After the lamination step, an incision was made in the laminate layer. Additionally, pressure was applied on the device during ECL measurements to achieve even contact with the working electrode. After the introduction of the sample to the assay, the potential is stepped from 0 to 1.15 for a short period to initiate the ECL. The initiation can be accomplished by shifting the potential to a level more positive than the oxidation potential of the ruthenium complex. In these experiments, chronoamperometry was adopted to generate ECL based on the fact that it provides control over reaction time (Fig. 15G).

This detection mechanism requires readouts to be taken in the dark since the detection is independent of ambient light. ECL must be used with mechanical camera phone housing units to darken the conditions of the sensing region to block the external light. Furthermore, ECL requires connection to the mobile phone battery and a short pulse of low voltage is required. In addition to these drawbacks, this detection mechanism requires a photomultiplier tube which is costly in a miniaturised form. Processing data was accomplished by analysing the red pixel intensity of the ECL emission and this was coupled with a calibration curve. The analyte concentration can be correlated to the intensity of the pixel.

Chemiluminescence (CL). This detection mechanism, not to be confused with fluorescence, is based on the emission of light generated by a chemical reaction. In the presence of reactants A (*e.g.* luminol) and B (*e.g.* hydrogen peroxide), and a catalyst or excited intermediate (*e.g.* 3-aminophthalate), light can be produced along with other products (eqn (14)). Here, hydrogen peroxidase catalyses the oxidation of luminol to 3-aminophthalate and the decay of the excited state, ◇, to a lower energy level results in light emission. The emission of light can be enhanced by using modified phenols (*e.g.* *p*-iodophenol) in the range of 10–100 fold. A common of example of CL is the glow stick which is based on the chemical reaction of peroxide with a phenyl oxalate ester.

$$[\mathrm{A}] + [\mathrm{B}] \rightarrow [\diamond] \rightarrow [\textit{products}] + \textit{light} \quad (14)$$

In paper-based microfluidics, CL has been exploited for biological analytes[253,254] and tumour markers.[255,272] The studies on glucose and uric acid determinations were based on oxidase reactions coupled with chemiluminescence reactions of a rhodanine derivative with the generated hydrogen peroxide in an acid medium[253] (Fig. 15H). Uric acid can also be determined through a chemiluminescence reaction between rhodanine derivative (3-*p*-nitrylphenyl-5-(40-methyl-20-sulfonophenylazo) rhodanine) and hydrogen peroxide.[254] Studies on the detection of tumour markers involved building sandwich-type immunoassays with a typical luminol-H_2O_2 chemiluminescence system and catalysed by Ag nanoparticles.[255] Other studies on detecting tumour markers focused on sandwich CL-ELISA with antibodies that were covalently immobilised on a chitosan modified paper zone through glutaraldehyde cross-linking.[272] Quantitative analysis was achieved based on the correlation between the concentration of the analyte and the peak intensity of the emitted light.

Fluorescence. This detection mechanism was first demonstrated on paper microzone plates. Although paper-based plates are well known in the literature,[103–106] they have only recently been suggested for quantitative fluorescence measurements. These paper plates were (i) relatively thinner, (ii) required smaller volumes of samples and were (iii) low-cost. Early studies have shown that 12.5 pmol of fluorescein isothiocyanate-labeled bovine serum albumin generated a relative fluorescence of 2700 ± 850.[256] Although concentration sensitivity and mass sensitivity were comparable with plastic plates, the average relative standard deviation for the replicates of all concentrations was higher. This limitation was attributed to scattering of light on the cellulose fibres and the influence of the index of refraction between cellulose and air. Additional attempts were not successful at improving the precision of the measurements. Although paper-based plates are suggested as alternatives to conventional plastic multiwell plates, their interpretation requires microplate readers. Other notable studies adopting fluorescent sensing includes paper strips containing DNA-conjugated microgels (MG) for the detection of DNA. Sensing DNA was accomplished in a number of steps: (i) targeting DNA promoted ligation of a DNA primer to the MG-bound DNA, (ii) rolling circle amplification (RCA) between the primer and a circle DNA, and (iii) hybridization of the RCA products and fluorescent DNA probe.[257] Another study reported a portable device for the growth of bacteria or the amplification of bacteriophages. In this study, a fluorescent mCherry reporter was used to quantify the growth of bacteria and the concentration of arabinose[215] (Fig. 15I). Another paper-based platform involving fluorescent sensing described the use of non-enzymatic nucleic acid circuits based on strand exchange reactions for the detection of target sequences.[258] Overall, although fluorescence sensing brings new capabilities to paper-based microfluidics, the feasibility of fluorescence sensing will be dependent on the advances in cost reduction and miniaturisation of fluorescence readers.

Hybrid sensors. An interesting sensing approach to paper-based microfluidic devices involved the realisation of a dual-detection mechanism. The first hybrid paper-based assay comprised of colourimetric and electrochemical sensing for the simultaneous detection of Au(III) and Fe(III) in industrial waste solutions.[262] In this study, electrodes were screen printed on patterned paper. These electrodes are comprised of carbon as the working electrode and counter electrode, and silver/silver chloride as the reference electrode as well as conductive pads. The inks were cured in an oven after each printing step. However, because Fe(III) interferes with Au(III)

 This journal is © The Royal Society of Chemistry 2013

Published on 08 May 2013. Downloaded by University of Cambridge on 31/05/2013 13:14:32.

determination, colourimetric detection of Fe(III) was also employed in the assay. Investigators demonstrated that the results were comparable with inductively coupled plasma-atomic emission spectrometry. Although hybrid detection mechanisms are a feasible alternative to single-type sensing assays, they require multiple readout mechanisms.

Genetically engineered bacterial whole-cells. Bacterial quorum signalling (QS) molecules, N-acylhomoserine lactones (AHLs), have been used as a sensing mechanism.[263] In this study, the bacterial cell-based sensing system comprised of two key components: (i) AHL-mediated QS regulatory system as recognition elements and (ii) β-galactosidase as the reporter enzyme. The bacterial cells were inoculated on paper by liquid drying. The paper strip biosensor was able to detect low concentrations (*i.e.* 1×10^{-8} M) of AHLs in saliva. The advent of synthetic biology will accelerate the efforts in developing whole-cell based biosensors in the future.

4.2 Readout

A unique selling point of lateral flow immunoassays has been their lack of requirement for readout devices over the last three decades. During early years of lateral flow assay development, manufacturers focused on cost and the ability to deliver a yes/no answer. This attractive attribute combined with low-cost, mobility and easy-to-read factors are the reasons for their popularity. However, their positive attributes also constituted their shortcomings: specifically, quantification had limited further exploitation of lateral flow assays. In addition to the quantification demand, subjective interpretation often resulted in false positives and negatives. They also did not possess the capabilities of connectivity, multiplexing and high-throughput. However, this is no longer the case. Recently developed rapid tests have demonstrated that these assays can be produced with manufacturing CV's of <10%, making them effectively quantitative, that they can be multiplexed, and, in association with handheld or small benchtop reader systems, can be applied at the point of interest more than adequately.

Today, the focus is shifting towards more sensitivity and quantification while the market's demand for automated systems is growing. Parallel to emerging biochemical techniques, a number of novel readers have been proposed. An ideal reader platform must address low-cost, simple operation, mobility, and connectivity. Despite the agreements on optimised assay characteristics, the views on interpretation of the assays have diverged. In this section, we evaluate three proposed reader platforms for rapid diagnostics: (i) handheld, (ii) mobile phones and (iii) on-chip quantification, and highlight their advantages and drawbacks. The evaluation in this section is aligned with WHO's ASSURED non-equipment criterion. However, although equipment-free technologies are desired, most detection techniques still require external electronic readers for quantitative analysis.

Hand-held readers. Reading technologies differ depending on the labelling and detection technologies used in lateral flow assays. Handheld readers comprising of optical sensors are used for the detection of colloidal gold or coloured monodisperse latex particles. Monodisperse particles with fluorescent dyes can be read by LED excitation *via* optical sensors. Today there are a number of commercial readers that can read colourimetric, fluorescent and paramagnetic-particle assays.[273,274] There are commercial products such as RDS-1500 Pro (Detekt Biomedical, Austin, TX), Defender TSR™ R-5001 (Alexeter Technologies LLC, Wheeling, IL), LFDR101 (Forsite Diagnostics Ltd, York, U.K.), UNISCAN™ Immunoassay Rapid Test Reader (Unison Biotech, Taiwan) and Magnetic Particle Reader (Magnasense, Finland). Currently, LRE[275] and Wiagen readers lead the market in fidelity and sensitivity. These semi-quantitative lateral flow assay readers offer adequate sensitivity, but come with high price tags ($1000–$2200). Many of the devices in the market have features such as internal displays, connection to other digital devices (*i.e.* printers) *via* USB, barcode readers, connection to printers and ID management systems (*i.e.* patient information). Wireless data transfer *via* Bluetooth and GSM is also available. The reader systems on the market today, from companies like ESE (Qiagen), Skannex (Norway), or Alverix (San Jose, CA) all have high end connectivity options. High throughput on these types of systems is an issue, although camera-based systems have the ability to change that also.

Camera phones and smartphones. High mobile phone penetration and rapidly growing telecommunications infrastructure in emerging markets has created an opportunity to deliver healthcare through telemedicine. Over the last decade, mobile phone penetration in the developing world has increased tremendously and now surpasses 4.8 billion subscriptions.[276] This can be attributed to unreliable fixed landline infrastructure. Currently, Africa stands as the second largest mobile phone market after Asia. With a 30% growth rate, there are 620 million mobile phone users as of 2011 in Africa.[277] Mobile phones have transformed the social and work lives of people in the developing world and contributed to local economies.[278–282] Notably, reduction in travelling needs has made a positive impact on the people living in rural areas, which now have the potential to access healthcare advice/information without travelling *via* poor roads, paying high costs and devoting large amounts of time.

Most mobile phones come with a built in camera and this represents a low-cost route to quantify paper-based microfluidic assays. Complementary metal-oxide-semiconductor (CMOS), also called active pixel sensors, dominate the camera phone market due to their low power consumption, fast readout, few components and cheap cost to manufacture. Although colourimetric techniques only require a calibration chart and do not require external instrumentation, their interpretation based on colour and intensity is subjective and is influenced by ambient lighting and the condition of dry and wet paper. The use of camera phones for on-site biomedical diagnostics has been previously demonstrated in dermatology,[283] microscopy,[284] ophthalmology[285] and lateral-flow assays.[286] There are two potential approaches to scale up of quantitative diagnostics with camera phones: (i) on-site readout with a preinstalled app and (ii) telemedicine. Both of these approaches have their benefits and drawbacks.

Image processing on phone. Lower-end Android smartphones ($75–200) with pre-installed apps can be distributed to healthcare workers. The image of the detection zones can be

Published on 08 May 2013. Downloaded by University of Cambridge on 31/05/2013 13:14:32.

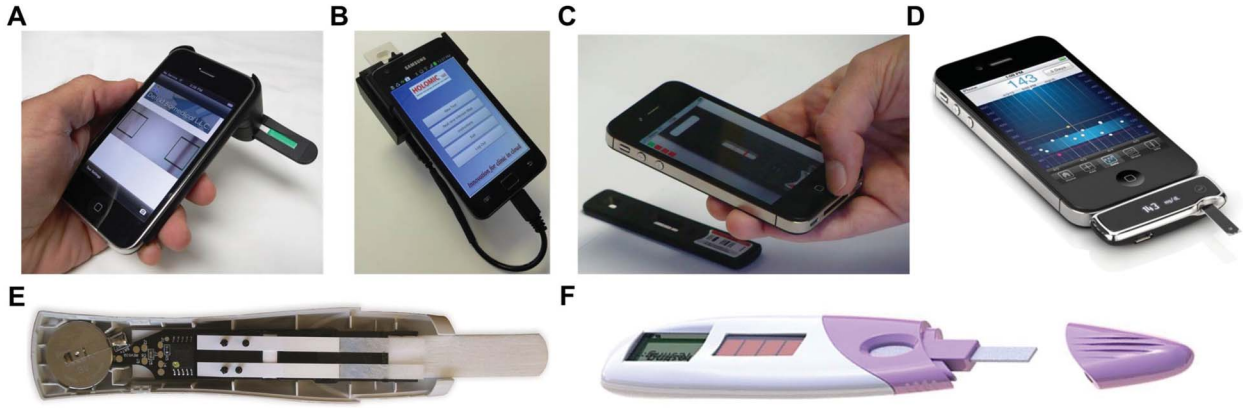

Fig. 17 Commercial readout devices (A) iPhone rapid diagnostic lateral flow reader. Courtesy of Detekt Biomedical L.L.C. (B) Android smartphone-based lateral flow reader. Courtesy of Holomic L.L.C. (C) Novarum reader. Courtesy of British Biocell International. (D) iBG star. Courtesy of Sanofi. (E) ClearblueDigital Pregnancy Test. © 2012 Swiss Precision Diagnostics GmbH. Clearblue is a trademark of SPD. (F) A solar powered digital strip reader. Taken from www.bioamd.com with permission from Bio-Alternative Medical Devices Ltd. (Cheshire, U.K.).

captured and processed by the native smartphone application. If required, the healthcare worker can send out the results *via* SMS or e-mail to a server for data mining. The method represents high capital cost, but low operating costs to quantify diagnostic results. The earliest examples are smartphone-based lateral flow test readers, which come with hardware that is mechanically attached to the smartphone. The advantage of using a reader is that the reading conditions can be standardised. An iPhone-based reader was introduced to the market by Detekt Biomedical L.L.C. and this reader comes with a price tag of $875 (Fig. 17A). The camera captures the images of the detection lines and processes the images through an app. The iPhone device is self-powered, supplying power to low-power LEDs. Depending on the assay format, which involves custom machining of parts, a customised unit can be delivered in 2–3 weeks. These units are expected to last 5–8 years depending upon work load and maintenance.[287] Recently, another iPhone-based lateral flow reader was reported to measure thyroid stimulating hormone.[288] There are also Android phone-based readers that comprises of a light-emitting diode based illumination (Fig. 17B).[289] This reader is now commercialised by Holomic L.L.C. (Los Angeles, CA). A smartphone app can enable the transmission of the results along with the images to a central server for geotagging and data mining. A real-time map with a web interface to monitor emerging epidemics can be generated. A rapid diagnostic test cloud information service is provided by SCC Soft Computer (Clearwater, Florida).

Another industrial partner, Novarum DX (Cardiff, U.K.), a joint venture of British Biocell International (Alere) and Albagaia Ltd. (Linlithglow, U.K.), introduced an Android and iOS phone-based Novarum reader without additional hardware (Fig. 17C). The company claims that the application can provide qualitative and quantitative results without being influenced by the ambient conditions and it can be adapted to function with any existing assay.[290] The platform requires a 5 Mpixel camera with autofocus. Because Novarum is a bespoke service, the application needs to be customised to the characteristics of the assay. A similar technology entitled Mobile Image Ratiometry[291,292] for testing seeds is marketed by Mobile Assay Inc. (Boulder, CO). In addition to smartphone-based optical readers, iBG star (Sanofi) introduced an iPhone-based electrochemical reader ($76) for the determination of glucose concentration in whole blood (Fig. 17D).

Despite their attractiveness, smartphone-based readers also have limitations. All these readers are demonstrated by current high-end smartphones and none of these platforms are available in open source. Additionally, these technologies are not originally designed for heavy duty: this means that a healthcare worker who needs to process many samples will drain the battery within 3–4 h (due to the energy-consuming screen and camera mode). Moreover, many of these technologies are not water-proof and this will be a barrier in extreme conditions. Also, currently, the Android hardware changes more quickly than the iPhone and as such it is difficult to accommodate so many versions of devices.[287] Platform obsolescence is a big issue for smart phone based systems. Ambient lighting and focal distance are huge factors in the quality of the read. These systems are in fact far more prone to error than the previous category discussed, which have hardware designed to overcome the issues listed. Smartphone Apps will also likely fall under FDA regulation very soon. In the developed world, the industry will ultimately accept these technologies: however, in low resource environments for undemanding infectious disease applications, these types of systems might not be useful for quantification or other highly demanding functions without some associated hardware.[47]

Telemedicine. In this service, a healthcare worker captures the image of the rapid test (*e.g.* colourimetric) and sends it to a server *via* Multimedia Messaging Service (MMS) or e-mail. The server analyses the image based on greyscale or RGB/chromaticity values using imaging software and the RGB values and grey values correlated with the concentration of the target analyte. The results are sent back to the healthcare worker *via* SMS. In this case, capital costs are lower, but operating costs are high. Although telemedicine allows real-

 This journal is © The Royal Society of Chemistry 2013

Published on 08 May 2013. Downloaded by University of Cambridge on 31/05/2013 13:14:32.

time data acquisition, its practicality is limited in sites without a signal or reception. All these processes can be accomplished by open source software. For example, the FrontlineSMS is an open source software solution that is capable of distributing and collecting SMS/MMS from multiple users.[293] The software only requires a computer and a mobile phone. Additionally, a patient information recording capability can be achieved through other platforms such as Medic Mobile.[293] Potentially, telemedicine can be adopted by these platforms to deliver diagnostically relevant information.

The major drawbacks of telemedicine are challenges in standardizing shading and lighting conditions, sensitivity, resolution, focus, and the background noise of paper. Camera phones are not optimised for capturing the images of colourimetric assays. They comprise of automated functions (*e.g.* auto white balance) which adjusts the RGB values at various ratios resulting in bright images. For example, embedded functions such as integrated colour balancing are tailored to photography (bright lighting conditions). Small alterations in colours can render RGB image analysis challenging for quantitative analysis. However, reference charts could be employed during readouts. Known colour intensities can allow the camera phone to process the image while compensating for ambient light differences. For example, calibration curves of the analyte concentrations can be built based on chromaticity values.[266]

On-chip quantification. The ClearblueDigital Pregnancy Test with conception indicator (Swiss Precision Diagnostics GmbH, Geneva, Switzerland) is a semi-quantitative assay. It comprises of blue latex particles that function as markers of hCG and it measures the density of the lines by an optical sensor (Fig. 17E).[93,294–296] The sensor (*i.e.* a miniaturised chromameter) illuminates the detection zone with a red light and converts the reflected light to an electrical signal, therefore determining the concentration of hCG. A fork-shaped assay consists of a main channel that branches into two strips with low and high sensitivities of detection. The control line is on the low-sensitivity strip. For 1–2 weeks of conception, the result line on the high-sensitivity channel exceeds the threshold set for the 1–2 week average hCG level, but not the 2–3 week average hCG level. For 2–3 weeks of conception, the result line on the high-sensitivity strip exceeds the threshold set for the 2–3 week average hCG levels, but the result line on the low-sensitivity strip does not exceed the threshold set for the 3+ week average hCG levels. For 3 weeks of conception, the result line on the low-sensitivity strip exceeds the threshold set for the 3+ week average hCG levels. A battery-powered screen displays a yes/no answer and the duration of conception in writing. Such on-chip readers can also be powered by solar energy (Fig. 17F).

5. High-volume manufacturing

The time to market must be as short as possible. In the expansion of the new diagnostics platforms to international markets, the feasibility for high volume manufacturing will be a determining factor. Scaling up in excess of 100 million test units per year to meet the market demand requires manufacturing capabilities that can function 24/7.

The early core intellectual property of manufacturing processes belonged to a few large companies, but the development methods were quickly adopted by many smaller companies in the 1990s. Later, relatively small size companies developed their own manufacturing processes, which were initially designed for acceptable performance, but not quantitative measurements. Other challenges included the treatment of different components of the assays with complex fluids (*i.e.* surfactants and proteins) in a consistent manner. The reproducibility of lateral flow and flow-through assays differ in market segments due to their performance requirements. These assays also have a reputation of not being reproducible for applications that require quantitative analysis. The inter-assay variation stems from their multi-material nature and inconsistency in the manufacturing techniques. Recent market needs have evolved assays with true quantitative formats while demanding improvements in manufacturing coefficients of variation. Although the academic community claims that paper-based microfluidic devices might be a player to fill this gap, this statement is highly disputed by the *in vitro* diagnostics industry.[47] The strongly opinionated industrial partners expressed that paper will create more variability in the final product.

A key step to enter the market is compatibility with the current manufacturing practices which might enable easy adaptation of paper-based microfluidic devices. A potential demand to adopt paper-based microfluidics might force the standards of manufacturing processes to evolve. Modern manufacturing techniques consist of (i) batch (ii) in-line processes. While the batch process is more labour intensive and convenient for small-size production, in-line process is fully automated and tailored to meet the needs of a specific application. Both of these processes consist of four key steps: (i) reagent dispensing, (ii) drying, (iii) slitting (required for materials in wide webs) and (iv) laminating (Fig. 18A). In batch processing, lateral-flow test components are loaded in card stocks and processed individually. Batch processing is vulnerable to variation due to the uptake of the fluids, control of the dissolved components and inconsistencies in the drying processes. Because each material is processed independently, it entails operator interference. Batch processing has been the dominant technique due to its ease in being scaled up from low-volume development, but it suffers from low-quality that is heavily influenced by manual operations. Although it has lower capital costs, its manufacturing capacity is limited (*i.e.* 10 million units per year). Batch systems can be used up to a capacity of 1 million units per year; beyond this, batch processing becomes relatively slow and costly, and the greater capital expenditure on equipment for in-line processing becomes more economical. The automated systems comprising of quantitative dispensers and in-line drying offer test strips with less variability than batch processing.[297] In-line process starts multitasked manner as they move along the conveyor system (Fig. 18B). Many of the high-volume lateral

Published on 08 May 2013. Downloaded by University of Cambridge on 31/05/2013 13:14:32.

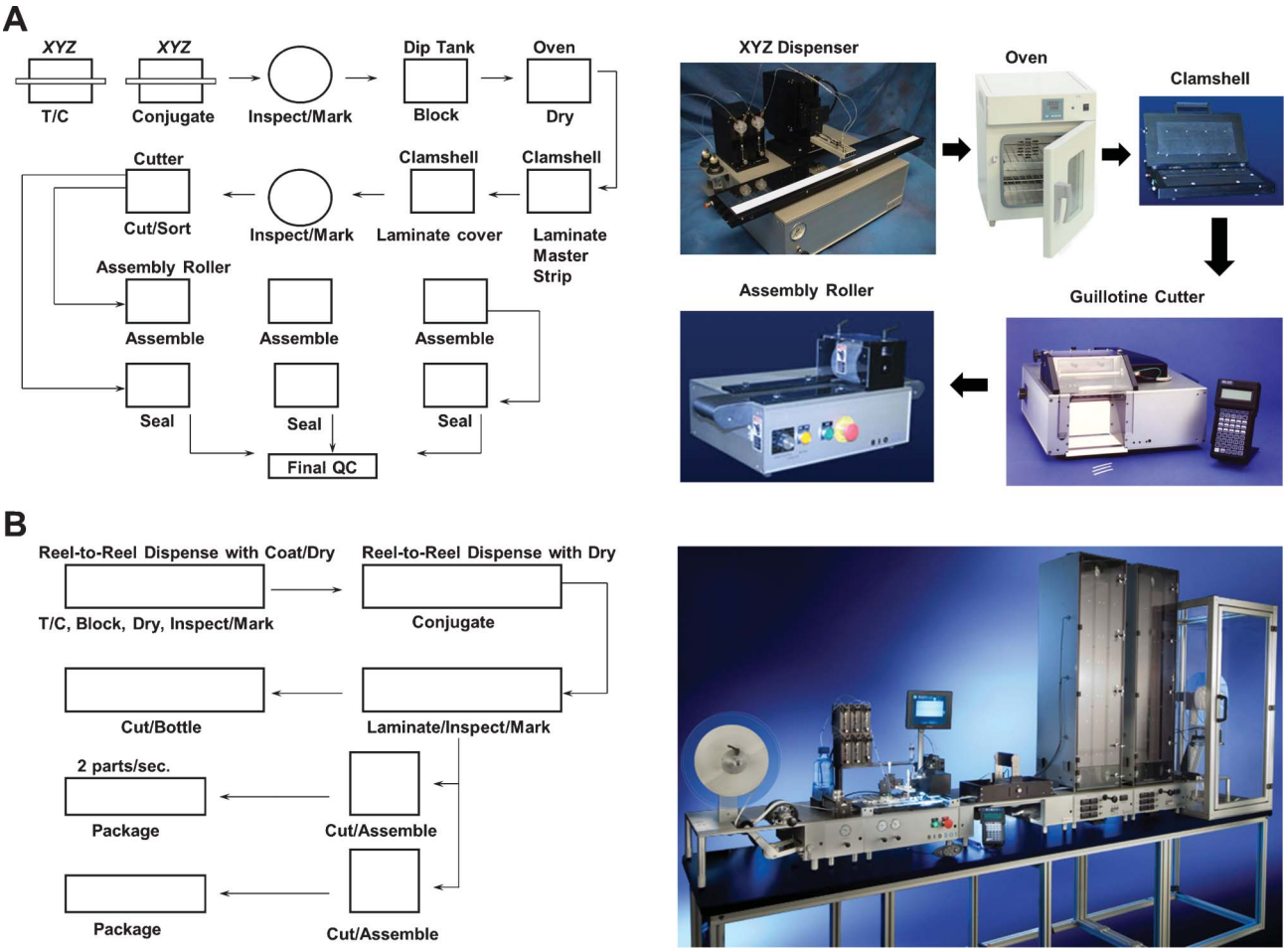

Fig. 18 Modern rapid test manufacturing. (A) Batch process and (B) in-line process. Courtesy of Biodot Inc.

flow tests (*i.e.* 100 million units per year) are manufactured in China. The batch systems and in-line systems cost about \$75–150 K and \$150–500 K, respectively.

5.1 Rapid test fabrication

The fabrication process starts with reagent dispensation. Impregnation is the process of saturating a material with a reagent. Historically, reagents are applied to the materials in two ways: (i) submergence of the material in a reagent reservoir followed by squeezing and drying in a tunnel and (ii) non-contact or contact dispensation. The easiest way to impregnate materials with reagents is dipping them into fluid tanks. The materials, in card stock or roll stock, can be submerged into a dip tank that comprises of fluid level sensors and metering control for consistent impregnation. However, glass fibre and polyester pads take a long time to impregnate due to their hydrophobicity; and to ensure impregnation in the batch format, the sheets are often stirred by ultrasonic vibration, whence the surface moisture is removed by blotting or squeezing. Nevertheless, the saturation and drying process can be the source of variation in batch to batch processes. More controlled results can be obtained if the process is executed in a continuous process. However, the submergence technique is ruled out for paper or nitrocellulose-based microfluidic devices.

A quantitative way of dispensing reagents on to the materials is by using dispensing sprays to cover a specific region by either discrete droplets or lines. If the materials are in card stocks, the dispensers are mounted on a robotic head. However, if the materials are in roll stocks, the dispensers are used in a reel-to-reel configuration for continuous dispensing. Reagents can be dispensed on the components quantitatively in three techniques: (i) non-contact, pump-driven solenoid dispensers,[298] (ii) contact tip dispensers (BioDot, Inc. (Irvine, CA) and Imagene Technology, Inc. (Hanover, NH) and Zeta Corporation (Korea)) and (iii) airbrush dispensers[298] (Kinematics Automation, Inc., Twain Harte, CA). Typically, most of these systems can process membranes running at speeds of 25 mm s^{-1}. Non-contact dispensers functionalise drop actuators such as solenoid systems (Fig. 19A). The pressure built by a hydraulic pump with a positive displacement system allows the dispensation of the reagents in a non-contact manner. In a reaction matrix, the protein solutions are absorbed quickly on impact of the drop. Hence, the width size of the hemispherical drop determines the dimensions of the developed protein line. The solenoid valves are capable of

 This journal is © The Royal Society of Chemistry 2013

Published on 08 May 2013. Downloaded by University of Cambridge on 31/05/2013 13:14:32.

dispensing small volumes of 15–20 nL which can eventually produce lines with widths of 0.5 mm. Contact tip dispensers comprise of a reagent reservoir, a syringe and a flexible tip that can be dragged across the surface of the membrane (Fig. 19B). Although, the amount of reagent dispensed can be quantified by the accuracy of the syringe or pump, the absorption rate of membrane is often uncontrolled. Other key factors that affect the absorption rate include protein concentration, viscosity of the fluids, pore size and the environmental conditions (*e.g.* ambient relative humidity and temperature), surface smoothness and other contaminants (*e.g.* dust). However, the contact tip might disturb the substrate as it is dragged across the membrane surface and potentially cause false positives. Another quantitative way of depositing reagents on the materials is airbrush dispensers. These dispensers consist of a positive displacement system and pneumatic spraying heads. They are capable of dispensing microliters of reagents quantitatively on the substrate (Fig. 19C). This setup is also capable of delivering spots with a minimum size of 0.5 mm in diameter. However, this system is not suitable for forming sharp edges, and therefore, it is adopted in coating and impregnation of the assay components. Such pad impregnation processes include pretreatment of the sample and conjugate pads in order to make them hydrophilic, adjust the pH and control the flow rates. Another application of airbrush dispensers is blocking.[299] The cost of adopting airbrush dispensers is low; however, it is limited in quantitation, bubble formation influences their reproducibility, and environmental conditions such as temperature and humidity may have to be controlled for reagent processing. Humidity in the range of 40–60% during reagent incorporation and 20% relative humidity prior to packaging are preferred.

Consistency in the immobilisation of immunologically active proteins onto the test and control bands of nitrocellulose membranes is a key parameter in order to obtain high sensitivities and reproducibility. If the proteins are unable to bind covalently and directionally to the reaction matrix, they cannot maintain their immunological activity after binding. Hence, electrostatic attraction is adopted to achieve long-term binding with electrostatic, hydrophobic and hydrogen bonding forces in nitrocellulose membranes. Conditions for the optimisation of binding are 25–50% relative humidity at room temperature. Other concerns related to binding include the contact tip and non-contact deposition techniques, their impact on protein binding and spread throughout the membrane. Non-contact dispensing methods are preferred due to their quantitative dispensation of proteins on membranes.[97]

The assay components can be blot dried or dried in high temperature furnaces. This process is often overlooked and it can be a source of variation in humidity. The duration of drying and the method of drying have an impact on the activity of the proteins within the membrane. The purpose of drying test and control lines is to prevent unstable coating of immuno-active proteins. There are a number of stages for the deposition of proteins on the material surface. Initial binding to the surface starts with electrostatic interactions; this is followed by the evaporation of water and the unfolding of the hydrophobic interior of the protein. At this point,

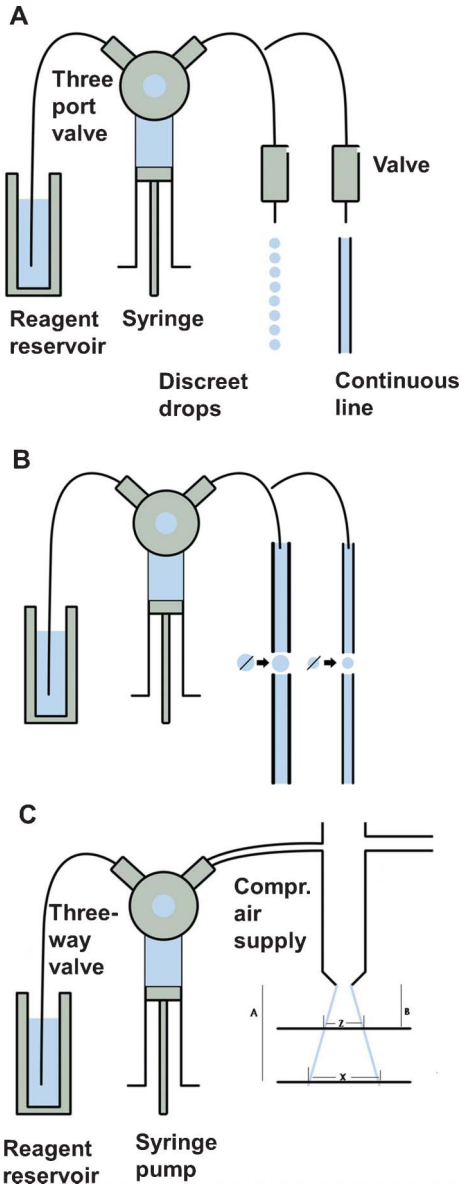

Fig. 19 Schematics of modern dispensing methods. (A) Noncontact dispensers (B) Contact dispensers. (C) Airjet applications of liquids.

hydrophobic binding takes over and eventually leads to the final configuration of the protein. Hence, achieving consistency in the evenness and stabilisation of the protein depends on the drying methods and timing. Forced air at high temperature and the less adopted method of lyophilisation are the two drying methods practiced by the diagnostics industry. Forced air drying can take place in (i) batch ovens (Fig. 20A) or (ii) in-line drying ovens (Fig. 20B). For card stocks, temperature controlled ovens with infrared sensors allow an even distribution of airflow in order to dry consistently across all the cards. However, conditions of batch drying can cause inherent variation in the assay performance. For in-line processing, the reel-to-reel system includes convection-based drying towers, which allow consistent temperature air to flow

Published on 08 May 2013. Downloaded by University of Cambridge on 31/05/2013 13:14:32.

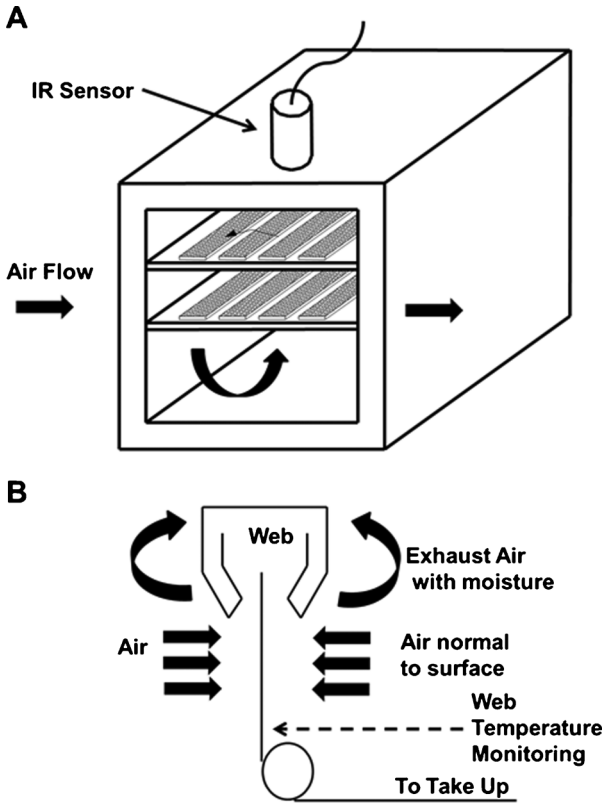

Fig. 20 Drying (A) batch processing (B) in-line drying.

through to achieve a controlled and uniform drying of the web material.

In lamination, the assay components are assembled together in this step. In lateral-flow tests, a typical test requires a plastic adhesive backing card. This process also differs in card stock and roll stock configurations. The simplest assembly is achieved using a clamshell laminator, in which, the materials are manually placed into an insert that aligns the components. The device comprises of vacuum and mechanical alignment fixtures to assemble the components into a complete card. In in-line processing, automated laminator systems operate with card and roll stocks.

Guillotine or rotary cutters singulate the complete cards into individual tests. Because edges have a profound effect on the flow characteristics, the processes of slitting and cutting must be controlled to achieve consistent assays. Slitting can take place before or after reagent treatment. Cutting perpendicular to the web axis to form individual strips can be performed by guillotine and rotary cutters. In guillotine cutting, a blade moving down works against an anvil to cut the material, whilst the rotary system comprises of a blade set spaced $\geqslant 4$ mm and this configuration enables cutting at one time.

5.2 Mass manufacturing of paper-based microfluidics

Paper-based microfluidics can easily be incorporated into mass manufacturing processes. One of the manufacturing techniques may involve the following steps: (1) dispense wax on paper or nitrocellulose, (2) melt wax, (3) dispense reagents, (4) dry reagents, (5) laminate (optional), (6) cut into individual strips and (7) package. Other methods such as dispensing AKD, CO_2 laser cutting and other methods can also be integrated in mass scale processes. Especially, CO_2 laser cutting strikes a good balance in quantity and quality, where mass manufacturing and close precision can be realised. However, the establishment of such advanced manufacturing systems might not be established in rural settings with limited resources. Existing mass manufacturing methods are capable of accommodating paper-based microfluidics in 2D, but 3D microfluidics will require custom-made in-line equipment. The compatibility with the existing assembly lines can eventually drive costs down. In this milestone, a one-step process for forming hydrophobic barriers (or hydrophobic channels) in the paper or nitrocellulose will ease the potential adoption by the industry. This milestone might be achieved by selectively depositing surfactants on nitrocellulose to form hydrophilic channels.

While much of the early (and even current) work focuses on methods for fabricating microfluidic channels, equally simple and efficient methods are needed for depositing assay reagents in the appropriate regions on the devices. In a manufacturing scheme, the deposition of reagents can be accomplished using computer-guided pipettes, or by spraying reagents through a mask in a reel-to-reel process. In the laboratory, and in small-scale manufacturing, reagents are deposited either by spraying, inkjet printing, drawing (*e.g.* graphite)[300] and manually pipetting. The reagents are deposited as solutions in most cases, but are stored dry on paper. For sensitive reagents (such as proteins), extra effort is required to stabilise the reagents on paper, such as depositing the protein reagent in a solution of the sugar, trehalose. Additional studies geared towards stabilizing reagents on porous media is required in this context, as will the development of assay reagents that are substantially more stable than native proteins.

6. Challenges and future directions

6.1 Market

The global *in vitro* diagnostics (IVD) market was valued at $44 billion (B) in 2011 and growing at a compound annual growth rate (CAGR) of 7.8%.[301] The largest share of the market is with the United States at 47%, while the fastest growing market is China with a CAGR of 18.8%.[301] Current UK spending on diagnostics is £2.5 B per year.[302] The important market segments are given in Fig. 21. The largest segment at 36% is point-of-care testing, in which lateral flow tests constitute the majority of this segment.[302] The fastest growing area is the integration of molecular diagnostics with point-of-care testing.[302]

6.2 Competitive advantage over existing technologies

There is an urgent need for low cost diagnostics for the developing world (see Section 1.1). Due to a lack of modern infrastructure, central laboratory facilities are few and far between; therefore, user-friendly technologies are required

 This journal is © The Royal Society of Chemistry 2013

Published on 08 May 2013. Downloaded by University of Cambridge on 31/05/2013 13:14:32.

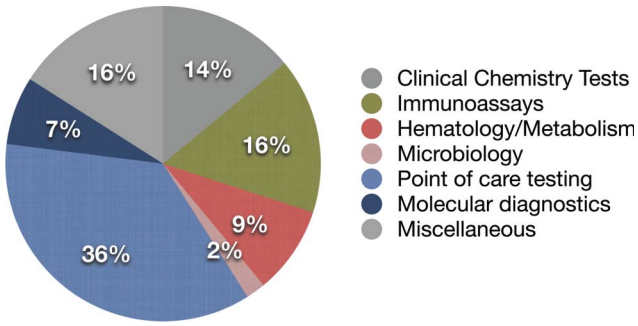

Fig. 21 *In vitro* Diagnostics Market Segments. Segments of the *in vitro* diagnostics market are presented according to the targeted therapeutics area. Modified from ref. 301 and 302. Copyright (2011) Markets and Markets, Copyright (2006) Business Insights Ltd.

which can be used in a variety of environments without any significant input from an expert. Low-cost lateral flow tests seem to be an ideal candidate to fill this gap since they can be manufactured for \$0.10–3.00 per test. The development costs for lateral-flow immunoassays are also low and range from \$30 K to \$100 K per test if the target analyte and necessary antibodies are available.[97]

Paper substrates are one of the many researched options to achieve this goal of low cost diagnostics.[303] The cost savings come from a reduction in the cost of goods, especially reagent pads that have microfluidic channels to carry out the reactions. It is calculated that paper-patterning costs can be as low as <\$0.01,[303] including the price of the paper, which is considerably lower than the cost of moulded plastic microfluidic patterning per test.[304] The microfluidic plastic should not be confused with the inexpensive housing laminates which are common to most formats of lateral flow tests. The silk-based platform (Fab-chips)[173] also offers a low cost alternative.[304] Fig. 22A shows the breakdown of a transaminase test developed on a paper substrate by Diagnostics for All and Fig. 22B gives breakdown of costs for a fabric-based immunoassay developed by Achira Labs (India). The costs are amortised over the production of 10 million chips. It needs to be acknowledged that adequate cost generalisations cannot be made until a large number of tests reach the market and achieve comparable economies of scale for production. For both parts of Fig. 22, the costs are calculated for manufacturing in India, which definitely lowers the cost of manpower and equipment but prices for specialised reagents are comparatively higher than the developed world. Antibodies make the major proportion of Fab chips but even if cost of the

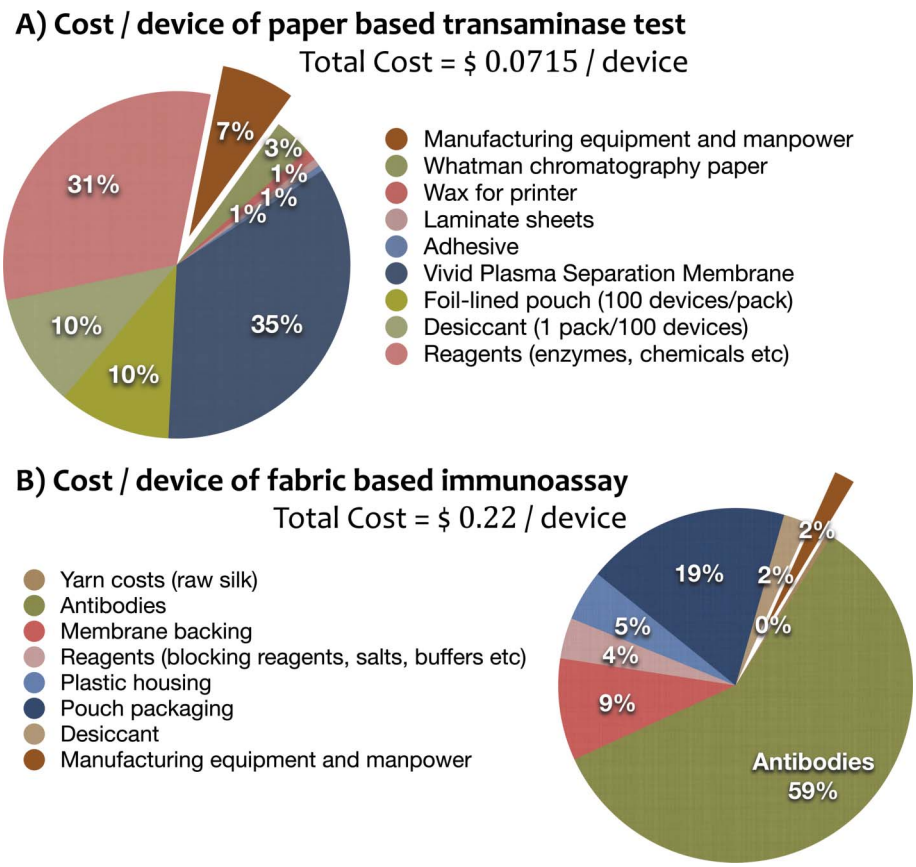

Fig. 22 (A) The breakdown of cost/device of paper based transaminase test. The total costs per tests are calculated to be \$ 0.0715. These costs are based upon Indian market and in the U.S., it would 2 to 3 fold higher. The figure is drawn from a supplementary table given by Diagnostics for All in ref. 143. (B) The breakdown cost/device is given for Fabric based chips developed by Achira labs (India). The total cost of a device is \$0.22. For both A & B, costs are amortised over 10 million devices. The exploded pieces of the pie charts represent the fixed costs as compared to consumables.

Published on 08 May 2013. Downloaded by University of Cambridge on 31/05/2013 13:14:32.

antibodies is removed from the calculations, paper based tests are 3 fold less expensive than the fabric chips. However, the social impact of Fab chips is commendable as it is putting artisans of India to use. Sample preparation is another area where innovation is required to bring the costs down as it can be seen that plasma separation membranes are the most expensive component of the paper based blood tests. However, Diagnostics for All believes that the cost of these tests can be reduced to as low as $0.10, which is significantly lower than the current cheapest point-of-care instruments for blood chemistries, which cost about $2500 for the reading unit and $5 for each test.[305]

6.3 Commercialisation of paper-based microfluidics

It will be very challenging, yet not impossible, for a biotechnology or a diagnostic company, research group or investors to capture value from paper-based microfluidics. Despite the perceived potential advantages in terms of reduction of costs with the use of the paper, there are number of factors which will define the commercialisation strategy. Different strategies need to be considered based on the geographical placement (developed or the developing world) of the product and also on the therapeutic area (established or new).

If the market is mature for a particular therapeutic area, then expecting a shift from current diagnostic methods to paper-based microfluidics is unrealistic. Any company considering this shift would have to incur heavy costs in relation to the changing existing assembly lines (infrastructure) and creating new proprietary technology around paper or in-licensing existing patents, which may require modifications to already patented reagents. Unless, and until, there is a significant technological advantage in using paper, there is no impetus for these companies to shift. The maturity of the market is fairly evident for diseases such as HIV/AIDS, cardiovascular and lysosomal storage diseases, respiratory infections and blood chemistries.[302] This is further evident from consolidation in the industry, where the leading 15 companies account for 90% of the global IVD market and, out of these 15 top companies, only 6 are pure diagnostic companies,[302] the rest being diagnostics divisions of big pharma companies. Most of the larger diagnostic companies have been acquired *e.g.* Dade Behring, Diagnostic Product Company, TheraStat, i-STAT and MediSense (Table 6). The acquisitions are not only limited to developed economies; small manufacturing companies and distributors have also been acquired in the developing world *e.g.* the acquisitions of

Table 6 Consolidation in the diagnostics market

Diagnostic companies	Revenues	($ million)	Major acquisitions of diagnostic companies	Value of acquisitions ($ million)
Roche[314]	Pharma	34 571	Boehringer Mannheim[309]	11 000
	Diagnostics	10 654	Ventana Medical Systems[315]	3400
			Igen[316]	1400
			Bio Veris[317]	600
Abbott[314]	Pharma	31 774	TheraSense[318]	1200
	Diagnostics	4126	Medisense[319]	876
			i-STAT[320]	392
			Vysis[321]	355
Siemens Medical Solutions[322]		15 800	Dade Behring[323]	7000
			Bayer Healthcare's Diagnostic[a324]	5380
			Diagnostic Product Company[324]	1860
Becton Dickinson & Co[314]	Medical	4007	Handylab[325]	275
	Diagnostics	2480	GeneOhm Sciences[326]	255
	Biosciences	1341		
Danaher[327]	Diagnostics	6300	Beckman Coulter[328]	6800
			AB SCIEX & Molecular Devices[329]	1100
			Tektronix[330]	2800
			IRIS International[331]	352
			LabIndia[306]	0.69
Hologic[332]		1783	Cytyc[333]	6200
			Gen-Probe[334]	3800
			Third Wave Technologies[121]	580
			GTI Diagnostics[335]	53
			Sentinelle Medical[336]	85
Alere[314] (Formerly Inverness Medical Innovations)		2363	Axis-Shield plc[337]	356
			eScreen[338]	270
			Standard Diagnostics[339]	224
			Epocal Inc[339]	175

[a] Not including the Bayer's Diabetes Care Division.

 This journal is © The Royal Society of Chemistry 2013

Published on 08 May 2013. Downloaded by University of Cambridge on 31/05/2013 13:14:32.

IndiaLab by Danaher[306] and TCT International Co. (Chinese distributor) by Hologic.[307]

Furthermore, it can be seen from the acquisition data that most of big pharma has invested in small or mid-sized diagnostic firms and these companies are generating healthy revenues from their sales. Combining these acquisitions and investments with a pipeline of future products tells us that the diagnostics sector is not under severe downward pressure as faced by the slowing pharmaceutical sector, due to the patent cliff, health service constraints and burgeoning research and development costs.[308] Roche Diagnostics maintains its position as a market leader since its acquisition of Boehringer Mannheim in 1997 for $11 B.[309] They made an attempt to acquire Illumina for $5.7 B earlier last year (2012),[310] which, although unsuccessful, re-iterates the strong intent of established pharma and diagnostics companies to acquire mid-sized diagnostic companies. For any small diagnostic company with a strong proprietary technology, which can sustain itself on venture funding for a period of around 4–5 years and can raise funds of around $5–10 million, would have a fair chance to exit on a good trade sale. However, to make it to the market, it will be of utmost importance that a company's products fill a genuine gap in the market rather than acting as a replacement product. One such opportunity is the field of theranostics where large pharmaceuticals want inexpensive diagnostics for the monitoring of drugs during their clinical trials, *e.g.* Diagnostics for All has been approached by pharmaceutical companies to create accompanying sensors to monitor liver toxicity during the clinical trials for their drugs for HIV and TB.[305]

Stifled growth in the developed world has given way to viable business propositions in the developing economies[311]. On one hand, it is forecast that seven countries (China, India, Russia, Brazil, Mexico, Indonesia and Turkey) from the developing world will treble their GDP (Gross Domestic Product) by 2020[312] and, by 2050, Asia alone will account for 51% of the world's GDP,[313] thus making them an ideal place to invest. On the other hand, their healthcare systems have not yet evolved, good clinical laboratories are scarce and reimbursement routes are unclear. For most of the poorer countries, the proportion of patients paying out of their pockets is much higher than those paying through government schemes or public money. In this scenario, the rich/poor gap becomes increasingly important and any modestly expensive drug or diagnostic test is effectively inaccessible for the poorest sector of the population. Unfortunately, this inequality gap is increasing,[340] which makes it even more important that diagnostics should be made cheaper and designed keeping in mind the purchasing power of these poorer populations.

Fortunately, this challenge has been realised by some philanthropic organisations and exploited by a handful of fledgling diagnostic companies. The ideal business model appears to drive product development through grants from governmental or non-governmental organisations. The governmental organisations that have invested in low cost diagnostics are the Department of Defense (DoD) through Defense Advanced Research Projects Agency (DARPA), Small Business Innovation Research (SBIR); USAID; National Institutes of Health (NIH) through the National Institute of Allergy and Infectious Diseases (NIAID) and the National Institute of Biomedical Imaging and Bioengineering (NIBIB); Centers for Diseases Control and Prevention (CDC); Department of International Development (DFID) and Grand Challenges Canada. The non-profit organisations that have invested significantly in low-cost diagnostics are the Bill & Melinda Gates Foundation and PATH.

One additional aspect that can help in raising funds from private sources is to focus on a working diagnostic device as an end product in a particular therapeutic area rather than as a technology platform. For *in vitro* diagnostics, too many competing technologies have been suggested and this just adds to the complexity and lack of investor interest. Moreover, it is not judicious to try to fund fundamental science through investors' money, as product development on its own is expensive. Identifying when a technology is ready to be commercialised for product development is the key to success of a company. George Whitesides, in his recent editorial, explains this very well "If the science of something is still interesting, the 'something' is probably not ready to be a product".[3]

Most of the rules that apply to winning academic grants also apply to raising funds for businesses as well. For developing countries it can be very useful to pick certain therapeutic areas, *e.g.* diseases that are perceived as huge problems in that geographical area, makes it easier not only to raise funds but also to get reimbursements for the product. In Africa, it is very useful to target a disease, which is on the priority list of the World Health Organisation (WHO) and the United Nations (UN). For low cost diagnostics, Diagnostics for All[341] in Africa has very successfully targeted assessment of liver damage from HIV medication (*e.g.* lactate dehydrogenases, transaminases and albumin) and at risk pregnancy; similarly, Achira Labs in India is about to market a cheap diagnostic test for thyroid diseases.[342]

6.4 Regulatory issues

Understanding of regulatory issues is extremely important for the development of low cost diagnostics. Device safety regulations are in place to ensure the impact of the diagnostic test or effect of the device on the health of the patients, especially in relevance to false positives and false negatives. The final marketing approval of a product also specifies the claims that a manufacturer can make; therefore, it essentially defines the patient population of the test. All the products are classified according to the risk where Class 1 diagnostics are subjected to the least and Class 3 diagnostics are subject to the most stringent regulatory process.[343]

On average, the development of a new diagnostic test or device takes 7 years.[302,344] The time also depends on the route taken for the approval process. In Europe, the '*In vitro* diagnostics directive' regulates all new devices and it entails all the essential requirements for design, production, labelling and information provided to the user. The product needs to go through the 'Conformity Assessment Procedure' to get CE marking, which once obtained, allows the manufacturers to test or sell their device across Europe.

There is a dual system in the USA, where manufactures of medical devices are regulated by the 'Office of IVD Device

Published on 08 May 2013. Downloaded by University of Cambridge on 31/05/2013 13:14:32.

Evaluation and Safety' of the Food and Drugs Administration (FDA), and a separate system, where diagnostics are regulated under the Clinical Laboratory Improvement Amendment (CLIA). If a test gets CLIA approval then it doesn't need FDA approval. There are three major regulatory pathways for devices to get to the market Exempt from FDA review 510(k) clearance process Pre-market approval (PMA) review

It is not within the remit of this review to discuss the finer differences between different approval routes; however, it should be noted that these pathways affect the development times, *e.g.* the review time for 510(k) submission is 90 to 120 days, as compared to one year for PMA. The 510(k) submission is used for new devices for which comparable devices are present on the market and manufacturers simply prove that the new device is as effective as the one already in the market. However, if the FDA determines that the data provided suggests that the new device raises new safety or effectiveness issues, the device automatically becomes a class 3 and needs to go through PMA review or a product development protocol (PDP), which allows relatively faster approval of class 3 devices with established technology.

Almost all PMA submission requires clinical data and, prior to starting clinical trials, a company needs to obtain Investigational Device Exemption (IDE).[343] There are three levels of CLIA approval depending on the complexity of the test. For simple tests, CLIA is waived and for moderate and high complexity, tests have to go through CLIA approval. For inexpensive point-of-care diagnostics, it is advisable that the test should be simple enough to be CLIA waived and a reference test included or it should be self-calibrating. For the developing world, it is essential that tests can be used and interpreted without expert personnel. The development pathway and the average time and costs to commercialise a diagnostic test are given in Fig. 23. This represents the average time to market once the technology underpinning it is established. The development costs show average values for medical devices;[302] however, lateral flow tests are significantly less expensive to develop.

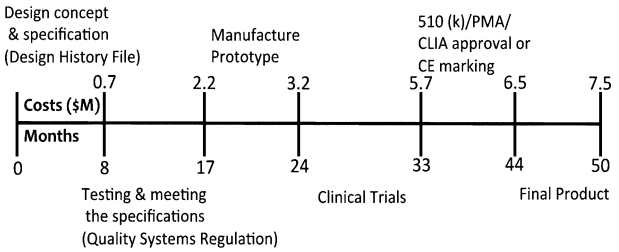

Fig. 23 Medical Device and IVD Development Pathway. A detailed design history file should be created and updated on a regular basis for FDA. The quality systems regulation (QSR) ensures that standard operating procedures are taken care of. It is advisable to have frequent meetings with the FDA at a preclinical stage to agree upon the plan and throughout the clinical trials to mitigate any safety issues. The development costs are given for medical devices but for lateral flow tests, costs are significantly less.

7. Conclusion

Paper-based microfluidics is still in an early development stage.[42–44] In order to create real-world products, capabilities of paper-based microfluidics must evolve to become a mature platform. Extending beyond the characteristics of commercial papers to novel paper-biofunctional material hybrids, and the integration of novel materials into paper can lead to more biocompatible substrates. The control over structural properties of paper, advances in deposition of hydrophobisation materials through printing will play greater roles in the realisation of paper-based microfluidics. Studies on paper-protein/enzyme interactions, surface energy, release characteristics, paper decay, the impact of temperature and moisture will gain momentum in the realisation of paper-based microfluidics beyond R&D. Understanding the fundamentals of capillary flow in paper-based microfluidics will allow construction of assays with improved control. To date, limited studies have employed unprocessed samples. Incorporation of sample preparation must not be overlooked.

Sensing and detection technologies will also evolve. Furthermore, the quality of paper after long-term storage, and time-consuming sensors (*e.g.* full colour development) require further improvements. The search for quantitative equipment will play a greater role in future diagnostics. According to some commentators, these attributes may include user-friendly fool-proof text/quantity-reporting capabilities and unexplored sensing mechanisms such as paramagnetic particles, quantum dots, coloured latex particles, diffraction gratings and genetically engineered whole cells (*i.e.* synthetic biology). Some of these sensing mechanisms might not require physical blocking or shaping of the substrate for multiplexing.

Although significant time has been devoted to quantitation with camera phones/handheld readers, the attribute of ASSURED equipment-free criterion must not be overlooked. The use of external readers is a barrier for existing assays, yet this requirement will be a greater challenge in adopting capillary-based microfluidics. Although the fast-growing mobile phone market in the developing world has made camera phones a potential platform for the delivery of rapid diagnostics, mobile phone connectivity must be increased and communications costs must be reduced.[345] Advances in the development of high-resolution cameras, the standardisation of image quality, the improvements in battery life and the development of waterproof smartphones will accelerate the efforts towards the realisation of telemedicine.

One may predict that novel approaches towards instrument free detection of amplicons along with the development of PCR-on-paper or nitrocellulose, whole cell detection on paper/nitrocellulose, tissue-on-paper and all-in-one assays will be important contributions to the field. There are some grounds for suggesting that the multiplex assay formats (Fig. 2H) will be exploited further by the *in vitro* diagnostics industry. All these advances will lead to multiplexed assays that are capable of identifying the specific etiological agent that causes a particular syndrome.

 This journal is © The Royal Society of Chemistry 2013

Published on 08 May 2013. Downloaded by University of Cambridge on 31/05/2013 13:14:32.

Intensive effort is required to transform the prototypes into a highly reproducible diagnostics platform. Having performance data does not always yield efficacy after deployment. Possible trials must establish the feasibility and cost-effectiveness after scaling up. The ultimate test in the realisation of paper-based microfluidics depends on experts in the commercial diagnostics industry and this may require evidence for acceptance. One challenge for the academic community is to justify the feasibility of the proposed technologies. Today, the rapid diagnostics business is based on a standard lateral flow format, involving the use of nitrocellulose as the reaction matrix. The lateral-flow format is the only ubiquitous, universally applicable platform that can be utilised for simple, qualitative, low cost point-of-care applications, while also having enough capability to be utilised in highly sensitive, fully quantified, multiplexed assays. Paper is an inconsistent matrix and it might not have many of the required characteristics for *in vitro* diagnostics.[47] The industrial partners still need to be persuaded whether paper is good enough for performance characteristics and large scale manufacturing basis, even for relatively low-performance requirements. The major markets in rapid diagnostics are in fact going the opposite direction, and demanding more rather than less of the assays. According to Brendan O'Farrell (Diagnostic Consulting Network, Carlsbad, CA), in terms of impact in market terms, lower performing tests might not have a large market impact in the developed world. In developing world markets, some applications may be found, but even there purchasing decisions tend to go through the tender process from organizations like the WHO or other large foundations and governmental agencies, who look for performance as well as price. It may be expected that low cost on its own will not be enough to achieve market penetration.

The value of diagnostics can only be realised if they meet the performance requirements, manufactured at high-volume and actions can be taken towards treatment. The killer app for the lateral flow format was the pregnancy strip and all other applications followed that. In capillary-based microfluidics, we need something similar.[346]

Acknowledgements

The authors thank Paul Yager, Scott T. Phillips, Andres W. Martinez, Brendan O'Farrell, Bernhard Weigl, Jason Rolland, Camilla Benfield, Charles S. Henry, Elain S. Fu, Barry R. Lutz, Damon Borich, Ken Banks, Leon Chen, Ketaki Sood, Juan L. Martinez-Hurtado, Anthony Haynes, Sai Krishna Nanduri, Linan Jiang, Peter Corish, Neil Polwart, Emma Browne, Jim Whelan, Andrew Clementson, Wanida Laiwattanapaisal, Barbara Mcintosh, Andrew Sweet, John Witton, Simon Taylor, Richard Hughes, Jamie Yacco, Xin Liu, Pratik Shah, Barbara J. Hunter, Helen Rabbitte, Shawn Gaskell, Jody Vacala, Dhananjaya Dendukuri, Colin Davidson and Helen Lee.

References

1 G. M. Whitesides, *Nature*, 2006, **442**, 368–373.
2 E. Berthier, E. W. Young and D. Beebe, *Lab Chip*, 2012, **12**, 1224–1237.
3 G. M. Whitesides, *Lab Chip*, 2013, **13**, 11–13.
4 H. Lee, personal communication.
5 N. Blow, *Nat. Methods*, 2009, **6**, 683–686.
6 A. W. Martinez, S. T. Phillips, M. J. Butte and G. M. Whitesides, *Angew. Chem., Int. Ed.*, 2007, **46**, 1318–1320.
7 A. W. Martinez, S. T. Phillips, E. Carrilho, S. W. Thomas, 3rd, H. Sindi and G. M. Whitesides, *Anal. Chem.*, 2008, **80**, 3699–3707.
8 Swiss Precision Diagnostics GmbH, Geneva, Switzerland, http://www.swissprecisiondiagnostics.com, Accessed January 14, 2013.
9 Chemstrip® Test Strips, http://www.poc.roche.com, Accessed January 12, 2013.
10 Multistix® 10 SG Reagent Strips, http://www.medical.siemens.com, Accessed January 12, 2013.
11 Medi-Test Combi 11, http://www.mn-net.com, Accessed January 12, 2013.
12 Arkray AUTION Sticks, http://www.arkray.co.jp/english, Accessed January 12, 2013.
13 YD Diagnostics URiSCAN Strips, http://www.yd-diagnostics.com, Accessed January 12, 2013.
14 Chemstrip® Micral Test Strips, http://www.poc.roche.com, Accessed January 12, 2013.
15 CLINITEK® Microalbumin Reagent Strips, http://www.medical.siemens.com, Accessed January 12, 2013.
16 Alere Inc. (Waltham, MA), http://www.alere.com, Accessed January 14, 2013.
17 Beckton Dickinson (Franklin Lakes, NJ), http://www.bd.com, Accessed January 14, 2013.
18 QUIDEL Corporation (San Diego, CA), http://www.quidel.com, Accessed January 14, 2013.
19 Beckman Coulter, Inc., Diagnostics Division (Brea, CA), http://www.beckmancoulter.com, Accessed January 14, 2013.
20 Meridian Bioscience, Inc. (Cincinnati, OH), http://www.meridianbioscience.com, Accessed January 14, 2013.
21 Audit Diagnostics (Carrigtwohill, Ireland), http://www.auditdiagnostics.ie/products/veterinary, Accessed January 14, 2013.
22 Abaxis Inc. (Union City, CA), http://www.abaxis.com/veterinary/, Accessed January 12, 2013.
23 Biomedica MedizinProdukte GmbH & Co KG, Vienna, Austria, http://www.biomedica.co.at, Accessed January 10, 2013.
24 Henry Schein, Inc. (Langen, Germany), http://www.henryscheinbrand.com, Accessed January 12, 2013.
25 Romer Labs, Inc. (Union, MO), http://www.romerlabs.com, Accessed January 5, 2013.
26 Neogen Corporation, (Lansing, MI), http://www.neogen.com, Accessed January 7, 2013.
27 Charm Sciences, Inc. (Lawrence, MA), http://www.charm.com, Accessed January 8, 2013.

Published on 08 May 2013. Downloaded by University of Cambridge on 31/05/2013 13:14:32.

28 Kwinbon Biotechnology Co., Ltd. (Beijing, China), http://www.kwinbon.com, Accessed January 6, 2013.
29 Wagtech WTD, Palintest Ltd (Gateshead, U. K.), http://www.wagtech.co.uk, Accessed January 9, 2013.
30 LaMotte Company (Chestertown, Maryland), http://www.lamotte.com, Accessed January 6, 2013.
31 YSI Inc. (Yellow Springs, Ohio), http://www.ysi.com, Accessed January 5, 2013.
32 Obreco-Hellige (Sarasota, FL), http://www.orbeco.com/, Accessed January 10, 2013.
33 HANNA instruments US Inc. (Woonsocket, RI), http://www.hannainst.com, Accessed January 14, 2013.
34 Industrial Test Systems, Inc. (Rock Hill, SC), http://www.sensafe.com, Accessed January 8, 2013.
35 Southern Scientific Ltd (Henfield, U.K.), http://www.southernscientific.co.uk, Accessed January 12, 2013.
36 Alexeter Technologies LLC (Chicago, IL), http://www.alexeter.com, Accessed January 13, 2013.
37 miprolab GmbH (Göttingen, Germany), http://www.miprolab.com, Accessed January 10, 2013.
38 American Bio Medica Corporation (Kinderhook, New York), http://www.abmc.com, Accessed January 11, 2013.
39 MP Biomedicals (Santa Ana, CA), http://www.mpbio.com, Accessed January 12, 2013.
40 Craig Medical Distribution, Inc. (Vista, CA), http://www.craigmedical.com, Accessed January 9, 2013.
41 Alfa Scientific Designs, Inc. (Poway, CA), http://www.alfascientific.com, Accessed January 7, 2013.
42 X. Li, D. R. Ballerini and W. Shen, *Biomicrofluidics*, 2012, **6**, 11301–1130113.
43 D. R. Ballerini, X. Li and W. Shen, *Microfluid. Nanofluid.*, 2012, **13**, 769–787.
44 D. D. Liana, B. Raguse, J. J. Gooding and E. Chow, *Sensors*, 2012, **12**, 11505–11526.
45 C. Parolo and A. Merkoci, *Chem. Soc. Rev.*, 2013, **42**, 450–457.
46 P. Shah, X. Zhu and C. Z. Li, *Expert Rev. Mol. Diagn.*, 2013, **13**, 83–91.
47 B. O'Farrell, personal communication.
48 *World Urbanization Prospects – The 2011 Revision, Department of Economic and Social Affairs, Population Division*, UN, New York, 2012.
49 K. Tontisirin, G. Nantel and L. Bhattacharjee, *Proc. Nutr. Soc.*, 2002, **61**, 243–250.
50 *Rethinking Poverty: Report on the World Social Situation 2010*, Department of Economic and Social Affairs, United Nations, New York, 2009.
51 T. Acharya, A. S. Daar, E. Dowdeswell, P. A. Singer and H. Thorsteinsdottir, *Genomics and Global Health*, University of Toronto Joint Centre for Bioethics, Toronto, Ontario, Canada, 2004.
52 *Water Quality for Ecosystem and Human Health*, GEMS/Water Programme Office, UN, Burlington, Ontario, Canada, 2008.
53 *Report, Animal Health and the Millennium Development Goals*, Animal Production and Health Division, Food and Agriculture Organization of the United Nations.
54 T. Aluwong and M. Bello, *Vet. Ital.*, 2010, **46**, 137–145.
55 *Global Strategy for Food Safety: Safer Food for Better Health*, F. S. Department, Food Safety Department, WHO, Geneva, Switzerland, 2002.
56 Millennium Development Goals, United Nations, http://www.un.org/millenniumgoals/, Accessed January 18, 2013.
57 G. M. Whitesides, A lab the size of a postage stamp, TEDX Boston, 2009 http://www.ted.com/talks/george_whitesides_a_lab_the_size_of_a_postage_stamp.html.
58 J. N. Nkengasong, T. Mesele, S. Orloff, Y. Kebede, P. N. Fonjungo, R. Timperi and D. Birx, *Am. J. Clin. Pathol.*, 2009, **131**, 852–857.
59 M. J. Schull, H. Banda, D. Kathyola, L. Fairall, A. Martiniuk, B. Burciul, M. Zwarenstein, S. Sodhi, S. Thompson, M. Joshua, M. Mondiwa and E. Bateman, *Trials*, 2010, **11**, 118.
60 H. H. Lee and J. P. Allain, *Vox Sang.*, 2004, **87**, 176–179.
61 B. Allegranzi, S. Bagheri Nejad, C. Combescure, W. Graafmans, H. Attar, L. Donaldson and D. Pittet, *Lancet*, 2011, **377**, 228–241.
62 M. Urdea, L. A. Penny, S. S. Olmsted, M. Y. Giovanni, P. Kaspar, A. Shepherd, P. Wilson, C. A. Dahl, S. Buchsbaum, G. Moeller and D. C. Hay Burgess, *Nature*, 2006, **444**, 73–79.
63 P. N. Newton, M. D. Green, F. M. Fernandez, N. P. Day and N. J. White, *Lancet Infect. Dis.*, 2006, **6**, 602–613.
64 P. Yager, G. J. Domingo and J. Gerdes, *Annu. Rev. Biomed. Eng.*, 2008, **10**, 107–144.
65 D. C. Hay Burgess, J. Wasserman and C. A. Dahl, *Nature*, 2006, **444**, 1–2.
66 R. W. Peeling and D. Mabey, *Clin. Microbiol. Infect.*, 2010, **16**, 1062–1069.
67 *Integrated Management of Childhood Illness*, MOPH&P, WHO/CHD, UNICEF, HCMC/CDP.
68 E. A. M. Bokkers, *Farming for Health: Green-Care Farming Across Europe and the United States of America*, Springer, 2006, 13, pp. 31–41.
69 I. D. Robertson, P. J. Irwin, A. J. Lymbery and R. C. Thompson, *Int. J. Parasitol.*, 2000, **30**, 1369–1377.
70 B. H. Hahn, G. M. Shaw, K. M. De Cock and P. M. Sharp, *Science*, 2000, **287**, 607–614.
71 J. Yuan, C. C. Hon, Y. Li, D. Wang, G. Xu, H. Zhang, P. Zhou, L. L. Poon, T. T. Lam, F. C. Leung and Z. Shi, *J. Gen. Virol.*, 2010, **91**, 1058–1062.
72 R. J. Webby and R. G. Webster, *Philos. Trans. R. Soc. London, Ser. B*, 2001, **356**, 1817–1828.
73 *Foodborne Disease Outbreaks: Guidelines for Investigation and Control*, WHO, France, 2008.
74 C. A. Sullivan, J. R. Meigh, A. M. Giacomello, T. Fediw, P. Lawrence, M. Samad, S. Mlote, C. Hutton, J. A. Allan, R. E. Schulze, D. J. M. Dlamini, W. Cosgrove, J. D. Priscoli, P. Gleick, I. Smout, J. Cobbing, R. Calow, C. Hunt, A. Hussain, M. C. Acreman, J. King, S. Malomo, E. L. Tate, D. O', S. Milner and I. Steyl, *Nat. Resour. Forum*, 2003, **27**, 189–199.
75 S. Luthra, Meet the Water Canary, TEDGlobal, 2011 http://www.ted.com/talks/sonaar_luthra_meet_the_water_canary.html.
76 A. H. Free, E. C. Adams, M. L. Kercher, H. M. Free and M. H. Cook, *Clin. Chem.*, 1957, **3**, 163–168.
77 C. M. Plotz and J. M. Singer, *Am. J. Med.*, 1956, **21**, 888–892.
78 S. A. Berson and R. S. Yalow, *J. Clin. Invest.*, 1959, **38**, 1996–2016.

 This journal is © The Royal Society of Chemistry 2013

Published on 08 May 2013. Downloaded by University of Cambridge on 31/05/2013 13:14:32.

79 F. D. Miles, *Cellulose Nitrate*, Interscience, New York, 1955.
80 E. M. Southern, *J. Mol. Biol.*, 1975, **98**, 503.
81 H. Towbin, T. Staehelin and J. Gordon, *Proc. Natl. Acad. Sci. U. S. A.*, 1979, **76**, 4350–4354.
82 D. A. Goldberg, *Proc. Natl. Acad. Sci. U. S. A.*, 1980, **77**, 5794–5798.
83 R. Hawkes, E. Niday and J. Gordon, *Anal. Biochem.*, 1982, **119**, 142–147.
84 A Timeline of Pregnancy Testing, http://history.nih.gov/exhibits/thinblueline/timeline.html, Accessed March 6, 2013.
85 J. L. Vaitukaitis, G. D. Braunstein and G. T. Ross, *Am. J. Obstet. Gynecol.*, 1972, **113**(6), 751–758.
86 J. H. W. Leuvering, *US Pat.*, 4313734, 1982.
87 G. S. David and H. E. Greene, *US Pat.*, 4376110, 1983.
88 D. J. Litman and R. F. Zuk, *US Pat.*, 4435504, 1984.
89 R. L. Campbell, J. P. O'Connell and D. B. Wagner, *US Pat.*, 4703017, 1987.
90 T. G. Bloomster and R. W. Rosenstein, *US Pat.*, 4855240, 1989.
91 J. C. Russell, H. Yang and D. Yost, *US Pat.*, 4954452, 1990.
92 P. Hunsinger and A. Zwarun, *US Pat.*, 4983416, 1991.
93 P. J. Davis, M. E. Prior and K. May, *European Pat.*, 0810436A1, 1997.
94 *Detection (sensor systems) – Biological, Jane's Nuclear, Biological and Chemical Defence*, Janes Information Group, 2012.
95 J. Whelan, personal communication.
96 IDEXX Laboratories (Westbrook, ME), http://www.idexx.com, January 30, 2013.
97 R. C. Wong and H. Y. Tse, *Lateral Flow Immunoassay*, Humana Press, Springer, 2009.
98 G. Fomovska, Filters, membranes, and bioseparation equipment for today's IVDs, IVD Technology, 2011.
99 Catalog, Clinical Diagnostics without boundaries, Whatman, GE Healthcare, 2007.
100 B. J. Stewart, R. L. Houghton, W. J. W. Morrow and S. Raychaudhuri, *IVD Technology*, April, 2006.
101 Astute Medical, Inc. (San Diego, CA), http://www.astute-medical.com, Accessed January 30, 2013.
102 F. Girosi, S. S. Olmsted, E. Keeler, D. C. Hay Burgess, Y. W. Lim, J. E. Aledort, M. E. Rafael, K. A. Ricci, R. Boer, L. Hilborne, K. P. Derose, M. V. Shea, C. M. Beighley, C. A. Dahl and J. Wasserman, *Nature*, 2006, **444**, 3–8.
103 K. Dieterich, *US Pat.*, 691249, 1902.
104 H. Yagoda, *Ind. Eng. Chem., Anal. Ed.*, 1937, **9**, 79–82.
105 H. Yagoda, *US Pat.*, 2129754, 1938.
106 J. L. Johnson, *Microchim. Acta*, 1967, **55**, 756–762.
107 R. H. Müller and D. L. Clegg, *Anal. Chem.*, 1949, **21**, 1123–1125.
108 D. E. Fonner, *US Pat.*, 3001915, 1961.
109 R. H. Jordan, *US Pat.*, 3006735, 1961.
110 M. E. Deutsch, *US Pat.*, 3011874, 1961.
111 H. F. Meyer, *US Pat.*, 3127281, 1964.
112 H. Hochstrasser, *US Pat.*, 3964871, 1976.
113 J. Y. Wang, *US Pat.*, 4618475, 1986.
114 B. O. Basore, K. J. Forney, M. B. O'Connell, R. G. Parsons and P. J. Ropella, *US Pat.*, 5209904, 1993.
115 Y. S. Yu, *US Pat.*, 6723500, 2004.
116 L. P. Fenocketti and M. C. Rapkin, *US Pat.*, 4160008, 1979.
117 M. C. Rapkin and D. L. Tabb, *US Pat.*, 4301115, 1981.
118 S. J. Chudzik and M. J. Hamilton, *US Pat.*, 5707818, 1998.
119 X. Chen, J. Chen, F. Wang, X. Xiang, M. Luo, X. Ji and Z. He, *Biosens. Bioelectron.*, 2012, **35**, 363–368.
120 P. Yager, T. Edwards, E. Fu, K. Helton, K. Nelson, M. R. Tam and B. H. Weigl, *Nature*, 2006, **442**, 412–418.
121 B. Weigl, G. Domingo, P. Labarre and J. Gerlach, *Lab Chip*, 2008, **8**, 1999–2014.
122 L. Y. Yeo, H. C. Chang, P. P. Chan and J. R. Friend, *Small*, 2011, **7**, 12–48.
123 H. Sharma, D. Nguyen, A. Chen, V. Lew and M. Khine, *Ann. Biomed. Eng.*, 2011, **39**, 1313–1327.
124 C. D. Chin, V. Linder and S. K. Sia, *Lab Chip*, 2007, **7**, 41–57.
125 W. G. Lee, Y. G. Kim, B. G. Chung, U. Demirci and A. Khademhosseini, *Adv. Drug Delivery Rev.*, 2010, **62**, 449–457.
126 J. C. Roberts, *The Chemistry of Paper*, The Royal Society of Chemistry, 1996.
127 Paper and Board Today: Part 2, http://www.paperacademy.net, Accessed January 30, 2013.
128 Nitrocellulose, Dow Wolff Cellulosics GmbH, www.dowwolffcellulosics.com, Accessed January 30, 2013.
129 Encyclopædia Britannica Online.
130 Protran® Nitrocellulose Membranes (Whatman), http://www.whatman.com/ProtranNitrocelluloseMembranes.aspx, Accessed January 30, 2013.
131 Catalog, Whatman papers, http://www.whatman.com/, Accessed January 14, 2013.
132 Z. W. Zhong, Z. P. Wang and G. X. D. Huang, *Microsyst. Technol.*, 2012, **18**, 649–659.
133 A. Doty, S. Gaskell and F. Sultan, *IVD Technology*, October, 2012.
134 Catalog, Rapid Lateral Flow Test Strips: Considerations for Product Development, vol. Millipore Corporation, Bedford, MA.
135 M. A. Harvey, C. A. Audette and R. McDonogh, *IVD Technology*, May, 1996.
136 W. Goldberg, M. Tilley and J. Rudolph, *Design Solutions Using Microporous Hydrophobic Membranes, Medical Plastics and Biomaterials*, March, 1997.
137 J. Alter, *Genet. Eng. News*, 1996, **16**, 28.
138 J. Alter, *Genet. Eng. News*, 1996, **16**, 30.
139 X. Yang, O. Forouzan, T. P. Brown and S. S. Shevkoplyas, *Lab Chip*, 2012, **12**, 274–280.
140 T. Songjaroen, W. Dungchai, O. Chailapakul, C. S. Henry and W. Laiwattanapaisal, *Lab Chip*, 2012, **12**, 3392–3398.
141 Vivid™ Plasma Separation Membrane, http://www.pall.com/main/oem-materials-and-devices/product.page?id=46962, Accessed January 21, 2013.
142 S. J. Vella, P. Beattie, R. Cademartiri, A. Laromaine, A. W. Martinez, S. T. Phillips, K. A. Mirica and G. M. Whitesides, *Anal. Chem.*, 2012, **84**, 2883–2891.
143 N. R. Pollock, J. P. Rolland, S. Kumar, P. D. Beattie, S. Jain, F. Noubary, V. L. Wong, R. A. Pohlmann, U. S. Ryan and G. M. Whitesides, *Sci. Transl. Med.*, 2012, **4**, 152ra129.
144 W. Dungchai, O. Chailapakul and C. S. Henry, *Analyst*, 2011, **136**, 77–82.
145 *US Pat.*, 12/150,607 (Application), 2008.

Published on 08 May 2013. Downloaded by University of Cambridge on 31/05/2013 13:14:32.

146 E. M. Fenton, M. R. Mascarenas, G. P. Lopez and S. S. Sibbett, *ACS Appl. Mater. Interfaces*, 2009, **1**, 124–129.
147 E. Fu, B. Lutz, P. Kauffman and P. Yager, *Lab Chip*, 2010, **10**, 918–920.
148 E. Fu, P. Kauffman, B. Lutz and P. Yager, *Sens. Actuators, B*, 2010, **149**, 325–328.
149 A. W. Martinez, S. T. Phillips, B. J. Wiley, M. Gupta and G. M. Whitesides, *Lab Chip*, 2008, **8**, 2146–2150.
150 Q. H. He, C. Ma, X. Hu and H. Chen, *Anal. Chem.*, 2012, **85**(3), 1327–1331.
151 D. A. Bruzewicz, M. Reches and G. M. Whitesides, *Anal. Chem.*, 2008, **80**, 3387–3392.
152 K. Abe, K. Suzuki and D. Citterio, *Anal. Chem.*, 2008, **80**, 6928–6934.
153 K. Abe, K. Kotera, K. Suzuki and D. Citterio, *Anal. Bioanal. Chem.*, 2010, **398**, 885–893.
154 X. Li, J. Tian, T. Nguyen and W. Shen, *Anal. Chem.*, 2008, **80**(23), 9131–9134.
155 Y. Lu, W. Shi, L. Jiang, J. Qin and B. Lin, *Electrophoresis*, 2009, **30**, 1497–1500.
156 E. Carrilho, A. W. Martinez and G. M. Whitesides, *Anal. Chem.*, 2009, **81**, 7091–7095.
157 X. Li, J. Tian, G. Garnier and W. Shen, *Colloids Surf., B*, 2010, **76**, 564–570.
158 J. Olkkonen, K. Lehtinen and T. Erho, *Anal. Chem.*, 2010, **82**, 10246–10250.
159 G. Chitnis, Z. Ding, C. L. Chang, C. A. Savran and B. Ziaie, *Lab Chip*, 2011, **11**, 1161–1165.
160 T. Songjaroen, W. Dungchai, O. Chailapakul and W. Laiwattanapaisal, *Talanta*, 2011, **85**, 2587–2593.
161 A. L. Zhang and Y. Zha, *AIP Adv.*, 2012, **2**(2), 022171.
162 E. W. Washburn, *Phys. Rev.*, 1921, **17**, 273–283.
163 X. Li, D. R. Ballerini and W. Shen, *Biomicrofluidics*, 2012, **6**(1), 11301.
164 A. W. Martinez, S. T. Phillips and G. M. Whitesides, *Proc. Natl. Acad. Sci. U. S. A.*, 2008, **105**, 19606–19611.
165 G. G. Lewis, M. J. DiTucci, M. S. Baker and S. T. Phillips, *Lab Chip*, 2012, **12**, 2630–2633.
166 H. Liu and R. M. Crooks, *J. Am. Chem. Soc.*, 2011, **133**, 17564–17566.
167 H. Liu, Y. Xiang, Y. Lu and R. M. Crooks, *Angew. Chem., Int. Ed.*, 2012, **51**, 6925–6928.
168 A. V. Govindarajan, S. Ramachandran, G. D. Vigil, P. Yager and K. F. Bohringer, *Lab Chip*, 2012, **12**, 174–181.
169 A. Nilghaz, D. H. Wicaksono, D. Gustiono, F. A. Abdul Majid, E. Supriyanto and M. R. Abdul Kadir, *Lab Chip*, 2012, **12**, 209–218.
170 M. Reches, K. A. Mirica, R. Dasgupta, M. D. Dickey, M. J. Butte and G. M. Whitesides, *ACS Appl. Mater. Interfaces*, 2010, **2**, 1722–1728.
171 *US Pat.*, 12/934,702 (Application), 2012.
172 X. Li, J. Tian and W. Shen, *ACS Appl. Mater. Interfaces*, 2010, **2**, 1–6.
173 P. Bhandari, T. Narahari and D. Dendukuri, *Lab Chip*, 2011, **11**, 2493–2499.
174 W. G. Meathrel and R. Malik, *Adhesives in Diagnostics, Medical Device + Diagnostic Industry*, vol. 33, 8.
175 K. M. Schilling, A. L. Lepore, J. A. Kurian and A. W. Martinez, *Anal. Chem.*, 2012, **84**(3), 1579–1585.
176 H. Noh and S. T. Phillips, *Anal. Chem.*, 2010, **82**, 8071–8078.
177 S. T. Phillips and N. K. Thom, *Methods Mol. Biol.*, 2013, **949**, 185–196.
178 H. Liu and R. M. Crooks, *Anal. Chem.*, 2012, **84**, 2528–2532.
179 N. K. Thom, K. Yeung, M. B. Pillion and S. T. Phillips, *Lab Chip*, 2012, **12**, 1768–1770.
180 K. Yeung, K. M. Schmid and S. T. Phillips, *Chem. Commun.*, 2013, **49**, 394–396.
181 R. F. Carvalhal, E. Carrilho and L. T. Kubota, *Bioanalysis*, 2010, **2**, 1663–1665.
182 A. R. Rezk, A. Qi, J. R. Friend, W. H. Li and L. Y. Yeo, *Lab Chip*, 2012, **12**, 773–779.
183 A. C. Siegel, S. T. Phillips, B. J. Wiley and G. M. Whitesides, *Lab Chip*, 2009, **9**, 2775–2781.
184 A. W. Martinez, S. T. Phillips, Z. Nie, C. M. Cheng, E. Carrilho, B. J. Wiley and G. M. Whitesides, *Lab Chip*, 2010, **10**, 2499–2504.
185 B. R. Lutz, P. Trinh, C. Ball, E. Fu and P. Yager, *Lab Chip*, 2011, **11**, 4274–4278.
186 R. F. Carvalhal, M. S. Kfouri, M. H. Piazetta, A. L. Gobbi and L. T. Kubota, *Anal. Chem.*, 2010, **82**, 1162–1165.
187 J. L. Osborn, B. Lutz, E. Fu, P. Kauffman, D. Y. Stevens and P. Yager, *Lab Chip*, 2010, **10**, 2659–2665.
188 P. Kauffman, E. Fu, B. Lutz and P. Yager, *Lab Chip*, 2010, **10**, 2614–2617.
189 H. Noh and S. T. Phillips, *Anal. Chem.*, 2010, **82**, 4181–4187.
190 H. Chen, J. Cogswell, C. Anagnostopoulos and M. Faghri, *Lab Chip*, 2012, **12**, 2909–2913.
191 M. Li, J. Tian, M. Al-Tamimi and W. Shen, *Angew. Chem., Int. Ed.*, 2012, **51**, 5497–5501.
192 B. Lutz, T. Liang, E. Fu, S. Ramachandran, P. Kauffman and P. Yager, presented in part at the MicroTAS, Okinawa, Japan, 2012.
193 A. C. Siegel, S. T. Phillips, M. D. Dickey, N. S. Lu, Z. G. Suo and G. M. Whitesides, *Adv. Funct. Mater.*, 2010, **20**, 28–35.
194 G. G. Lewis, M. J. DiTucci and S. T. Phillips, *Angew. Chem., Int. Ed.*, 2012, **51**, 12707–12710.
195 E. Fu, S. A. Ramsey, P. Kauffman, B. Lutz and P. Yager, *Microfluid. Nanofluid.*, 2011, **10**, 29–35.
196 B. Kirby, *Micro- and Nanoscale Fluid Mechanics: Transport in Microfluidic Devices*, Cambridge University Press, 2010.
197 G. Taylor, *Proc. Roy. Soc. Lond. A*, 1953, **219**, 186.
198 R. Aris, *Proc. R. Soc. London, Ser. A*, 1956, **235**, 67–77.
199 A. J. Bae, C. Beta and E. Bodenschatz, *Lab Chip*, 2009, **9**, 3059–3065.
200 H. Darcy, *Les Fontaines Publiques de la Ville de Dijon*, ed. V. Dalmont, Paris, 1856.
201 J. L. Auriault, L. Borne and R. Chambon, *J. Acoust. Soc. Am.*, 1985, **77**, 1641–1650.
202 J. M. Nordbotten, M. A. Celia, H. K. Dahle and S. M. Hassanizadeh, *Water Resour. Res.*, 2007, **43**(8), W08430.
203 A. W. Martinez, S. T. Phillips, E. Carrilho, S. W. Thomas, H. Sindi and G. M. Whitesides, *Anal. Chem.*, 2008, **80**, 3699–3707.
204 W. Dungchai, O. Chailapakul and C. S. Henry, *Anal. Chim. Acta*, 2010, **674**, 227–233.
205 S. M. Hossain, R. E. Luckham, M. J. McFadden and J. D. Brennan, *Anal. Chem.*, 2009, **81**, 9055–9064.

 This journal is © The Royal Society of Chemistry 2013

Published on 08 May 2013. Downloaded by University of Cambridge on 31/05/2013 13:14:32.

206 S. M. Hossain, R. E. Luckham, A. M. Smith, J. M. Lebert, L. M. Davies, R. H. Pelton, C. D. Filipe and J. D. Brennan, *Anal. Chem.*, 2009, **81**, 5474–5483.
207 C. M. Cheng, A. W. Martinez, J. Gong, C. R. Mace, S. T. Phillips, E. Carrilho, K. A. Mirica and G. M. Whitesides, *Angew. Chem., Int. Ed.*, 2010, **49**, 4771–4774.
208 M. S. Khan, G. Thouas, W. Shen, G. Whyte and G. Garnier, *Anal. Chem.*, 2010, **82**, 4158–4164.
209 M. Al-Tamimi, W. Shen, R. Zeineddine, H. Tran and G. Garnier, *Anal. Chem.*, 2011, **84**(3), 1661–1668.
210 S. A. Klasner, A. K. Price, K. W. Hoeman, R. S. Wilson, K. J. Bell and C. T. Culbertson, *Anal. Bioanal. Chem.*, 2010, **397**, 1821–1829.
211 S. M. Hossain and J. D. Brennan, *Anal. Chem.*, 2011, **83**, 8772–8778.
212 S. Pumtang, W. Siripornnoppakhun, M. Sukwattanasinitt and A. Ajavakom, *J. Colloid Interface Sci.*, 2011, **364**, 366–372.
213 M. Xu, B. R. Bunes and L. Zang, *ACS Appl. Mater. Interfaces*, 2011, **3**, 642–647.
214 T. Eaidkong, R. Mungkarndee, C. Phollookin, G. Tumcharern, M. Sukwattanasinitt and S. Wacharasindhu, *J. Mater. Chem.*, 2012, **22**, 5970–5977.
215 M. Funes-Huacca, A. Wu, E. Szepesvari, P. Rajendran, N. Kwan-Wong, A. Razgulin, Y. Shen, J. Kagira, R. Campbell and R. Derda, *Lab Chip*, 2012, **12**, 4269–4278.
216 J. C. Jokerst, J. A. Adkins, B. Bisha, M. M. Mentele, L. D. Goodridge and C. S. Henry, *Anal. Chem.*, 2012, **84**, 2900–2907.
217 S. Kim, E. Jung, M. J. Kim, A. Pyo, T. Palani, M. S. Eom, M. S. Han and S. Lee, *Chem. Commun.*, 2012, **48**, 8751–8753.
218 M. M. Mentele, J. Cunningham, K. Koehler, J. Volckens and C. S. Henry, *Anal. Chem.*, 2012, **84**, 4474–4480.
219 Y. Sameenoi, P. Panymeesamer, N. Supalakorn, K. Koehler, O. Chailapakul, C. S. Henry and J. Volckens, *Environ. Sci. Technol.*, 2013, **47**, 932–940.
220 B. M. Jayawardane, I. D. McKelvie and S. D. Kolev, *Talanta*, 2012, **100**, 454–460.
221 W. Dungchai, O. Chailapakul and C. S. Henry, *Anal. Chem.*, 2009, **81**, 5821–5826.
222 Z. Nie, F. Deiss, X. Liu, O. Akbulut and G. M. Whitesides, *Lab Chip*, 2010, **10**, 3163–3169.
223 Z. Nie, C. A. Nijhuis, J. Gong, X. Chen, A. Kumachev, A. W. Martinez, M. Narovlyansky and G. M. Whitesides, *Lab Chip*, 2010, **10**, 477–483.
224 S. N. Tan, L. Ge and W. Wang, *Anal. Chem.*, 2010, **82**(21), 8844–8847.
225 J. J. Shi, F. Tang, H. L. Xing, H. X. Zheng, L. H. Bi and W. Wang, *J. Braz. Chem. Soc.*, 2012, **23**, 1124–1130.
226 S. Ge, L. Ge, M. Yan, X. Song, J. Yu and J. Huang, *Chem. Commun.*, 2012, **48**, 9397–9399.
227 P. Wang, L. Ge, M. Yan, X. Song, S. Ge and J. Yu, *Biosens. Bioelectron.*, 2012, **32**, 238–243.
228 S. Wang, L. Ge, Y. Zhang, X. Song, N. Li, S. Ge and J. Yu, *Lab Chip*, 2012, **12**, 4489–4498.
229 D. Zang, L. Ge, M. Yan, X. Song and J. Yu, *Chem. Commun.*, 2012, **48**, 4683–4685.
230 M. Novell, M. Parrilla, G. A. Crespo, F. X. Rius and F. J. Andrade, *Anal. Chem.*, 2012, **84**, 4695–4702.
231 P. Rattanarat, W. Dungchai, W. Siangproh, O. Chailapakul and C. S. Henry, *Anal. Chim. Acta*, 2012, **744**, 1–7.
232 L. Y. Shiroma, M. Santhiago, A. L. Gobbi and L. T. Kubota, *Anal. Chim. Acta*, 2012, **725**, 44–50.
233 N. Dossi, R. Toniolo, A. Pizzariello, E. Carrilho, E. Piccin, S. Battiston and G. Bontempelli, *Lab Chip*, 2012, **12**, 153–158.
234 W. A. Zhao, M. M. Ali, S. D. Aguirre, M. A. Brook and Y. F. Li, *Anal. Chem.*, 2008, **80**, 8431–8437.
235 E. Fu, T. Liang, P. Spicar-Mihalic, J. Houghtaling, S. Ramachandran and P. Yager, *Anal. Chem.*, 2012, **84**, 4574–4579.
236 C. Z. Li, K. Vandenberg, S. Prabhulkar, X. Zhu, L. Schneper, K. Methee, C. J. Rosser and E. Almeide, *Biosens. Bioelectron.*, 2011, **26**, 4342–4348.
237 M. Ornatska, E. Sharpe, D. Andreescu and S. Andreescu, *Anal. Chem.*, 2011, **83**, 4273–4280.
238 A. Apilux, W. Siangproh, N. Praphairaksit and O. Chailapakul, *Talanta*, 2012, **97**, 388–394.
239 J. Liang, Y. Y. Wang and B. Liu, *RSC Adv.*, 2012, **2**, 3878–3884.
240 J. Nie, Y. Zhang, L. Lin, C. Zhou, S. Li, L. Zhang and J. Li, *Anal. Chem.*, 2012, **84**, 6331–6335.
241 N. Ratnarathorn, O. Chailapakul, C. S. Henry and W. Dungchai, *Talanta*, 2012, **99**, 552–557.
242 B. A. Rohrman and R. R. Richards-Kortum, *Lab Chip*, 2012, **12**, 3082–3088.
243 B. Veigas, J. M. Jacob, M. N. Costa, D. S. Santos, M. Viveiros, J. Inacio, R. Martins, P. Barquinha, E. Fortunato and P. V. Baptista, *Lab Chip*, 2012, **12**, 4802–4808.
244 J. Szucs and R. E. Gyurcsanyi, *Electroanalysis*, 2012, **24**, 146–152.
245 A. M. Lopez Marzo, J. Pons, D. A. Blake and A. Merkoci, *Anal. Chem.*, 2013, **85**(7), 3532–3538.
246 J. L. Delaney, C. F. Hogan, J. Tian and W. Shen, *Anal. Chem.*, 2011, **83**, 1300–1306.
247 L. Ge, J. Yan, X. Song, M. Yan, S. Ge and J. Yu, *Biomaterials*, 2012, **33**, 1024–1031.
248 W. Li, M. Li, S. Ge, M. Yan, J. Huang and J. Yu, *Anal. Chim. Acta*, 2013, **767**, 66–74.
249 J. Yan, L. Ge, X. Song, M. Yan, S. Ge and J. Yu, *Chem.–Eur. J.*, 2012, **18**, 4938–4945.
250 C. G. Shi, X. Shan, Z. Q. Pan, J. J. Xu, C. Lu, N. Bao and H. Y. Gu, *Anal. Chem.*, 2012, **84**, 3033–3038.
251 M. Zhang, L. Ge, S. Ge, M. Yan, J. Yu, J. Huang and S. Liu, *Biosens. Bioelectron.*, 2013, **41**, 544–550.
252 V. Mani, K. Kadimisetty, S. Malla, A. A. Joshi and J. F. Rusling, *Environ. Sci. Technol.*, 2013, **47**, 1937–1944.
253 J. Yu, L. Ge, J. Huang, S. Wang and S. Ge, *Lab Chip*, 2011, **11**, 1286–1291.
254 J. Yu, S. Wang, L. Ge and S. Ge, *Biosens. Bioelectron.*, 2011, **26**, 3284–3289.
255 L. Ge, S. Wang, X. Song, S. Ge and J. Yu, *Lab Chip*, 2012, **12**, 3150–3158.
256 E. Carrilho, S. T. Phillips, S. J. Vella, A. W. Martinez and G. M. Whitesides, *Anal. Chem.*, 2009, **81**, 5990–5998.
257 M. M. Ali, S. D. Aguirre, Y. Xu, C. D. M. Filipe, R. Pelton and Y. Li, *Chem. Commun.*, 2009, 6640–6642.
258 P. B. Allen, S. A. Arshad, B. Li, X. Chen and A. D. Ellington, *Lab Chip*, 2012, **12**, 2951–2958.
259 U. H. Yildiz, P. Alagappan and B. Liedberg, *Anal. Chem.*, 2013, **85**, 820–824.

Published on 08 May 2013. Downloaded by University of Cambridge on 31/05/2013 13:14:32.

260 M. O. Noor, A. Shahmuradyan and U. J. Krull, *Anal. Chem.*, 2013, **85**, 1860–1867.
261 B. S. Miranda, E. M. Linares, S. Thalhammer and L. T. Kubota, *Biosens. Bioelectron.*, 2013, **45C**, 123–128.
262 A. Apilux, W. Dungchai, W. Siangproh, N. Praphairaksit, C. S. Henry and O. Chailapakul, *Anal. Chem.*, 2010, **82**, 1727–1732.
263 A. Struss, P. Pasini, C. M. Ensor, N. Raut and S. Daunert, *Anal. Chem.*, 2010, **82**, 4457–4463.
264 A. K. Ellerbee, S. T. Phillips, A. C. Siegel, K. A. Mirica, A. W. Martinez, P. Striehl, N. Jain, M. Prentiss and G. M. Whitesides, *Anal. Chem.*, 2009, **81**, 8447–8452.
265 D. S. Lee, B. G. Jeon, C. Ihm, J. K. Park and M. Y. Jung, *Lab Chip*, 2011, **11**, 120–126.
266 L. Shen, J. A. Hagen and I. Papautsky, *Lab Chip*, 2012, **12**, 4240–4243.
267 J. Chandler, T. Gurmin and N. Robinson, *IVD Technology*, 2000, 6, pp. 37–59.
268 E. Fu, T. Liang, J. Houghtaling, S. Ramachandran, S. A. Ramsey, B. Lutz and P. Yager, *Anal. Chem.*, 2011, **83**, 7941–7946.
269 E. S. Fu, personal communication.
270 M. A. Nash, J. M. Hoffman, D. Y. Stevens, A. S. Hoffman, P. S. Stayton and P. Yager, *Lab Chip*, 2010, **10**, 2279–2282.
271 L. L. Xue, L. H. Guo, B. Qiu, Z. Y. Lin and G. N. Chen, *Electrochem. Commun.*, 2009, **11**, 1579–1582.
272 S. Wang, L. Ge, X. Song, J. Yu, S. Ge, J. Huang and F. Zeng, *Biosens. Bioelectron.*, 2012, **31**, 212–218.
273 D. V. Borich and W. P. Coffey, *US Pat.*, 7267799, 2007.
274 D. V. Borich, M. McAleer, A. Milder, D. Mitchell and S. Savoy, *US Pat.*, 7803322, 2010.
275 LRE Medical GmbH, Nördlingen, Germany, http://www.esterline.com/lremedical, Accessed January 29, 2013.
276 *Mobile-cellular subscriptions*, International Telecommunication Union, Place des Nations, Geneva, Switzerland, June 2012.
277 *African Mobile Observatory 2011: Driving Economic and Social Development through Mobile Services*, GSM Association, 2011.
278 R. Abraham, *International Conference on Information and Communication Technologies and Development*, 2006, pp. 48–56.
279 P. A. K. Kyem and P. K. Le Maire, *The Electronic Journal of Information Systems in Developing Countries*, 2006, **28**(5), 1–16.
280 B. Lane, S. Sweet, D. Lewin, J. Sephton and I. Petini, *The Economic and Social Benefits of Mobile Services in Bangladesh*, GSM Association, 2006.
281 J. C. Aker, *Does Digital Divide or Provide? The Impact of Cell Phones on Grain Markets in Niger*, The Center for Global Development, 2008.
282 O. Morawczynski, *Surviving in the 'Dual System:' How M-Pesa is Fostering Urban-to-Rural Remittances in a Kenyan Slum*, Mobile Active, 2008.
283 E. M. Wurm, R. Hofmann-Wellenhof, R. Wurm and H. P. Soyer, *J. Dtsch. Dermatol. Ges.*, 2008, **6**, 106–112.
284 D. N. Breslauer, R. N. Maamari, N. A. Switz, W. A. Lam and D. A. Fletcher, *PLoS One*, 2009, **4**, e6320.
285 V. F. Pamplona, A. Mohan, M. M. Oliveira and R. Raskar, Dual of Shack-Hartmann Optometry Using Mobile Phones, 2010.
286 A. F. Coskun, J. Wong, D. Khodadadi, R. Nagi, A. Tey and A. Ozcan, *Lab Chip*, 2013, **13**, 636–640.
287 D. Borich, personal communication.
288 D. J. You, T. S. Park and J. Y. Yoon, *Biosens. Bioelectron.*, 2013, **40**, 180–185.
289 O. Mudanyali, S. Dimitrov, U. Sikora, S. Padmanabhan, I. Navruz and A. Ozcan, *Lab Chip*, 2012, **12**, 2678–2686.
290 N. Polwart, personal communication.
291 D. C. Cooper, B. Callahan, P. Callahan and L. Burnett, Mobile Image Ratiometry: A New Method for Instantaneous Analysis of Rapid Test Strips, Nature Precedings, 2012.
292 D. C. Cooper, Mobile Image Ratiometry for the Detection of Botrytis Cinerea (Gray Mold), Nature Precedings, 2012.
293 http://www.frontlinesms.com/, Accessed January 29, 2013.
294 K. May, M. E. Prior and I. Richards, *US Pat.*, 6187598, 2001.
295 P. J. Davis, M. E. Prior and K. May, *US Pat.*, 6352862, 2002.
296 S. Ching, P. A. Billing and J. Gordon, *US Pat.*, 6534320, 2003.
297 T. Tisone, *IVD Technology*, 2000, 6(3), pp. 43–60.
298 T. C. Tisone, *US Pat.*, 5916524, 1999.
299 A. Weiss, *IVD Technology*, 1999, 5, pp. 48–57.
300 K. A. Mirica, J. G. Weis, J. M. Schnorr, B. Esser and T. M. Swager, *Angew. Chem., Int. Ed.*, 2012, **51**, 10740–10745.
301 *In vitro Diagnostics (IVD) Market (Applications, End-users & Types) Trends & Global Forecasts (Major & Emerging Markets - G7, Japan & BRIC), Markets and Markets*, 2011.
302 J. Marchant, *Innovations in Diagnostics (Next Generation Molecular & Point of Care Diagnostics Driving Personalised Healthcare), Business Insights Ltd*, 2006.
303 A. W. Martinez, S. T. Phillips, G. M. Whitesides and E. Carrilho, *Anal. Chem.*, 2009, **82**, 3–10.
304 D. Dendukuri, personal communication.
305 J. Rolland, personal communication.
306 Labindia divests businesses to AB Sciex and Leica, 2011 http://www.genengnews.com/gen-news-highlights/labindia-divests-businesses-to-ab-sciex-and-leica/81245950/, Accessed January 11, 2013.
307 Hologic acquires TCT International Co. Ltd., a leading distributor of Medical Products in China, News Release, 2011 http://investors.hologic.com/index.php?s=43&item=200, Accessed January 14, 2013.
308 An IMAP HEALTHCARE Report, Pharmaceuticals & Biotech Industry Global Report, 2011.
309 B. Bauer, An Executive Interview with Jean Luc Belingard, President of Roche's Diagnostic Business, 1997 http://www.casebauer.com/publications/library/p014.htm, Accessed January 10, 2013.
310 Roche disappointed by Illumina Inc's Board of Directors' rejection, World Pharma News, 2012 http://www.worldpharmanews.com/roche/2030-roche-disappointed-by-illumina-incs-board-of-directors-rejection, Accessed January 14, 2013.
311 P. Woodall, Hey big spenders, The World in 2012, The Economist, http://www.economist.com/node/21537925.
312 *Pharma 2020: The Vision*, PricewaterhouseCoopers, 2007.
313 S. Long, Tiger Traps, The World in 2012, The Economist.
314 *Annual Report*, Roche, 2011.
315 Roche to acquire Ventana for $89.50 per share, Media Release, 2008 http://www.roche.com/media/media_

 This journal is © The Royal Society of Chemistry 2013

Published on 08 May 2013. Downloaded by University of Cambridge on 31/05/2013 13:14:32.

releases/med-cor-2008-01-22.htm, Accessed January 8, 2013.
316 Roche completes acquisition of Igen, Media Release, 2004 http://www.roche.com/media/media_releases/med-cor-2004-02-16.htm, Accessed January 3, 2013.
317 Roche completes acquisition of BioVeris, Media Release, 2007 http://www.roche.com/investors/ir_update/inv-update-2007-06-26.htm, Accessed January 7, 2013.
318 L. S. Thomas, Abbott buys TheraSense for $1.2 billion, San Francisco Business Times, 2004 http://www.bizjournals.com/eastbay/stories/2004/01/12/daily9.html?page=all, Accessed January 8, 2013.
319 B. J. Feder, Abbott Laboratories to Buy Medisense for $876 Million, The New York Times, 1996, http://www.nytimes.com/1996/03/30/business/abbott-laboratories-to-buy-medisense-for-876-million.html.
320 Abbott Laboratories to Acquire i-STAT Corp., a Leading Manufacturer of Point-of-Care Diagnostics, PR Newswire, 1995 http://www.prnewswire.co.uk/news-releases/abbott-laboratories-to-acquire-i-stat-corp-a-leading-manufacturer-of-point-of-care-diagnostics-155236705.html, Accessed January 3, 2013.
321 B. Japsen, Abbott to acquire biotech firm Vysis, Chicago Tribune, 2001 http://articles.chicagotribune.com/2001-10-25/business/0110250381_1_vysis-abbott-chief-executive-miles-white, Accessed January 6, 2013.
322 *Annual Report, Siemens at a glance*, 2011.
323 Press Release, Siemens to acquire Dade Behring, 2007 http://www.siemens.by/en/press/releases/2007/behring/, Accessed January 11, 2013.
324 Press Release, Siemens to acquire Diagnostic Products Corporation, 2006 http://www.medical.siemens.com/siemens/en_GLOBAL/gg_diag_FBAs/files/About_Us/DPCPressRelease4_27_06.pdf, Accessed January 11, 2013.
325 News & Events, BD announces agreement to acquire HandyLab, Inc., 2009 http://www.bd.com/contentmanager/b_article.asp?Item_ID=24217&ContentType_ID=1&BusinessCode=20001&d=BD+Worldwide&s=&dTitle=&dc=&dcTitle=, Accessed January 8, 2013.
326 News & Events, BD announces agreement to acquire GeneOhm Sciences, Inc., 2006 http://www.bd.com/contentmanager/b_article.asp?Item_ID=22369&ContentType_ID=1&BusinessCode=20001&d=&s=&dTitle=&dc=&dcTitle=, Accessed January 12, 2013.
327 *Quarter 3 Report, Danaher*, 2012.
328 Press Release, Danaher to acquire Beckman Coulter, Inc. for $83.50 per share or $6.8 Billion, 2011 http://phx.corporate-ir.net/phoenix.zhtml?c=82105&p=irol-newsArticle&ID=1525238&highlight=, Accessed January 14, 2013.
329 Press Release, DHR to acquire Life Sciences Instrumentation businesses from MDS Inc. & Life Technologies Corp., 2009 http://www.absciex.com/company/news-room/dhr-to-acquire-life-sciences-instrumentation-businesses-from-mds-inc-and-life-technologies-corp, Accessed January 11, 2013.
330 S. G. Langlois and S. Danaher to acquire Tektronix for $2.8 billion, 2007, The Wall Street Journal, http://articles.marketwatch.com/2007-10-15/news/30796010_1_tektronix-danaher-fluke.
331 T. Stynes, Danaher to acquire Iris International for $352 mln, The Wall Street Journal, 2012 http://www.marketwatch.com/story/danaher-to-acquire-iris-international-for-352-mln-2012-09-17, Accessed January 12, 2013.
332 *Form 10-K*, Hologic Inc., 2011.
333 M. Allison, Shareholders approve Hologic's $6.2 Billion acquisition of Cytyc, 2007 http://www.xconomy.com/boston/2007/10/18/shareholders-approve-hologics-62-billion-acquisition-of-cytyc/, Accessed January 9, 2013.
334 Hologic completes acquisition of Gen-Probe, http://investors.hologic.com/2012-08-01-Hologic-Completes-Acquisition-Of-Gen-Probe, Accessed January 14, 2013.
335 Gen-Probe acquires GTI Diagnostics for $53 million in cash, 2010 http://www.gen-probe.com/news/PressReleaseText.asp?releaseID=1508519, Accessed January 14, 2013.
336 Hologic to acquire Sentinelle Medical, http://investors.hologic.com/index.php?s=43&item=406, Accessed January 13, 2013.
337 Acquisition of outstanding Axis-Shield shares, 2011 http://www.investegate.co.uk/article.aspx?id=201111090700487395R, Accessed January 14, 2013.
338 eScreen, Inc. and Alere announce acquisition, 2012 http://www.escreen.com/About/Newsroom/AlereAcquireseScreen.aspx, Accessed January 13, 2013.
339 C. A. Burkhardt, Buyer's market prevails for Medtech firms, 2010, MD+DI, vol. 32, 12, http://www.mddionline.com/article/buyers-market.
340 C. Dodge and M. Dorning, Rich-Poor Gap Widens to Most Since 1967 as Income Falls, Bloomberg, http://www.bloomberg.com/news/2012-09-12/u-s-poverty-rate-stays-at-almost-two-decade-high-income-falls.html, Accessed January 11, 2013.
341 Diagnostics for all, http://www.dfa.org/projects/projects-overview.php, Accessed January 11, 2013.
342 Achira Labs, http://www.achiralabs.com/products.html, Accessed January 14, 2013.
343 S. S. Mehta, *Commercializing Successful Biomedical Technologies: Basic Principles for the Development of Drugs, Diagnostics and Devices*, Cambridge University Press, 2008.
344 C. D. Chin, V. Linder and S. K. Sia, *Lab Chip*, 2012, **12**, 2118–2134.
345 M. Mars, *Yearb. Med. Inform.*, 2010, 87–93.
346 W. Bernhard, personal communication.